



UNIVERSITÀ DELLA CALABRIA

DOTTORATO DI RICERCA IN MECCANICA COMPUTAZIONALE
XXI CICLO

Tesi di Dottorato

**The Implicit Corotational Method:
General theory and FEM implementation**

Antonio Madeo

SETTORE SCIENTIFICO DISCIPLINARE ICAR-08

Dissertazione presentata per il conseguimento del titolo di Dottore di
Ricerca in Meccanica Computazionale

Novembre 2008


UNIVERSITÀ DELLA CALABRIA

Data: Cosenza, Novembre 2008

Autore: **Antonio Madeo**

Titolo: **The Implicit Corotational Method: General theory and FEM implementation**

Dipartimento: **Modellistica per l'Ingegneria**



Firma dell'autore

Supervisore:



Prof. Giovanni Garcea

Supervisore:



Prof. Raffaele Casciaro

Coordinatore:



Prof. Maurizio Aristodemo

a Laura...

Contents

1	Introduction	1
2	Nonlinear structural analysis	4
2.1	From linear to nonlinear analysis	4
2.2	Solution strategies in nonlinear analysis	5
2.3	Modeling requirements	6
3	Implicit Corotational Method	8
3.1	Kinematics and statics of continuum body	8
3.2	Corotational observer equations	10
3.2.1	Quadratic approximations	11
3.2.2	Further insight	11
3.3	Use of linear solutions to set up a nonlinear modeling	12
3.4	ICM basic items	13
4	Some tutorial implementation of ICM	16
4.1	Planar beam in bending and shear	16
4.1.1	Recovering linear solutions	16
4.1.2	Galerkin approximation	17
4.1.3	Kinematic equations	18
4.1.4	Corotational setup	19
4.1.5	Further insights	21
4.2	Thin walled beam subjected to axial force and torsion	24
4.2.1	Recovering linear solution	24
4.2.2	Galerkin approximation	25
4.2.3	Kinematics equations	26
4.3	Some further considerations	26
5	Nonlinear 3D beam model based on Saint Venant general rod theory	28
5.1	Recovering linear solution–stress	28
5.2	Recovering linear solution–kinematics	29

5.3	Galerkin approximation	30
5.4	Kinematics equations	31
5.5	The quadratic strain model	31
6	Nonlinear plate model	32
6.1	Recovering linear solution	32
6.2	Galerkin approximation	33
6.3	Kinematics equations	33
6.4	Kirchoff's thin plate	34
7	FEM implementation	36
7.1	Corotational strategy	37
7.2	Total-Lagrangian strategy	38
7.3	The asymptotic method (Koiter analysis)	38
7.4	The path-following method	41
7.4.1	The arc-length iterative scheme	42
8	FEM implementation of the Saint Venánt nonlinear beam model-Corotational formulation	44
8.1	3D rotation algebra	44
8.2	Corotational formulation	46
8.2.1	Strain energy in the CR frame	46
8.2.2	A remark on the corotational description	48
8.2.3	Strain energy in the fixed frame	48
8.3	Local beam modeling	52
8.3.1	Linear local modeling for the beam	53
8.3.2	The CR transformation for the beam	54
8.3.3	The assemblage matrix	58
8.3.4	The quadratic local modeling for the beam	58
8.4	Some further detail for Riks analysis	60
8.4.1	Updated scheme	60
8.4.2	The CR transformation for the beam	61
8.4.3	Expressions for the strain variations for linear model	62
8.4.4	Computational remarks	63
8.5	Numerical results	64
8.5.1	Planar beams	64
8.5.2	Spatial beams	66
8.5.3	Modal interaction test: 3D tower	69
9	FEM implementation of the Saint Venánt nonlinear beam model-Total Lagrangian formulation	72
9.1	Mixed strain energy	72

9.2	Finite element	74
9.2.1	Energy derivatives	75
9.2.2	Discrete energy derivatives	75
9.2.3	Energy equivalences	76
10	FEM implementation of nonlinear plate model	78
10.1	The finite element of the plate	78
10.1.1	Displacements interpolation	79
10.1.2	Numerical integration	79
10.2	Numerical results	80
10.2.1	The Eulero beam and Roorda Frame	81
10.2.2	C section beam	84
10.2.3	C section with stress redistribution	84
11	Concluding remarks	87
A	Some remarks on polar decomposition	97
A.1	Recursive evaluation of polar decomposition	97
B	Objective interpolation	99
B.1	Objective Interpolation	99
B.1.1	Equivalence with Corotational Formulation	101
C	The use of material-spatial model in Koiters analysis	103
C.1	Shallow Frame - Analytical Solution	103
C.1.1	Shallow frame solution using - material model	114

Abstract

A method, called implicit corotational, is proposed. It allows to obtain, in a simple way, objectivity coherent nonlinear modelings for structural continua, as beams or shells, undergoing finite rotations and small strains. The basic idea is to apply a corotational description to the neighbor of each continuum point. This allows to recover an objective nonlinear modeling while reusing information gained from its linear counterpart. The formulation implicitly satisfies the energy independence from rigid body motions and is well suited to be implemented in FEM nonlinear analysis, particularly when using a Koiter-like asymptotic approach, where this objectivity requirements has to be exactly guaranteed.

The theoretical guidelines and the general motivations of the method are discussed in detail. It is then applied for generating nonlinear models for 3d beams and plates from the Saint Venant rods and Mindlin–Reissner plates linear theories, respectively. Both models maintain full detail of their linear counterpart, so somewhere overpassing similar models available in literature. A finite element implementation of the beam model, suitable for asymptotic post-buckling and path-following analysis of 3d frames and plate model, is then presented. Numerical tests in both case of monomodal and multimodal buckling show the effectiveness and accuracy of the proposed approach, also in this context which is strongly sensitive to the geometrical coherence of the model.

Chapter 1

Introduction

The reliability and the accuracy for nonlinear analysis of slender elastic structures require appropriate nonlinear modeling. The objectivity of the models, that is strain measures must be independent from finite rigid body motions in order to assure a coherent expression for the strain energy, is sure a fundamental requirement.

The usual approach to nonlinear analysis, that is the so-called *path-following approach*, is based on an incremental-iterative step-by-step solution algorithm which actually exploits the first derivatives of the energy to check the equilibrium and makes use of the second ones to obtain a suitable iteration matrix. Only the former have to be expressed exactly, while even a rather rough estimate for the second derivatives could be sufficient to satisfy the convergence requirements. Furthermore, displacements can be made small enough by an appropriate updating of the reference configuration within the incremental step, using the so called Updating Lagrangian or Corotational solution strategies. Therefore, full objectivity, while obviously desirable, is not really required and approximate *technical* models aimed to be only second-order accurate could be viewed as an acceptable compromise in this analysis context, at least if combined with a robust and accurate configuration updating.

Koiter-like asymptotic approach as that described in [1, 3, 4, 5] represents a powerful and potentially convenient tool for the analysis of slender nonlinear structures, being able to provide an accurate syntectic answer about their overall buckling and post-buckling behavior, including the effects due to possible load imperfections and geometrical defects. The analysis is based on a fourth-order expansion of the energy and needs both the structural modeling and its finite element discretization to be also, at least, fourth-order accurate in order to obtain results reliability. Corotational formulation and technical models are recently been introduced also in this kind of approach [102] but the presence of fourth order derivative of the strain energy penalize

the formulation that, especially when used for structural model requiring the use of 3D rotations, need of complex manipulations.

Furthermore to define appropriate nonlinear modeling, which satisfy objectivity exactly while being suitable for FEM implementations without missing the richness of 3d solutions, could be however a difficult task, in general. Actually, it is quite easy to model 3d bodies using the Cauchy continuum and Green–Lagrange strain tensor, but it can become difficult to get a coherent, simply enough modeling for slender structural components as beams or shells which are more conveniently described as one- or two-dimensional structured continua characterized by 3d displacements and rotations fields.

Even if the literature is very rich of nonlinear structural modeling, developed in different fashion, the general picture is somewhere unsatisfactory. Beam or shell models based on a direct assumption of constitutive laws in terms of stress/strain resultants, as those developed by Cosserat [15], Reissner [20, 27, 30, 31], Antmann [19, 46], Simo [33, 35], Rubin [32] are generally based on a simplified kinematics and tend to miss the richness of the 3d solution by loosing important detail, as the shear/torsional coupling, covered by the linear theories. Conversely, models generated as direct Galerkin reduction of the 3d nonlinear continuum appear to complex for being suitable for FEM implementations and tend to be affected by locking in the nonlinear range due to even small kinematical incoherencies made in displacement interpolations. So they require some ad hoc simplifications and a-posteriori treatments to be actually used as a computational tool (see Kim [52, 69, 98], Pacoste [55], Petrov [66, 67], Bradford [76, 77, 99], Chen [62, 70, 75, 100]).

On the other hand the availability of linear model developed in the frame of small displacements/rotations hypothesis is notable. The theories are enough consolidated and generally the models account the richness of 3d solution. The possibility of reusing the linear model as a basis for generating appropriate nonlinear models appear fashionable, allowing a complete recovering of all effort in developing linear theory in nonlinear context and overpassing the drawbacks present in nonlinear models. This possibility could be exploited extending with appropriate hypothesis at continuum level the corotational idea proposed by Rankin [34, 37, 40] in FEM context.

All previous considerations leading to an automatic and elegant method that we call *Implicit Corotational Method* or simply ICM allowing to recover objective nonlinear models for structure undergoing finite rotations and small strains, starting from the corresponding linear ones, so allowing to completely reuse the information gained by the linear analysis in the nonlinear context. The main idea is to associate a corotational reference frame to each neighbor of the 3d continuum points. This allows to split the neighbor motion in its rotational and pure deformative parts, according to the decomposition theo-

rem [18], and to transfer to the nonlinear modeling the information provided by the existing linear theories. In particular linear stress and strain, which are assumed to be small, are directly taken as Biot's stress and strain tensors in the nonlinear model, while nonlinear rotations are recovered from the linear ones exploiting the internal properties of a rotation tensor. The final expression for the strain energy, in terms of stress/strain resultants, is then obtained through a mixed variational formulation which also provide a convenient framework for the numerical implementation. It is worth mentioning that the approach proposed appear somewhat similar to that by Nayfeh and Pai [49, 65, 95]. It is however more connected to the corotational formulation and exploit in a deeper and more automatic way the reuse of linear models in a nonlinear context.

Chapter 2

Nonlinear structural analysis

2.1 From linear to nonlinear analysis

The ability in predicting the structural behavior consequent to assigned external loadings is a traditional need for engineering. Such implies a proper theoretical framework, accurate modeling and suitable analysis strategies be available. A great effort has been actually spent in this direction, particularly in the last two Centuries, leading to the classical Cauchy's theory of elastic three-dimensional bodies, the Saint Venant's rods theory, the plates and shells theories and, more recently, exploiting the wide improvements in computational tools, powerful numerical approaches as the Finite Element Method.

The so called "small displacements" assumption, allowing to refer to relatively simple linearized equations, have played a strong role in this evolution. A large amount of results obtained by the research, in particularly the derivation of structured models as plates and beams from the 3D continuum and their description in terms of finite elements, are strictly related to this assumption. The use of high strength materials and slender structures, leading to complex instability phenomena and strong imperfection sensitivity which can not be recovered by linear theories, however enforces the research to nonlinear formulations and solution strategies.

Nonlinear analysis usually refers to a structure subjected to an assigned loading path $p[\lambda] = \lambda \hat{p}$, λ being a load amplifier factor controlling the loading process. The structure behavior is governed by the stationarity condition of its total potential energy $\Pi[u; \lambda]$, associated to the external load p and to the configuration u of the structure, with respect to all admissible changes of configuration δu . Using compact notations this condition is expressed by

$$\Pi' [u, \lambda] \delta u = 0 \quad , \quad u \in \mathcal{U} \quad , \quad \delta u \in \mathcal{T} \quad (2.1)$$

where \mathcal{U} is the manifold of the admissible configurations, \mathcal{T} its tangent

space and the prime stands for Frechét differentiation. Condition (2.1) states a relationship between λ and u describing a curve in the $\{u, \lambda\}$ space. The goal of the analysis is to determine this curve, the so called *equilibrium path* with a particular accuracy in the evaluation of the maximum value λ_c of the load multiplier.

Usually (and conveniently) the configuration is described according \mathcal{U} to be a linear manifold, so \mathcal{T} becomes independent from u , and the potential energy can be split in two separate terms, the first expressing the internal strain energy and the second the external load work:

$$\Pi[u, \lambda] := \Phi[u] - \lambda \hat{p} u \quad (2.2)$$

We also know (see [10, 11]) that, with an appropriate choice of configuration variables $u := \{\sigma, d\}$, being σ the stress and d the displacements fields, energy (2.2) can be expressed in mixed form. The kinematical relationship between displacements and strains, plays an important role in the analysis: if assuming that the relationship are linear, we get a linear formulation. So we can translate from a linear to a geometrically nonlinear formulation simply by referring to a proper nonlinear expression for compatibility relationships.

2.2 Solution strategies in nonlinear analysis

Using a suitable interpolation rules which allows to define the configuration fields d and σ through a discrete vector \mathbf{u} , condition (2.1) can be reduced to a nonlinear vector equation

$$\mathbf{r}[\mathbf{u}, \lambda] := \mathbf{s}[\mathbf{u}] - \lambda \hat{\mathbf{p}} = \mathbf{0} \quad (2.3)$$

to be solved numerically. Roughly speaking, two solution approaches are currently available for this purpose.

The first, usually referred as *path-following analysis* recovers the equilibrium path by a sequence of sufficiently close equilibrium points each of them being obtained by the Riks iteration scheme [2]. Obviously this approach needs the first variation \mathbf{r} be evaluated accurately, the solution being directly defined by condition $\mathbf{r} = \mathbf{0}$. Conversely, the same accuracy is not actually needed for the second variation that is only utilized for defining the iterations matrix and its accuracy only influences the convergence of the iterative process. A quite rough approximation could be sufficient for that purpose (see [10]). The need of an exact evaluation for \mathbf{r} can also be relaxed if using an Updating Lagrangian (UL) solution strategy. According to the step smallness, a simple second-order accurate modeling could be generally sufficient, even if a certain care has always to be taken in the end-step configuration

updating in order to reduce, as much as possible, geometrical incoherencies and avoiding objectivity errors can cumulate in the loading process.

The second approach, referred as *asymptotic analysis* develops as a finite element implementation of Koiter's nonlinear instability theory [1], and it is based on a 4th order Taylor expansion of the strain energy. This solution approach presents several advantages: i) it provides a synthetic representation of the solution allowing to easily recover the main features of the structural behavior, including complex instability phenomena as coupled buckling and modal jumps ; ii) it is computationally fast, of the same order of linearized stability analysis; iii) the effects of additional imperfections can be taken into account with negligible extra-costs, so allowing an inexpensive imperfection sensitivity analysis. Conversely, it strongly uses information attained from the 4th-order expansion of the strain energy and then requires that all terms of this expansion be accurately evaluated. Even small inaccuracies in this evaluation, coming from geometrical incoherencies in the higher-order terms of the expansion of the kinematical relationship or in its finite element representation, strongly affect the solution accuracy and can render it to become unreliable. For a discussion about all these topics, the reader can refer to [3] and their citations.

2.3 Modeling requirements

Both solution strategies require an appropriate expression for the total potential energy be explicitly allowable. Its correctness with respect to the objectivity requirements, is crucial for the results reliability of path-following analysis, and even more for asymptotic analysis which needs full 4th-order accuracy in both the finite element modelings and in their underlayered continua. In view of this demand, the current state of knowledge is however not completely satisfactory. Although a lot of theoretical results and finite element technologies are available for the linear case, the experience in deriving suitable nonlinear models is poorer than in the linear case, particularly with respect to the nonlinear structural modeling (e.g. beams, plates and shells).

Current proposals for nonlinear models available in literature are not free from inconveniences. Autonomous models, as those proposed by Cosserat [15], Reissner [20, 27, 30, 31], Simo [33, 35] and Antman [19, 46], Rubin [32] defined in terms of a rigid motion of the cross section and simplified constitutive laws, are little related to 3d Cauchy nonlinear continuum equations and appear somewhat poorer than the richness and complexity of the linear theories. In fact, the section warping, stress distribution and other relevant details characterizing the linear solution are completely neglected in this approach, and possible generalizations are not so obvious and can

lead to so complex expressions to be of little use in practical applications. Models obtained through a Galerkin approximation of the equations of the 3d nonlinear continuum (see Kim [52, 69, 98], Pacoste [55], Petrov [66, 67], Bradford [76, 77, 99], Chen [62, 70, 75, 100]) are also unsatisfactory. Even if using a displacement interpolation based on the Cauchy solution, as made for instance by Petrov and Geradin [66, 67], an interpolation locking tends to be produced. This is due to a disturbing interaction, between the assumed displacement fields and the use of a strain energy based on the Green–Lagrange tensor, which generates spurious high–order energy terms which have to be a–posteriori deleted through at–hands simplifications. In both cases, an algebraically complex formulation is obtained, little suited for finite element implementations and some care is required for avoiding interpolation and extrapolation locking (see [11] for a discussion of this topic).

The corotational approach, based on polar decomposition theorem [18], because it allows to decoupling the kinematical coherency from the elastic response, represents a potentially suitable way for generating coherent nonlinear models, particularly when, as in the case of beams or shells, rotation variables are directly involved in the description. It has been followed by Nayfeh and Pai which presented in [95] a wide number of nonlinear models covering a large range of structural cases, including beams, layered plates and shells. The amplitude of this contribution is impressive. However, the corotational description is mainly used for providing a–priori geometrical coherence to the modeling than as a general automatic tool for fully transfer to the nonlinear context the wide theoretical experience and the refined numerical technologies already available in linear analysis. So the full potentialities of corotational approach, devised in the natural modes approach by Argyris [24], clearly stated in continuum and FEM context by Belytschko [23], and by Rankin [34, 37, 40] in reusing all linear FEM tradition for nonlinear analysis, seems to be not completely fulfilled.

The need of an organic methodology, which could render fully automatic the derivation of the nonlinear model fully exploiting all information gained by its linear counterpart, avoiding heuristic assumptions for each particular case, is clear. A full attention to minor but crucial details such as the parametrization of rotations, the equation formats and other implementation details which result however crucial for FEM implementations, are also necessary in order to get models suitable for practical applications.

Chapter 3

Implicit Corotational Method

The goal of the **Implicit Corotational Method** (ICM) is to reuse, in a non-linear context, the results of linear theories in order to obtain objective structural models (e.g. beam, shell) suitable for FEM implementations. An appropriate stress/strain representation for the description of the nonlinear elastic continuum, the use of corotational algebra for splitting the body motion in the rigid and deformative parts and some assumptions on the reinterpretation of linear theory in nonlinear context, constitute the basis of the ICM.

3.1 Kinematics and statics of continuum body

Each material point P is referred by its position $\mathbf{X} = \{X_1, X_2, X_3\}$ in a reference configuration (usually the *initial undeformed* one) and denoted with \mathcal{B} and by its current position \mathbf{x} defined in terms of the displacement $\mathbf{u}[\mathbf{X}]$ as:

$$\mathbf{x}[\mathbf{X}] := \mathbf{X} + \mathbf{u}[\mathbf{X}]$$

The deformation gradient defines the motion of the infinitesimal neighbor of \mathbf{X}

$$\mathbf{F}[\mathbf{X}] := \nabla \mathbf{x} = \mathbf{I} + \nabla \mathbf{u} \quad \text{with} \quad \nabla(\cdot) := \partial(\cdot)/\partial \mathbf{X}$$

\mathbf{I} being the identity tensor.

From the decomposition theorem (see [18]) the positive defined tensor $\mathbf{F}[\mathbf{X}]$ can be decomposed into a unique product of a rotation tensor $\mathbf{R}[\mathbf{X}]$ and a symmetric, positive definite, stretch tensor $\mathbf{U}[\mathbf{X}]$:

$$\mathbf{F} = \mathbf{R}\mathbf{U} \tag{3.1}$$

An objective description requires that the strain to be independent from \mathbf{R} , so possible objective strain measure are expressed in the form

$$\boldsymbol{\varepsilon}^{(n)} := \frac{1}{n} (\mathbf{U}^n - \mathbf{I}) \tag{3.2}$$

which, for $n = 1$ and $n = 2$, provides the *Biot strain tensor* $\boldsymbol{\varepsilon}_b$ and the *Green-Lagrange strain tensor* $\boldsymbol{\varepsilon}_g$, respectively:

$$\boldsymbol{\varepsilon}_b = \mathbf{R}^T \mathbf{F} - \mathbf{I} \quad , \quad \boldsymbol{\varepsilon}_g = \frac{1}{2}(\mathbf{F}^T \mathbf{F} - \mathbf{I}) \quad (3.3)$$

Green-Lagrange strain $\boldsymbol{\varepsilon}_g$ can be easily evaluated from \mathbf{F} to which is related by a simple quadratic expression and for this is the most frequently used measure while Biot strain $\boldsymbol{\varepsilon}_b$ has a more complex expression in terms of \mathbf{F} . Really the following relations between the two strain measure holds:

$$\boldsymbol{\varepsilon}_g = \boldsymbol{\varepsilon}_b + \frac{1}{2}\boldsymbol{\varepsilon}_b^2 \quad , \quad \boldsymbol{\varepsilon}_b = \sqrt{2\boldsymbol{\varepsilon}_g + \mathbf{I}} - \mathbf{I} \quad (3.4)$$

Dealing with problems characterized by large displacements but small strain we can generally assume $\|\mathbf{U} - \mathbf{I}\| \ll 1$ and then also $\|\boldsymbol{\varepsilon}_g\| \ll 1$. This enables the use of a Taylor expansion to obtain $\boldsymbol{\varepsilon}_b$ and \mathbf{R} as

$$\begin{aligned} \boldsymbol{\varepsilon}_b &= \boldsymbol{\varepsilon}_g - \frac{1}{2}\boldsymbol{\varepsilon}_g^2 + \frac{1}{2}\boldsymbol{\varepsilon}_g^3 + \dots \\ \mathbf{R} &= \mathbf{F}(\mathbf{I} - \boldsymbol{\varepsilon}_g + \frac{3}{2}\boldsymbol{\varepsilon}_g^2 - \frac{5}{2}\boldsymbol{\varepsilon}_g^3 + \dots) \end{aligned} \quad (3.5)$$

that can be expressed in terms of \mathbf{F} and then of $\nabla \mathbf{u}$ using eq. (3.3). Kinematics description is completed by the boundary condition on $\partial \mathcal{B}_u$.

Letting \mathbf{b}_0 the external body forces with $\partial \mathcal{B}_f$ the boundary in witch the external tractions \mathbf{f}_0 are assigned and with $\mathbf{n}_0[\mathbf{X}]$ the unit versor to $\partial \mathcal{B}_f$ in \mathbf{X} , the equilibrium equations in terms of the symmetric second Piola–Kirchhoff stress $\boldsymbol{\sigma}_g$, work conjugate with $\boldsymbol{\varepsilon}_g$ are:

$$\begin{cases} \operatorname{div}[\mathbf{F}\boldsymbol{\sigma}_g] + \mathbf{b}_0 &= \mathbf{0} & \text{in } \mathcal{B} \\ \mathbf{F}\boldsymbol{\sigma}_g \mathbf{n}_0 &= \mathbf{f}_0 & \text{in } \partial \mathcal{B}_f \end{cases} \quad (3.6)$$

Defining the Biot stress, work conjugate with $\boldsymbol{\varepsilon}_b$ as the symmetric part of

$$\boldsymbol{\sigma}_b = \frac{1}{2}(\mathbf{P} + \mathbf{P}^T) \quad , \quad \mathbf{P} = \mathbf{U}\boldsymbol{\sigma}_g$$

eq.(3.6) becomes

$$\begin{cases} \operatorname{div}[\mathbf{R}\mathbf{P}] + \mathbf{b}_0 &= \mathbf{0} & \text{in } \mathcal{B} \\ \mathbf{R}\mathbf{P} \mathbf{n}_0 &= \mathbf{f}_0 & \text{in } \partial \mathcal{B}_f \\ \mathbf{R}\mathbf{P}\mathbf{F}^T &= \mathbf{F}\mathbf{P}^T \mathbf{R}^T & \text{in } \mathcal{B} \end{cases}$$

Note as \mathbf{P} is the rotated by \mathbf{R} first Piola–Kirchhoff stress. In case of isotropic material for which $\mathbf{U}\boldsymbol{\sigma}_g = \boldsymbol{\sigma}_g\mathbf{U}$ we also have

$$\mathbf{P} = \boldsymbol{\sigma}_b$$

and the equilibrium equations simplify to

$$\begin{cases} \operatorname{div}[\mathbf{R}\boldsymbol{\sigma}_b] + \mathbf{b}_0 & = \mathbf{0} & \text{in } \mathcal{B} \\ \mathbf{R}\boldsymbol{\sigma}_b \mathbf{n}_0 & = \mathbf{f}_0 & \text{in } \partial\mathcal{B}_f \end{cases} \quad (3.7)$$

Note as in this case the symmetry and comutativity assure rotation equilibrium

$$\mathbf{R}\boldsymbol{\sigma}_b \mathbf{U} \mathbf{R}^T = \mathbf{R} \mathbf{U} \boldsymbol{\sigma}_b \mathbf{R}^T$$

Also note as $\boldsymbol{\sigma}_g \mathbf{n}_0$ represent the force for unity of reference area pull-back by \mathbf{F} while $\boldsymbol{\sigma}_b \mathbf{n}_0$ the same quantities but pull-back by \mathbf{R} .

3.2 Corotational observer equations

Denoting with a bar quantities viewed by a new observer, defined by a rotation tensor \mathbf{Q} we have [18] that the deformation quantities $\bar{\mathbf{F}} = \bar{\mathbf{R}}\bar{\mathbf{U}}$ transforms as

$$\bar{\mathbf{F}} := \mathbf{I} + \nabla \bar{\mathbf{u}} = \mathbf{Q}^T \mathbf{F} \quad , \quad \bar{\mathbf{R}} := \mathbf{Q}^T \mathbf{R} \quad , \quad \bar{\mathbf{U}} := \mathbf{U} \quad (3.8)$$

that is the material strain don't change with a change of observer and the same occurs for stresses.

It the case of $\mathbf{Q} = \mathbf{R}$ eqs.(3.3) become

$$\boldsymbol{\varepsilon}_b = \bar{\mathbf{E}} \quad \text{and} \quad \boldsymbol{\varepsilon}_g = \bar{\mathbf{E}} + \frac{1}{2} \bar{\mathbf{E}}^2 \quad (3.9a)$$

being

$$\bar{\mathbf{E}} = \frac{1}{2} (\nabla \bar{\mathbf{u}} + \nabla \bar{\mathbf{u}}^T) \quad , \quad \bar{\mathbf{W}} = \frac{1}{2} (\nabla \bar{\mathbf{u}} - \nabla \bar{\mathbf{u}}^T) \quad (3.9b)$$

that is the Biot strain is exactly the symmetric part of $\nabla \bar{\mathbf{u}}$, that is the small linear strain tensor in CR frame, while $\boldsymbol{\varepsilon}_g \approx \bar{\mathbf{E}}$ only if $\bar{\mathbf{E}} \ll 1$.

Letting $\mathbf{Q} = \mathbf{R}$ the linear equilibrium equations in terms of the linear stress tensor $\bar{\boldsymbol{\sigma}}_l$ and using a material description are

$$\begin{cases} \mathbf{R} \operatorname{div}[\bar{\boldsymbol{\sigma}}_l] + \mathbf{b}_0 & = \mathbf{0} & \text{in } \mathcal{B} \\ \mathbf{R} \bar{\boldsymbol{\sigma}}_l \mathbf{n}_0 & = \mathbf{f}_0 & \text{in } \partial\mathcal{B}_f \end{cases} \quad (3.10)$$

Note as second equation in (3.10) has exactly the same forms of nonlinear corresponding one in terms of Biot stress. Some differences occurs in the terms that define the body force equilibrium being

$$\operatorname{div}[\mathbf{R}\boldsymbol{\sigma}_b] = \mathbf{R} \left(\operatorname{div}[\boldsymbol{\sigma}_b] + \sum_{j=1}^3 \chi^{(j)} \boldsymbol{\sigma}_b \right) \neq \mathbf{R} \operatorname{div}[\boldsymbol{\sigma}_b]$$

with a difference respect to the linear equilibrium equation terms that depend by the curvature $\chi^{(j)} \equiv \mathbf{R}^T \mathbf{R}_{,j}$ tha we supposed to be small. However also in this case we have an expression more similar to the corresponding nonlinear equilibrium equation in terms of Biot stress that in terms of the second Piola one. From previous consideration appears natural to consider the linear solution quantities as an accurate estimate of the corresponding Biot stress and strain assuming then

$$\boldsymbol{\sigma}_b \approx \bar{\boldsymbol{\sigma}}_l, \quad \boldsymbol{\varepsilon}_b \approx \bar{\mathbf{E}} \quad (3.11)$$

when all the linear quantities are described in a suitable corotational observer defined by \mathbf{R} .

3.2.1 Quadratic approximations

Let be the case that CR observer be characterized by a rotation \mathbf{Q} almost, but not exactly coincident with, \mathbf{R} that is let be

$$\mathbf{R} = \mathbf{Q}\bar{\mathbf{R}} \quad , \quad \|\bar{\mathbf{R}} - \mathbf{I}\| \ll 1$$

Assuming $\bar{\mathbf{R}}$ small from (3.5) we gets

$$\bar{\mathbf{R}} \approx \mathbf{I} + \bar{\mathbf{W}} + \frac{1}{2}\bar{\mathbf{W}}^2 - \frac{1}{2}(\bar{\mathbf{E}}\bar{\mathbf{W}} + \bar{\mathbf{W}}\bar{\mathbf{E}}) + \mathcal{O}[\bar{\mathbf{E}}^2, \bar{\mathbf{W}}^2] \quad (3.12)$$

and from eq.(3.3) we have the quadratic approximation of $\boldsymbol{\varepsilon}_b$ as

$$\boldsymbol{\varepsilon}_b \approx \bar{\mathbf{E}} + \frac{1}{2}(\bar{\mathbf{E}}\bar{\mathbf{W}} - \bar{\mathbf{W}}\bar{\mathbf{E}} - \bar{\mathbf{W}}^2) \quad (3.13)$$

Note as $\boldsymbol{\varepsilon}_b$ could also simply be obtained remembering its expression in terms of Green tensor and then neglecting in eq.(3.5) higher order terms

$$\boldsymbol{\varepsilon}_b \approx \boldsymbol{\varepsilon}_g - \frac{1}{2}\bar{\mathbf{E}}^2 \quad \text{being} \quad \boldsymbol{\varepsilon}_g = \mathbf{E} + \frac{1}{2}(\bar{\mathbf{E}}^2 + \bar{\mathbf{E}}\bar{\mathbf{W}} - \bar{\mathbf{W}}\bar{\mathbf{E}} - \bar{\mathbf{W}}^2)$$

Linear stresses, are always considered as that viewed by the observer rotated of \mathbf{R} and then don't change.

3.2.2 Further insight

The CR formulations can be look from another point of view. When structural models are considered, the kinematics are described in terms of generalized kinematics parameters that will be denoted synthetically whit \mathbf{d} . The fully nonlinear kinematics relationship is generally is not known, in particular non linear gradient $\mathbf{F}[\mathbf{d}]$ is not given, but however if the linear model available a linear approximation for the deformation can be obtained:

$$\mathbf{F}[\mathbf{d}] = \mathbf{E}[\mathbf{d}] + \mathbf{W}[\mathbf{d}] + \mathbf{I} \quad (3.14)$$

The use of corotational description allow to recover fully nonlinear deformation gradient starting from linear ones (3.14). Introducing a CR frame, defined by a finite rotation \mathbf{Q} function of generalized kinematics parameters \mathbf{d} obtained from small rotation \mathbf{W} , we can assume that \mathbf{F} is a corotational quantities than (3.14) is rewritten as:

$$\bar{\mathbf{F}}[\bar{\mathbf{d}}] = \bar{\mathbf{E}}[\bar{\mathbf{d}}] + \bar{\mathbf{W}}[\bar{\mathbf{d}}] + \mathbf{I} \quad (3.15)$$

In CR frame using expression (3.13) Biot's stress and polar decomposition rotation (3.12) can be evaluated:

$$\varepsilon_b \approx \bar{\mathbf{E}} + \frac{1}{2} (\bar{\mathbf{E}}\bar{\mathbf{W}} - \bar{\mathbf{W}}\bar{\mathbf{E}} - \bar{\mathbf{W}}^2) , \quad \bar{\mathbf{R}} \approx \mathbf{I} + \bar{\mathbf{W}} + \frac{1}{2}\bar{\mathbf{W}}^2 - \frac{1}{2}(\bar{\mathbf{E}}\bar{\mathbf{W}} + \bar{\mathbf{W}}\bar{\mathbf{E}}) \quad (3.16)$$

Thereby the fully nonlinear deformation gradient using (3.8) is obtained as:

$$\mathbf{F} = \mathbf{Q}\bar{\mathbf{R}}(\varepsilon_b + \mathbf{I}) \quad (3.17)$$

The recovered gradient (3.17) of deformation describe exactly the rigid body motion defined by \mathbf{Q} . The approximation is only contained in the description of small rotation $\bar{\mathbf{R}}$. The accuracy of nonlinear gradient of deformation increase when $|\bar{\mathbf{R}}| \ll 1$. This imply that the CR could be fixed so that $\bar{\mathbf{W}}$ is small. Generally previous condition when structured continua is considered the small rotation $\bar{\mathbf{W}}$ is not small for each point by only on average $|\bar{\mathbf{W}}| \ll 1$. Then, the approximations in (3.17) are related to the difference between $\bar{\mathbf{W}}$ and its average $|\bar{\mathbf{W}}|$.

3.3 Use of linear solutions to set up a nonlinear modeling

Previous considerations suggest that a nonlinear modeling can be obtained from the corresponding linear one, reusing the linear solution in an appropriate corotational frame that rotating with the material. This is a great potentiality because the literatures on linear theory is very rich and enough consolidated.

Really linear theory, during its long evolution, has produced many complex and elegant solutions can be used for a sophisticated detailed modeling in specific structural contexts: the rods theory by Saint Venant, the Vlasov theory for thin walled structures, the plates theory by Mindlin, to cite only some classical results. Moreover all these results have been obtained by the assumption that displacements (rotations) are small enough to allow to identify the deformed configuration with the undeformed one, and their derivation implies the use of appropriate reference systems that avoid rigid

rotations in order to minimize this difference. Therefore, the corotational idea is in some way implicit in linear theories.

In corotational frame linear solution gives a first-order accurate evaluation for the Biot's stress $\boldsymbol{\sigma}_b$ and for the displacement gradient $\nabla \bar{\mathbf{u}}$, and so for both $\bar{\mathbf{E}}$ and the *residual rotation* $\bar{\mathbf{W}}$ that, even if small, could be not identically zero. Then, Biot's strain $\boldsymbol{\varepsilon}_b$ can be estimate from $\bar{\mathbf{E}}$ and $\bar{\mathbf{W}}$ using linear or quadratic expression (3.13).

In this way we have an approximation for both the Biot's stress and strain fields that can be used in a variational principle to obtain, as Galerkin approximation, the nonlinear modeling which will be able to both exploit full detail of the corresponding linear solution and to satisfy objectivity requirements with respect to the rigid motion of the section exactly. The approximation will be as more accurate as the *residual rotation* $\bar{\mathbf{W}}$ while be as small as possible. Note that using Green strain and second Piola kirchhoff stresses the difference with respect to the linear solution will also contain terms in $\bar{\mathbf{E}}$ always not zero also if small (3.9a).

3.4 ICM basic items

The above discussion can be synthesized in the method that we call *Implicit Corotational Method* or ICM. The basic items and the hypothesis of the ICM are here schematically pointed out:

- *mixed variational formulation*

The nonlinear elastic continuum is described using Biot's stress/strain $\boldsymbol{\sigma}_b$ and $\boldsymbol{\varepsilon}_b$. Mixed form for the strain energy is used:

$$\Phi[\boldsymbol{\sigma}_b, \boldsymbol{\varepsilon}_b] := \mathcal{W} - \Phi_c, \quad \begin{cases} \mathcal{W} := \int_V \{\boldsymbol{\sigma}_b \cdot \boldsymbol{\varepsilon}_b\} dV \\ \Phi_c := \int_V \left\{ \frac{1}{2} \boldsymbol{\sigma}_b \cdot \mathbf{C}^{-1} \boldsymbol{\sigma}_b \right\} dV \end{cases} \quad (3.18a)$$

being \mathbf{C} bilinear compliance operator defining the constitutive law, that ICM assume equal to that of linear continuum and V the volume of the body in the undeformed reference configuration.

- *recovering linear solutions*

Through a corotational frame (CR) defined by a rotation $\mathbf{Q} \approx \mathbf{R}$, Biot's measure recalling (3.13) is expressed in terms of linear quantities $\bar{\boldsymbol{\sigma}}_l$, $\bar{\mathbf{E}}$ and $\bar{\mathbf{W}}$ as:

$$\boldsymbol{\sigma}_b = \bar{\boldsymbol{\sigma}}_l, \quad \boldsymbol{\varepsilon}_b \approx \bar{\mathbf{E}} + \frac{1}{2} (\bar{\mathbf{E}} \bar{\mathbf{W}} - \bar{\mathbf{W}} \bar{\mathbf{E}} - \bar{\mathbf{W}} \bar{\mathbf{W}}) \quad (3.18b)$$

When $\|\bar{\mathbf{W}}\| \ll 1$ we have also the Biot's strain is equal to linear strain tensor

$$\boldsymbol{\sigma}_b = \boldsymbol{\sigma}_l \quad , \quad \boldsymbol{\varepsilon}_b \approx \bar{\mathbf{E}} \quad (3.18c)$$

Biot's stress/strain representation therefore appear the most appropriate representations for recovering linear solutions.

- *Galerkin approximation*

When structured continua (e.g. beam, shell) are considered, linear solution stresses and displacements field are described in terms of global stress parameters $\mathbf{t}[s]$ and global kinematics parameters $\bar{\mathbf{d}}[s]$ begin s an n -dimensional abscissa depending on the model considered

$$\bar{\boldsymbol{\sigma}}_l = \bar{\boldsymbol{\sigma}}_l[\mathbf{t}] \quad , \quad \bar{\mathbf{E}} = \bar{\mathbf{E}}[\bar{\mathbf{d}}] \quad , \quad \bar{\mathbf{W}} = \bar{\mathbf{W}}[\bar{\mathbf{d}}] \quad (3.18d)$$

In the frame of a Galerkin approximation, mixed energy (3.18a) can be rewritten in terms of \mathbf{t} and $\bar{\mathbf{d}}$ as:

$$\Phi[\mathbf{t}, \mathbf{e}] = \int_s \left\{ \mathbf{t}^T \mathbf{e}[\bar{\mathbf{d}}] - \frac{1}{2} \mathbf{t}^T \mathbf{K}^{-1} \mathbf{t} \right\} ds \quad (3.18e)$$

being $\mathbf{e}[\bar{\mathbf{d}}]$ the strain work-conjugate with \mathbf{t} , \mathbf{K} a compliance operator. The constitutive law is obtained directly from (3.18e) as:

$$\mathbf{t} = \mathbf{K} \mathbf{e}[\bar{\mathbf{d}}] \quad (3.18f)$$

- *kinematics equations*

The relationships between generalized kinematical parameters $\bar{\mathbf{d}}$ in CR frame and \mathbf{d} in fixed frame complete the kinematics. The corotational transformations involve only geometrically laws depending from the particular definition of the kinematical parameters. Without loss of generality, when $\bar{\mathbf{d}} = \{\bar{\mathbf{u}}_{0,s}, \bar{\mathbf{R}}_{0,s}\}$ collects displacements and rotations derivatives of a particular point \mathbf{X}_0 of the continuum, corotational relationship assume the expressions:

$$\bar{\mathbf{u}}_{0,s} := \mathbf{Q}^T (\mathbf{X}_{0,s} + \mathbf{u}_{,s}) - \mathbf{X}_{0,s} \quad , \quad \bar{\mathbf{R}}_{0,s} := \mathbf{Q}^T \mathbf{R}_{0,s} \quad (3.18g)$$

Note that for structural model \mathbf{Q} depends on \mathbf{d} and the criteria $|\bar{\mathbf{W}}| = 0$ is, in general, satisfied only in an average. Different choice of CR frame can be done depending on the particular model at hand and on the average selection of \mathbf{Q} .

It is worth noting that the proposed method is a fully automated procedure for defining a nonlinear model, without needing any heuristic choices or at-hand approximations but only that the corresponding linear modeling

be already available. The model will satisfy exactly the objectivity requirements, apart for the rotation $\bar{\mathbf{W}}$ which is however taken within a second-order accuracy, while exploiting full detail of the linear solution. Note also that, being based on variational condition (2.1) through the mixed and a separate description for both the stress and the displacement fields, it provides a mixed approximate solution, the approximation error being however related to residual rotation $\bar{\mathbf{W}}$.

Chapter 4

Some tutorial implementation of ICM

To better illustrate the Implicit Corotational Method (ICM), it is convenient to start discussing its implementation in some simple tutorial contexts, in order to clarify how it can be actually implemented and what is the accuracy we can expect.

4.1 Planar beam in bending and shear

Consider a rectangular planar beam, with a cross section of area A and inertia J and denote with s a material abscissa along the beam axis.

4.1.1 Recovering linear solutions

A linear solution is provided in this case by Saint Venant–Jourasky (SV) theory. The solution is referred to an appropriate corotational reference system rotated by $\mathbf{Q} = \mathbf{Q}[\alpha]$, defined in this simple case by angle α , following the current section motion s , so that for $x = 0$ we have the quantities evaluated at s .

The linear stress tensor $\bar{\boldsymbol{\sigma}}_l[\mathbf{t}]$ given by SV solution is defined in current section ($x = 0$) as:

$$\boldsymbol{\sigma}_l[\mathbf{t}] := \begin{bmatrix} \bar{\sigma}[y] & \bar{\tau}[y] \\ \text{sym.} & 0 \end{bmatrix} \quad , \quad \begin{cases} \bar{\sigma}[y] = \frac{1}{A}N - \frac{y}{J}M \\ \bar{\tau}[y] = \frac{\psi_{,y}[y]}{A}T \end{cases} \quad (4.1a)$$

where $\psi[y]$ is the stress function expressed in this case as

$$\psi := \frac{3h^2y - 4y^3}{2h^3} \quad , \quad \int_S \psi \, dA = 0 \quad , \quad \int_S \psi_{,y} \, dA = A \quad (4.1b)$$

and the generalized stress $\mathbf{t} = \{N, T, M\}^T$ are the axial, shear and flexural strengths defined as

$$N[s] := \int_S \bar{\sigma}[y] dA \quad , \quad T[s] := \int_S \bar{\tau}[y] dA \quad , \quad M[s] := \int_S y \bar{\sigma}[y] dA \quad (4.1c)$$

The kinematics of SV solution is assumed in CR frame. The solution provides for the displacements field

$$\bar{\mathbf{u}}[x, y] := \begin{bmatrix} \bar{\varepsilon} x - (\bar{\varphi} + \bar{\chi} x)y + \bar{w}[y]\bar{\gamma} \\ (\bar{\gamma} + \bar{\varphi})x + \frac{1}{2} \bar{\chi} x^2 \end{bmatrix} \quad (4.2a)$$

where $\bar{\mathbf{d}} = \{\bar{\varepsilon}, \bar{\gamma}, \bar{\chi}\}$ are generalized strain parameters work-conjugate in SV solution with stress $\mathbf{t} = \{N, T, M\}$, $\bar{w}[y]$ is the warping function defined by

$$\bar{w}[y] := \frac{\psi}{k} - y \quad , \quad k := \frac{1}{A} \int_S \psi_{,y}^2 dA = \frac{6}{5} \quad (4.2b)$$

k being the shear factor. The evaluation of displacement gradient from (4.2a) gives, for the current section ($x=0$), in components for its symmetric and skew-symmetric part:

$$\bar{\mathbf{E}}[\bar{\mathbf{d}}] = \begin{bmatrix} \bar{\varepsilon} - \bar{\chi} y & \bar{\gamma} \psi_{,y}/2k \\ \text{sym.} & 0 \end{bmatrix} \quad , \quad \bar{\mathbf{W}}[\bar{\mathbf{d}}] = \begin{bmatrix} 0 & -\bar{\varphi} - (1 - \psi_{,y}/2k)\bar{\gamma} \\ \text{skew} & 0 \end{bmatrix} \quad (4.2c)$$

Introducing vectors

$$\bar{\boldsymbol{\varepsilon}} := \begin{bmatrix} \bar{\varepsilon} \\ \bar{\gamma} \end{bmatrix} \quad , \quad \bar{\boldsymbol{\chi}} := \begin{bmatrix} 0 & -\bar{\chi} \\ \bar{\chi} & 0 \end{bmatrix} \quad , \quad \mathbf{X} := \begin{bmatrix} x \\ y \end{bmatrix} \quad , \quad \mathbf{X}_0 := \begin{bmatrix} 0 \\ y \end{bmatrix} \quad (4.2d)$$

gradient of deformation (4.2c) can be also rewritten

$$\nabla \bar{\mathbf{u}}[\bar{\mathbf{d}}] = [\bar{\boldsymbol{\varepsilon}} + \bar{\boldsymbol{\chi}}(\mathbf{X} - \mathbf{X}_0)] \otimes \mathbf{e}_1 + \bar{\mathbf{W}}_0 + \bar{w}_{,y}[y] \mathbf{e}_1 \otimes \mathbf{e}_2 \quad (4.2e)$$

4.1.2 Galerkin approximation

As stated in the previous sections, we will assume that the Biot's stress field be directly described by eq. (4.1), then assuming:

$$\boldsymbol{\sigma}_b = \boldsymbol{\sigma}_l[\mathbf{t}]$$

and substituting into (3.18a), we obtain on the current section

$$\Phi_c := \frac{1}{2} \left(\frac{N^2}{EA} + \frac{k T^2}{GA} + \frac{M^2}{EJ} \right) \quad (4.3a)$$

Conversely, assuming for the symmetric and skew-symmetric part of displacements gradients into (3.18b) be coincident with those defined by eq. (4.2e)

$$\bar{\mathbf{E}} = \bar{\mathbf{E}}[\bar{\mathbf{d}}] \quad , \quad \bar{\mathbf{W}} = \bar{\mathbf{W}}[\bar{\mathbf{d}}]$$

and evaluating the Biot's strain ε_b using (3.18b), the internal work (3.18a) provides on the current section:

$$\mathcal{W} := N \varepsilon + T \gamma + M \chi \quad (4.3b)$$

where ε , γ and χ are defined by:

$$\varepsilon := \bar{\varepsilon} + \frac{19}{48} \bar{\gamma}^2 + \bar{\varphi} \left(\frac{1}{2} \bar{\varphi} + \bar{\gamma} \right), \quad \gamma := \bar{\gamma} - \bar{\varepsilon} \left(\bar{\varphi} + \frac{1}{2} \bar{\gamma} \right), \quad \chi := \bar{\chi} \quad (4.3c)$$

By relating expressions (4.3a) and (4.3b) through the Clapeyron's equivalence $2\Phi_c = \mathcal{W}$, we also obtain

$$N = EA \varepsilon \quad , \quad T = \frac{1}{k} GA \gamma \quad , \quad M = EJ \chi \quad (4.4)$$

which provides the elastic laws for the nonlinear model.

4.1.3 Kinematic equations

Eqs.(4.3) provide the explicit expressions for the local contribution of the current section s to the energy terms. The energy is locally defined by generalized strain $\bar{\varepsilon}$ and $\bar{\chi}$. The nonlinear beam model is completed by kinematics strain–displacements relationship. Introducing average displacements $\bar{\mathbf{u}}_0$ and rotations $\bar{\mathbf{W}}_0$ of current section

$$\bar{\mathbf{u}}_0 := \frac{1}{A} \int_A \bar{\mathbf{u}}[x, y] dA, \quad \bar{\mathbf{W}}_0[\bar{\varphi}] := \frac{1}{J} \int_A (\mathbf{X} - \mathbf{X}_0) \wedge \bar{\mathbf{u}}[x, y] dA \quad (4.5)$$

the SV displacements field (4.2a) can be rewritten as composed by a rigid body motion of the section described by average displacements $\bar{\mathbf{u}}_0$ and rotations $\bar{\mathbf{R}}_0[\bar{\varphi}]$, that in CR we can assume small $\bar{\mathbf{R}}_0 \approx \mathbf{I} + \bar{\mathbf{W}}_0[\bar{\varphi}]$ and by an out–plane warping $\bar{\mathbf{u}}_w$:

$$\bar{\mathbf{u}}[x, y] := \bar{\mathbf{u}}_0 + \bar{\mathbf{W}}_0(\mathbf{X} - \mathbf{X}_0) + \bar{\mathbf{u}}_w \quad (4.6)$$

then recalling (4.2d) hold that:

$$\bar{\varepsilon} := \bar{\mathbf{u}}_{0,s} - \bar{\mathbf{W}}_0 \mathbf{e}_1, \quad \bar{\chi} := \bar{\mathbf{W}}_{0,s} \quad (4.7)$$

Introducing in global fixed frame the displacements \mathbf{u}_0 and rotations $\mathbf{R}_0[\varphi]$ corresponding corotational displacements $\bar{\mathbf{u}}_0$ and rotations $\bar{\mathbf{R}}_0[\bar{\varphi}]$ in CR frame defined by $\mathbf{Q}[\alpha]$, using (3.18g) we have:

$$\bar{\varepsilon} := \mathbf{Q}^T(\mathbf{u}_{0,s} + \mathbf{e}_1) - \mathbf{e}_1 - (\mathbf{Q}^T \mathbf{R}_0 - \mathbf{I}) \mathbf{e}_1, \quad \bar{\chi} := \mathbf{R}_0^T \mathbf{R}_{0,s} \quad (4.8a)$$

Splitting the rotation \mathbf{Q} as:

$$\mathbf{Q}[\alpha] = \mathbf{R}_0[\varphi] \bar{\mathbf{Q}}[\bar{\alpha}], \quad \alpha = \varphi + \bar{\alpha} \quad (4.8b)$$

the expression of $\bar{\boldsymbol{\varepsilon}}$ into (4.8) can be rearranged as:

$$\bar{\boldsymbol{\varepsilon}} := \bar{\mathbf{Q}}^T \bar{\boldsymbol{\varepsilon}}_0, \quad \bar{\boldsymbol{\varepsilon}}_0 := \mathbf{R}_0^T(\mathbf{u}_{0,s} + \mathbf{e}_1) - \mathbf{e}_1 \quad (4.8c)$$

if the approximate expression is used we have that

$$\bar{\boldsymbol{\varepsilon}} := \bar{\mathbf{Q}}^T(\bar{\boldsymbol{\varepsilon}}_0 + \mathbf{e}_1) - \mathbf{e}_1 + \bar{\alpha} \mathbf{e}_2 \quad (4.8d)$$

finally in components for deformation $\bar{\boldsymbol{\varepsilon}}$ and $\bar{\chi}$

$$\begin{cases} \bar{\varepsilon} = (u_{,s} + 1) \cos \alpha + v_{,s} \sin \alpha - \cos(\varphi - \alpha) \\ \bar{\gamma} = v_{,s} \cos \alpha - (u_{,s} + 1) \sin \alpha - \sin(\varphi - \alpha) \\ \bar{\chi} = \varphi_{,s} \end{cases} \quad (4.8e)$$

while for local rotations

$$\bar{\varphi} = \varphi - \alpha \quad (4.8f)$$

4.1.4 Corotational setup

ICM is completed by the choice of rotation $\mathbf{Q}[\alpha]$, or simply in this case the angle α , defining CR frame. The general idea is to select the CR frame so that $|\bar{\mathbf{W}}| \ll 1$ almost on average. Two possible choices will be discussed in order to make clear how the setup of CR frame affects the beam nonlinear model.

1. A first choice is to setup the CR frame \mathbf{Q} zeroing in the $\bar{\mathbf{W}}[\bar{\mathbf{d}}]$ the contribution due to rotation of the cross section, this corresponds to the conditions:

$$\bar{\mathbf{W}}_0 = \mathbf{0}, \quad \bar{\varphi} = 0 \quad (4.9a)$$

and using (4.8f), this choice corresponds to assume:

$$\mathbf{Q}[\alpha] = \mathbf{R}_0[\varphi], \quad \alpha = \varphi \quad (4.9b)$$

Nonlinear kinematics relationships (4.8c) particularize as:

$$\bar{\boldsymbol{\varepsilon}} = \bar{\boldsymbol{\varepsilon}}_0, \quad \bar{\mathbf{Q}}[\bar{\alpha}] = \mathbf{0}$$

and then for strains (4.3c) hold:

$$\boldsymbol{\varepsilon} := \bar{\boldsymbol{\varepsilon}}_0 + \frac{19}{48} \bar{\gamma}_0^2, \quad \boldsymbol{\gamma} := \bar{\boldsymbol{\gamma}}_0 - \frac{1}{2} \bar{\boldsymbol{\varepsilon}}_0 \bar{\boldsymbol{\gamma}}_0, \quad \boldsymbol{\chi} := \bar{\boldsymbol{\chi}} \quad (4.9c)$$

and when warping is neglected $w[y] \approx 0$:

$$\varepsilon := \bar{\varepsilon}_0 + \frac{3}{8}\bar{\gamma}_0^2, \quad \gamma := \bar{\gamma}_0 - \frac{1}{2}\bar{\varepsilon}_0\bar{\gamma}_0, \quad \chi := \bar{\chi} \quad (4.9d)$$

The skew-symmetric part of the displacements gradient (4.2c) particularize as:

$$\bar{\mathbf{W}}[\bar{\mathbf{d}}] = \begin{bmatrix} 0 & \frac{1}{2}(\bar{w}_{,y}-1)\bar{\gamma}_0 \\ \text{skew} & 0 \end{bmatrix} \quad (4.9e)$$

thereby, the average rotations due to the shear deformation, with an amplitude $\bar{\gamma}/2$, and the contribution due to the warping is not accounting into CR frame but using quadratic expression of Biot's strain (3.18b). The total average rotation accounting for the model is then $\varphi + \bar{\gamma}/2$.

2. A more refined choice could be that of zeroing $\bar{\mathbf{W}}[\bar{\mathbf{d}}]$ in weighted average, i.e.

$$\int_{\bar{S}} \psi_{,y} (-\bar{\varphi} - (1 - \psi_{,y}/2k)) dA = 0 \quad (4.10a)$$

which provides

$$\bar{\varphi} = -\bar{\gamma}/2 \quad (4.10b)$$

Substituting (4.8f) and (4.3c) into (4.10b), holds

$$\sin(\varphi - \alpha) + v_{,s} \cos \alpha - (u_{,s} + 1) \sin \alpha = 0 \quad (4.10c)$$

which provide the condition on α . Using (4.8b) previous condition becomes

$$\sin \bar{\alpha} + (\bar{\varepsilon}_0 + 1) \sin \bar{\alpha} - \bar{\gamma}_0 \cos \bar{\alpha} \quad (4.10d)$$

and solving

$$\bar{\alpha} = \arctan \frac{\bar{\gamma}_0}{2 + \bar{\varepsilon}_0}$$

finally total rotation accounted by CR frame is

$$\alpha = \varphi + \bar{\alpha} = \varphi + \arctan \frac{\bar{\gamma}_0}{2 + \bar{\varepsilon}_0}$$

For this case the the skew-symmetric part of gradient of deformation (4.2c) particularize as:

$$\bar{\mathbf{W}}[\bar{\mathbf{d}}] = \begin{bmatrix} 0 & \frac{1}{2}\bar{w}_{,y}\bar{\gamma} \\ \text{skew} & 0 \end{bmatrix} \quad (4.10e)$$

and then includes only the point wise rotation due the the warping that is not filtered by CR frame. The quadratic formula (3.18b) allows

to accounting the point wise rotations (4.10e), and gives for the strain measures (4.3c):

$$\varepsilon := \bar{\varepsilon} + \frac{1}{48}\bar{\gamma}^2, \quad \gamma := \bar{\gamma}, \quad \chi := \bar{\chi} \quad (4.10f)$$

Note that when warping is neglected $w[y] \approx 0$, this choice allows to zeroing for each point $\bar{\mathbf{W}}[\bar{\mathbf{d}}] \approx \mathbf{0}$ moreover terms $\bar{\gamma}^2/48$ into (4.10) disappears and we have

$$\varepsilon := \bar{\varepsilon}, \quad \gamma := \bar{\gamma}, \quad \chi := \bar{\chi} \quad (4.10g)$$

$$\bar{\varepsilon} = \bar{\mathbf{Q}}^T \bar{\varepsilon}_0 \quad (4.11)$$

if is used the approximate formula

$$\bar{\varepsilon} := \bar{\mathbf{Q}}^T (\bar{\varepsilon}_0 + \mathbf{e}_1) - \mathbf{e}_1 + (\bar{\alpha})\mathbf{e}_2 \quad (4.12)$$

The two different choice differs only in the accounting of average rotation to due shear deformation $\bar{\gamma}$. The first choice account rotations $\bar{\gamma}/2$ using quadratic expression (3.18b) and then rotations $\bar{\gamma}/2$ is treated in approximate way. The second choice accounting the rotations $\bar{\gamma}/2$ directly in CR frame and so is treated as finite rotations. It is easy to check that latter expressions (4.9) coincide with eq. (4.10) if the strain measure ε, γ are rotated by an angle of amplitude $\bar{\gamma}/2$, than the two choices $\bar{\varphi} = -\bar{\gamma}/2$ and $\bar{\varphi} = 0$ provide equivalent results within the assumption $\bar{\gamma} \ll 1$. The second choice is generally is however complicated in the solution of condition for setup the CR frame in particular when finite 3D rotation are involved, then in the following the CR frame will be setup using the first strategy.

4.1.5 Further insights

Some considerations can be useful.

1. To better clarify the ICM, we discuss the case of nonlinear beam model with rigid cross-section with regard to the kinematics. The displacement field can be written as:

$$\mathbf{u} := \mathbf{u}_0 + (\mathbf{R}_0 - \mathbf{I})(\mathbf{X} - \mathbf{X}_0) \quad (4.13a)$$

The evaluation of displacements gradient starting from the latter gives

$$\mathbf{F} = \mathbf{R}_0 [(\bar{\varepsilon} + \bar{\chi}(\mathbf{X} - \mathbf{X}_0)) \otimes \mathbf{e}_1 + \mathbf{I}] \quad (4.13b)$$

being

$$\bar{\varepsilon} := \mathbf{R}_0^T (\mathbf{u}_{0,s} + \mathbf{e}_1) - \mathbf{e}_1, \quad \bar{\chi} := \mathbf{R}_0^T \mathbf{R}_{0,s} \quad (4.13c)$$

In CR frame rotated by $\mathbf{Q} \equiv \mathbf{R}_0$ deformation gradient (4.13b) becomes

$$\bar{\mathbf{F}} = \mathbf{R}_0^T \mathbf{F} = (\bar{\varepsilon} + \bar{\chi}(\mathbf{X} - \mathbf{X}_0)) \otimes \mathbf{e}_1 + \mathbf{I} \quad (4.13d)$$

or alternatively in components:

$$\bar{\mathbf{F}} = \begin{bmatrix} \bar{\varepsilon} + 1 - \bar{\chi}y & 0 \\ \bar{\gamma} & 1 \end{bmatrix}, \quad \begin{cases} \bar{\varepsilon} = (u_{,s} + 1) \cos \varphi + v_{,s} \sin \varphi - 1 \\ \bar{\gamma} = v_{,s} \cos \varphi - (u_{,s} + 1) \sin \varphi \\ \bar{\chi} = \varphi_{,s} \end{cases} \quad (4.13e)$$

The Biot strain for this case can be evaluated exactly, in particular hold

$$\varepsilon_b = \bar{\mathbf{R}}_0^T \bar{\mathbf{F}} \quad (4.13f)$$

being

$$\bar{\mathbf{R}}_0 = \bar{\mathbf{R}}_0[\bar{\alpha}] \quad , \quad \bar{\alpha} = \arctan \frac{\bar{\gamma}}{2 + \bar{\varepsilon} - y\bar{\chi}} \quad (4.13g)$$

Then the polar decomposition rotation $\mathbf{R}[\alpha]$ can be written as:

$$\mathbf{R}[\alpha] = \mathbf{R}_0 \bar{\mathbf{R}}_0 \quad , \quad \alpha = \varphi + \bar{\alpha} \quad (4.13h)$$

Using a linearized kinematics for the beam model, neglecting out-plane warping, the gradient of deformation in a CR frame rotated by $\mathbf{Q} = \mathbf{R}_0$ recalling (4.2e) is

$$\bar{\mathbf{F}} = (\bar{\varepsilon} + \bar{\chi}(\mathbf{X} - \mathbf{X}_0)) \otimes \mathbf{e}_1 + \mathbf{I} \quad (4.14)$$

thereby recalling CR transformation relationships (3.18g), the latter coincides with these evaluated using finite kinematics (4.13d). When approximate expression (3.18b) is used for the evaluation of Biot's strain, a linearization of polar decomposition rotation on CR frame is used:

$$\bar{\mathbf{R}}_0 \approx \mathbf{I} + \bar{\mathbf{W}} \quad , \quad \bar{\alpha} \approx \frac{1}{2} \bar{\gamma} \quad (4.15)$$

however a quadratic accuracy for Biot's strain is recovered (4.13f)

$$\varepsilon_b = \bar{\mathbf{R}}_0^T \bar{\mathbf{F}} \approx \begin{bmatrix} \bar{\varepsilon} - y\bar{\chi} + \frac{3}{8}\bar{\gamma}^2 & \frac{1}{2}\bar{\gamma} - \frac{1}{4}\bar{\gamma}\bar{\varepsilon} + \frac{1}{4}y\bar{\gamma}\bar{\chi} \\ \text{sym.} & -\frac{1}{8}\bar{\gamma}^2 \end{bmatrix} \quad (4.16)$$

- Assuming $\bar{\varphi} \approx \bar{\gamma} \approx 0$ and, consequently, $\bar{\mathbf{W}}[\bar{\mathbf{d}}] \approx \mathbf{0}$ and $\varepsilon_b \approx \bar{\mathbf{E}}[\bar{\mathbf{d}}]$, we obtain a direct identification of the linear solution for both the stress and the strain fields. The ICM beam kinematics (4.8) reduces to the well known Antman's beam kinematics [46]:

$$\begin{cases} \varepsilon = (1 + u_{,s}) \cos \varphi + v_{,s} \sin \varphi - 1 \\ \gamma = v_{,s} \cos \varphi - (1 + u_{,s}) \sin \varphi \\ \chi = \varphi_{,s} \end{cases} \quad (4.17)$$

3. By neglecting shear deformation at all, i.e. assuming $\bar{\gamma} := 0$, we can use the condition $\gamma = 0$ in the second of eqs. (4.17) for relating φ to $u_{,s}$ and $v_{,s}$. By some algebra, eqs. (4.17) become

$$\begin{cases} \varepsilon = \sqrt{(1 + u_{,s})^2 + v_{,s}^2} - 1 \\ \chi = \frac{v_{,ss} + v_{,ss} u_{,s} - v_{,s} u_{,ss}}{\sqrt{(1 + u_{,s})^2 + v_{,s}^2}} \end{cases} \quad (4.18)$$

that coincide with the kinematic relationships developed by Nayfeh and Pai in [95]. We can further mention that, accepting an error $\mathcal{O}^3(\varepsilon \gamma)$, previous equations can be simplified into

$$\begin{cases} \varepsilon \approx u_{,s} + \frac{1}{2} (u_{,s}^2 + v_{,s}^2) \\ \chi \approx v_{,ss} + v_{,ss} u_{,s} - u_{,ss} v_{,s} \end{cases} \quad (4.19)$$

which have been proposed and used in [103].

4. All previous variants only differ in the treatment of shear deformation γ . When, as generally can be assumed for slender beams, $\gamma \ll 1$ their differences become negligible. So expressions (4.10) and (4.17)–(4.19) can be considered as equivalent for practical purposes.
5. In some cases, we can assume $\varphi \ll 1$ and so make the local frame coincident with the global one. Taking $\varphi = 0$ and $\bar{\gamma} \ll \varphi$, $\bar{\varepsilon} \ll 1$ into (4.8) and (4.2e), are further simplified into

$$\begin{cases} \varepsilon = u_{,s} + \frac{1}{2} v_{,s}^2 \\ \chi = v_{,ss} \end{cases} \quad (4.20)$$

corresponding to the standard $2nd$ -order kinematics used in simplified modelings. Eqs. (4.20) could represent an acceptable compromise when working within an Updated Lagrangean or a Standard Corotational approach where the reference frame is continuously updated with the current configuration of the element, e.g. see [102].

6. The stress parameters N , T , implicitly defined by eq. (4.1c), do not coincide in general to the strengths \bar{F}_x and \bar{F}_y defined as components, in x and y direction, of the stress section resultant, nor they coincide with the normal and tangential resultants to the section. Analogously, the parameter M does not coincide (in general) to the resulting couple \bar{M} . Due to eq. (4.1c), from the virtual work condition

$$N \delta\varepsilon + T \delta\gamma + M \delta\chi = \bar{F}_x \delta\bar{\varepsilon} + \bar{F}_y \delta\bar{\gamma} + \bar{M} \delta\bar{\chi}$$

we obtain the relations

$$\bar{F}_x = N \quad , \quad \bar{F}_y = T + \frac{1}{24}\bar{\gamma}N \quad , \quad \bar{M} = M \quad (4.21)$$

It is worth mentioning that the same expressions can be obtained by integrating the normal and tangential components of the Biot's stresses:

$$\begin{aligned} \bar{F}_x &= \int_{\bar{S}} \left(\sigma_{xx} - \sigma_{xy} \frac{(k - \psi_{,y}) \bar{\gamma}}{2k} \right) dA \\ \bar{F}_f &= \int_{\bar{S}} \left(\sigma_{xx} \frac{(k - \psi_{,y}) \bar{\gamma}}{2k} + \sigma_{xy} \right) dA \end{aligned}$$

Terms $\frac{1}{48}\bar{\gamma}^2$ and $\frac{1}{24}\bar{\gamma}N$ appearing in eqs. (4.10) and (4.21) both derive from the warping function (4.2b). By neglecting the warping, assuming $w[y] = 0$, both term be canceled.

4.2 Thin walled beam subjected to axial force and torsion

Consider the spatial beam, width a thin-walled cross-shaped section and subjected to axial force and torsion, shown in fig. ??, the section thickness t being small when compared with its size h . As in the previous case, we will denote with s a material abscissa along the beam axis and by $u[s]$, $\varphi[s]$ and by $\bar{u}[s]$, $\bar{\varphi}[s]$ the average axial displacement and torsional rotation of the current section S referred to a global fixed frame $\{\mathbf{e}_1, \mathbf{e}_2, \mathbf{e}_3\}$ and a local corotational frame $\{\mathbf{i}_1, \mathbf{i}_2, \mathbf{i}_3\}$, respectively.

4.2.1 Recovering linear solution

We start, as before, recalling Saint Venant linear solution $\bar{\sigma}_l[\mathbf{t}]$. By assuming $t \ll h$ and denoting with $\bar{\sigma}_{xx}[x, y, z]$, $\bar{\sigma}_{xy}[x, y, z]$ and $\bar{\sigma}_{xz}[x, y, z]$ the relevant components of the stress field in the local frame, the solution is locally given by

$$\bar{\sigma}_{xx} = \frac{N}{A} \quad , \quad \bar{\sigma}_{xy} = (2\psi[y, z]_{,y} - z) \frac{M}{J_t} \quad , \quad \bar{\sigma}_{xz} = (2\psi[y, z]_{,z} + y) \frac{M}{J_t} \quad (4.22a)$$

where $A \approx 2bt$ and $J_t \approx 2t^3b/3$ are the area and torsional inertia of the section, $\mathbf{t} := [N, M]^T$ are the strength resultant on S

$$N := \int_S \bar{\sigma}_{xx} dA \quad , \quad M := \int_S (\bar{\sigma}_{xz} y - \bar{\sigma}_{xy} z) dA \quad (4.22b)$$

and $\psi[y, z]$ is the stress function, that can be evaluated as

$$\psi[y, z] \approx \begin{cases} \frac{1}{2} x y & \text{if } y \ll t \\ -\frac{1}{2} x y & \text{if } z \ll t \end{cases} \quad (4.22c)$$

and J_t is the so called torsional inertia of the section, defined by

$$J_t := \int_S \{(2\psi[y, z]_{,y} - z)^2 + (2\psi[y, z]_{,z} + y)^2\} dA \approx \frac{2}{3} t^3 h$$

Furthermore, denoting with $\bar{\mathbf{u}}[x, y, z]$, the displacement field by reference to the corotational frame, these are locally given by:

$$\bar{\mathbf{u}}[x, y, z] := \begin{bmatrix} \bar{\varepsilon} x + \bar{\chi} w[y, z] \\ -z \bar{\varphi} \\ y \bar{\varphi} \end{bmatrix} \quad (4.23a)$$

being $\bar{\mathbf{d}} := [\bar{\varepsilon}, \bar{\chi}]^T$ generalized strains work-conjugate in SV solution with generalized strain \mathbf{t} and $w[y, z]$ the warping function obtained solving the problem

$$w[y, z]_{,y} = 2\psi[y, z]_{,y} \quad , \quad w[y, z]_{,z} = 2\psi[y, z]_{,z} \quad (4.23b)$$

The previous expressions allow to recover the displacement gradient $\nabla \bar{\mathbf{u}}[\bar{\mathbf{d}}] = \mathbf{E}[\bar{\mathbf{d}}] + \mathbf{W}[\bar{\mathbf{d}}]$ field on the current section ($x=0$):

$$\bar{\mathbf{E}}[\bar{\mathbf{d}}] = \begin{bmatrix} \bar{\varepsilon}_{,s} & (\psi_{,y} - \frac{1}{2} z) \bar{\chi} & (\psi_{,z} + \frac{1}{2} y) \bar{\chi} \\ (\psi_{,y} - \frac{1}{2} z) \bar{\chi} & 0 & 0 \\ (\psi_{,z} - \frac{1}{2} y) \bar{\chi} & 0 & 0 \end{bmatrix} \quad (4.24a)$$

$$\bar{\mathbf{W}}[\bar{\mathbf{d}}] = \begin{bmatrix} 0 & (\frac{1}{2} z + \psi_{,y}) \bar{\chi} & -(\frac{1}{2} y - \psi_{,z}) \bar{\chi} \\ -(\frac{1}{2} z + \psi_{,y}) \bar{\chi} & 0 & 0 \\ (\frac{1}{2} y - \psi_{,z}) \bar{\chi} & 0 & 0 \end{bmatrix} \quad (4.24b)$$

4.2.2 Galerkin approximation

As before, we assume that the Biot's stress field $\boldsymbol{\sigma}_b$ will be directly described by the linear solution (4.22) $\bar{\boldsymbol{\sigma}}_l$. We obtain therefore

$$\Phi_c := \frac{1}{2} \left(\frac{N}{EA} + \frac{M}{GJ} \right) \quad (4.25)$$

The Biot's strain field is obtained by substituting expressions (4.24a) and (4.24b) into (3.18b). The evaluation of internal work provides

$$\mathcal{W} := N\varepsilon + M\chi \quad (4.26)$$

where

$$\varepsilon = \bar{\varepsilon} + \frac{1}{2} \frac{J_p}{A} \bar{\chi}^2 \quad , \quad \chi = \bar{\chi} \quad , \quad J_p = \int_S (y^2 + z^2) dA = \frac{1}{6} t b^3 \quad (4.27)$$

By relating expressions (4.25) and (4.26) through the Clapeyron's equivalence $2\Phi_c = \mathcal{W}$, we also obtain

$$N = EA\varepsilon \quad , \quad M = GJ\chi \quad (4.28)$$

which provides the elastic laws for the beam model.

4.2.3 Kinematics equations

Local kinematics provides the following local kinematics relationships

$$\bar{\varepsilon} := \bar{u}_{,s} \quad , \quad \bar{\chi} := \bar{\varphi}_{,s} \quad (4.29)$$

The corotational change for this case give for global strains (4.27)

$$\varepsilon = u_{,s} + \frac{1}{2} \frac{J_p}{A} \varphi_{,s}^2 \quad , \quad \chi = \varphi_{,s} \quad (4.30)$$

which defines the beam nonlinear kinematics and completes the definition of the nonlinear beam model.

It is worth mentioning that, expression (4.30), which coincides with that derived by Wagner in its study of beams in torsion [16], implies a coupling between axial elongation and torsional curvature. This effect comes from taking into account the section warping and is completely obliged in approaches as that of Simo [35] or Nayfeh and Pai [95] which are based on a rigid motion kinematics of the section. Note however that, at least in presence of torsion and thin-walled sections, warping is more due to the helicoid distortion due to torsion.

4.3 Some further considerations

Note that the ICM model is derived through a two-steps process. In the first step the corotational change (3.18g) is used to refer kinematical parameters to an appropriate reference frame, the second one is based on the use of stress and strain fields directly derived from a linear solution. While the former, being based on exact kinematics, does not introduce any approximation, the latter, which actually extend the linear solution in a nonlinear range, is affected by some approximations which came from the pointwise differences between the Biot's strains derived from the displacement field and those recovered from the stress field through the elastic laws. The error

came however as a second-order consequence of the warping, so it and can be generally neglected, especially if considering that the stress and displacement fields derived from the linear solution will be used into a mixed energy formulation, so the pointwise error is zeroed in the average, and the final error in the nonlinear modeling is consequently largely reduced.

In the discussed examples the linear solution as been derived from the Saint Venant rod theory. So the ICM model inherits all the approximations contained in this theory. More refined model can be obtained, by the same procedure, from more sophisticate theories, as those by Vlasov [17].

In absence of torsional distortions, the warping is only due to the tangential deformation γ so its effect is very small and can be generally neglected.

Chapter 5

Nonlinear 3D beam model based on Saint Venant general rod theory

The ICM is now applied in order to recover a nonlinear 3D beam model completely reusing the Saint Venant general rod theory [13]. The beam is referred to a local baricentric Cartesian system $\{x, y, z\}$ aligned according to the principal directions of the current section $\bar{S} := S[s]$. We will denote with $\bar{\Gamma}$ the cross-section contour and with $\bar{\mathbf{n}} = [n_y, n_z]$ its normal in the $\{y, z\}$ plane.

5.1 Recovering linear solution–stress

Exploiting Saint Venant solution results, the nonzero stress components $\bar{\sigma}_{xx}$, $\bar{\sigma}_{xy}$ and $\bar{\sigma}_{xz}$ are, in the current section s , expressed in terms of six strength parameters collected in the vectors $\mathbf{t}_\sigma := \{N_x, M_y, M_z\}^T$ and $\mathbf{t}_\tau := \{M_x, T_y, T_z\}^T$, as:

$$\bar{\boldsymbol{\sigma}}_l = \begin{bmatrix} \bar{\sigma} & \bar{\boldsymbol{\tau}}^T \\ \bar{\boldsymbol{\tau}} & \mathbf{0} \end{bmatrix}, \quad \begin{cases} \bar{\sigma} = \mathbf{D}_\sigma \mathbf{t}_\sigma \\ \bar{\boldsymbol{\tau}} = \mathbf{D}_\tau \mathbf{t}_\tau \end{cases}, \quad \begin{aligned} \mathbf{D}_\sigma &:= \begin{bmatrix} \frac{1}{A} & \frac{z}{J_y} & -\frac{y}{J_z} \end{bmatrix} \\ \mathbf{D}_\tau &:= \begin{bmatrix} \mathbf{d}_x & \mathbf{d}_y & \mathbf{d}_z \end{bmatrix} \end{aligned} \quad (5.1a)$$

where $\bar{\sigma} := \bar{\sigma}_{xx}$ and $\bar{\boldsymbol{\tau}} := [\bar{\sigma}_{xy}, \bar{\sigma}_{xz}]^T$ collects the shear components,

$$A := \int_{\bar{S}} dA, \quad J_y := \int_{\bar{S}} z^2 dA, \quad J_z := \int_{\bar{S}} y^2 dA$$

are the area and the inertias of the section. Vectors $\mathbf{d}_x, \mathbf{d}_y, \mathbf{d}_z$ are defined as

$$\mathbf{d}_x := (\nabla\psi_x - \mathbf{b}_x)/r_x, \quad \mathbf{d}_y := \nabla\psi_y - \mathbf{b}_y - r_y \mathbf{d}_x, \quad \mathbf{d}_z := \nabla\psi_z - \mathbf{b}_z - r_z \mathbf{d}_x \quad (5.1b)$$

where stress functions

$$\psi[y, z] := m \psi_x[y, z] + T_y \psi_y[y, z] + T_z \psi_z[y, z] \quad (5.1c)$$

is provided by the solutions of the Laplace/Neumann differential problem:

$$\begin{cases} \psi_{j,yy} + \psi_{j,zz} = 0 & \{y, z\} \in \bar{S} \\ \psi_{j,n} = \mathbf{b}_j^T \bar{\mathbf{n}} & \{y, z\} \in \bar{\Gamma} \end{cases} \quad (5.1d)$$

being $j = x, y, z$, vectors \mathbf{b}_j defined as

$$\mathbf{b}_x = \frac{1}{2} \begin{bmatrix} z \\ -y \end{bmatrix}, \quad \mathbf{b}_y = \frac{1}{2J_z} \begin{bmatrix} y^2 - \frac{\nu}{1+\nu} z^2 \\ 0 \end{bmatrix}, \quad \mathbf{b}_z = \frac{1}{2J_y} \begin{bmatrix} 0 \\ z^2 - \frac{\nu}{1+\nu} y^2 \end{bmatrix} \quad (5.1e)$$

and m given by

$$m = \frac{1}{r_x} (M_x - r_y T_y - r_z T_z), \quad r_j = 2 \int_{\bar{S}} (\mathbf{b}_j - \nabla \psi_j)^T \mathbf{b}_x dA \quad (5.1f)$$

Numerical solution of eq.(5.1d) are easily obtained through either finite element [93]. We obtain, by some algebra,

$$N = \int_{\bar{S}} \bar{\sigma} dA, \quad T_y = \int_{\bar{S}} \bar{\tau}_y dA, \quad T_z = \int_{\bar{S}} \bar{\tau}_z dA \quad (5.2a)$$

$$M_t = \int_{\bar{S}} (y \bar{\tau}_z - z \bar{\tau}_y) dA, \quad M_y = \int_{\bar{S}} z \bar{\sigma} dA, \quad M_z = - \int_{\bar{S}} y \bar{\sigma} dA \quad (5.2b)$$

so recovering the standard definition for the strength parameters.

5.2 Recovering linear solution–kinematics

The displacement field $\bar{\mathbf{u}}[x, y, z]$ is provided by Saint Venant solution and as function of six deformational parameters $\bar{\boldsymbol{\varepsilon}}_\sigma := \{\bar{\varepsilon}_x, \bar{\chi}_y, \bar{\chi}_z\}^T$ and $\bar{\boldsymbol{\varepsilon}}_\tau := \{\bar{\chi}_x, \bar{\gamma}_y, \bar{\gamma}_z\}^T$, in the form:

$$\begin{cases} \bar{u}_x[x, y, z] = \bar{\varepsilon}_x x - \bar{\chi}_z x y + \bar{\chi}_y x z + w[y, z] \\ \bar{u}_y[x, y, z] = \bar{\gamma}_y x + \frac{1}{2} \bar{\chi}_z x^2 - \bar{\chi}_x x z \\ \bar{u}_z[x, y, z] = \bar{\gamma}_z x - \frac{1}{2} \bar{\chi}_y x^2 + \bar{\chi}_x x y \end{cases} \quad (5.3a)$$

where $w[x, y]$ express the out-of-plane warping of the section. Evaluating the displacement gradient from eq. (5.3a), we obtain the following expressions for the symmetric and skew-symmetric components of the displacement gradient

$$\bar{\mathbf{E}} := \begin{bmatrix} \bar{\varepsilon} & \frac{1}{2} (\bar{\boldsymbol{\gamma}} + \nabla w)^T \\ \frac{1}{2} (\bar{\boldsymbol{\gamma}} + \nabla w) & \mathbf{0} \end{bmatrix}, \quad \bar{\mathbf{W}} := \begin{bmatrix} 0 & -\frac{1}{2} (\bar{\boldsymbol{\gamma}} - \nabla w)^T \\ \frac{1}{2} (\bar{\boldsymbol{\gamma}} - \nabla w) & \mathbf{0} \end{bmatrix} \quad (5.3b)$$

where

$$\begin{cases} \bar{\varepsilon} := \mathbf{A}_\epsilon \bar{\varepsilon}_\sigma \\ \bar{\gamma} := \mathbf{A}_\gamma \bar{\varepsilon}_\tau \\ \nabla w := \frac{1}{G} \boldsymbol{\tau} - \gamma \end{cases} \quad \text{with} \quad \mathbf{A}_\epsilon = \begin{bmatrix} 1 & z & -y \end{bmatrix}, \quad \mathbf{A}_\gamma = \begin{bmatrix} -z & 1 & 0 \\ y & 0 & 1 \end{bmatrix} \quad (5.3c)$$

5.3 Galerkin approximation

Following the the ICM procedure, we identify the Biot stress field with SV stress solution (5.1), and obtain the corresponding Biot strain field by entering the SV displacement solution (5.3) into formula (3.18b). Complementary energy (3.18a) becomes

$$\Phi[\boldsymbol{\sigma}, \boldsymbol{\tau}] := \frac{1}{2} (\mathbf{t}_\sigma^T \mathbf{H}_\sigma \mathbf{t}_\sigma + \mathbf{t}_\tau^T \mathbf{H}_\tau \mathbf{t}_\tau), \quad \begin{cases} \mathbf{H}_\sigma := \int_{\bar{S}} \mathbf{D}_\sigma^T \mathbf{D}_\sigma dA \\ \mathbf{H}_\tau := \int_{\bar{S}} \mathbf{D}_\tau^T \mathbf{D}_\tau dA \end{cases} \quad (5.4a)$$

while for the internal work can be splitted, using simplified linear express for Biot strain:

$$\mathcal{W} := \mathbf{t}_\sigma^T \boldsymbol{\varepsilon}_\sigma + \mathbf{t}_\tau^T \boldsymbol{\varepsilon}_\tau, \quad \boldsymbol{\varepsilon}_\sigma \equiv \bar{\varepsilon}_\sigma, \quad \boldsymbol{\varepsilon}_\tau \equiv \bar{\varepsilon}_\tau \quad (5.4b)$$

By relating expressions (5.4a) and (5.4b) though the Clapeyron's equivalence $2\Phi_c = \mathcal{W}$, we also obtain:

$$\mathbf{t}_\sigma := \mathbf{H}_\sigma^{-1} \boldsymbol{\varepsilon}_\sigma, \quad \mathbf{t}_\tau := \mathbf{H}_\tau^{-1} \boldsymbol{\varepsilon}_\tau \quad (5.5)$$

that define the elastic laws for the nonlinear beam model. For further develops it is convenient to rearrange the energy expression (5.4) in the more convenient form as:

$$\mathcal{W} = \mathbf{t}_\sigma^T \boldsymbol{\varepsilon}_\sigma + \mathbf{t}_\tau^T \boldsymbol{\varepsilon}_\tau = \mathbf{t}^T \boldsymbol{\varepsilon}, \quad \Phi_c = \frac{1}{2} (\mathbf{t}_\sigma^T \mathbf{H}_\sigma \mathbf{t}_\sigma + \mathbf{t}_\tau^T \mathbf{H}_\tau \mathbf{t}_\tau) = \frac{1}{2} \mathbf{t}^T \mathbf{H} \mathbf{t} \quad (5.6a)$$

being

$$\mathbf{t} := \begin{Bmatrix} \mathbf{n} \\ \mathbf{m} \end{Bmatrix}, \quad \boldsymbol{\varepsilon} := \begin{Bmatrix} \boldsymbol{\varepsilon} \\ \boldsymbol{\chi} \end{Bmatrix} \quad (5.6b)$$

and

$$\mathbf{n} := \begin{Bmatrix} N_x \\ T_y \\ T_z \end{Bmatrix}, \quad \mathbf{m} := \begin{Bmatrix} M_x \\ M_y \\ M_z \end{Bmatrix}, \quad \boldsymbol{\varepsilon} := \begin{Bmatrix} \bar{\varepsilon}_x \\ \bar{\gamma}_y \\ \bar{\gamma}_z \end{Bmatrix}, \quad \boldsymbol{\chi} := \begin{Bmatrix} \bar{\chi}_x \\ \bar{\chi}_y \\ \bar{\chi}_z \end{Bmatrix} \quad (5.6c)$$

collect the component of stress and strain parameters (5.2), $N_x \cdots M_z$, in different arrangement.

5.4 Kinematics equations

Introducing the average displacements $\bar{\mathbf{u}}_0[x]$ and rotations $\bar{\boldsymbol{\varphi}}_0[x]$ of the displacements SV solution $\bar{\mathbf{u}}[x, y, z]$:

$$\bar{\mathbf{u}}_0[x] = \int_{\bar{S}} \bar{\mathbf{u}}[x, y, z] dA, \quad \bar{\boldsymbol{\varphi}}_0[x] = \mathbf{J}^{-1} \int_{\bar{S}} (\bar{\mathbf{X}} - \bar{\mathbf{X}}_0) \wedge \bar{\mathbf{u}}[x, y, z] dA \quad (5.7a)$$

where $\mathbf{J} := \text{diag}[J_t, J_y, J_z]$, eq. (5.3a) is conveniently rewritten in compact form as

$$\bar{\mathbf{u}}[\bar{\mathbf{X}}] = \bar{\mathbf{u}}_0 + \bar{\mathbf{W}}_0(\mathbf{X} - \mathbf{X}_0) + w[y, z] \mathbf{e}_1 \quad (5.7b)$$

where

$$\mathbf{X} := \begin{Bmatrix} x \\ y \\ z \end{Bmatrix}, \quad \mathbf{X}_0 := \begin{Bmatrix} x \\ 0 \\ 0 \end{Bmatrix}, \quad \bar{\mathbf{W}}_0 := \text{spin}[\bar{\boldsymbol{\varphi}}_0] \quad (5.7c)$$

We obtain therefore the following kinematics relationships:

$$\boldsymbol{\varepsilon} := \bar{\mathbf{u}}_{0,s}, \quad \boldsymbol{\chi} := \bar{\boldsymbol{\varphi}}_{0,s} \quad (5.8)$$

so the Saint Venant displacement solution is completely defined as function of $\bar{\mathbf{u}}_{0,s}$ and $\bar{\boldsymbol{\varphi}}_{0,s}$. To complete the modeling we need to relate the average displacement and rotation derivatives $\bar{\mathbf{u}}_{0,s}$, $\bar{\boldsymbol{\varphi}}_{0,s}$, defined by reference to the local corotational frame $\{x, y, z\}$, with their representation $\bar{\mathbf{u}}_{,s}[s]$ and $\bar{\boldsymbol{\varphi}}_{0,s}[s]$ referred to the global fixed frame $\{X_1, X_2, X_3\}$. The relationship is already governed eqs.(3.18g). The two systems are rotated by an angle $\boldsymbol{\alpha} = \boldsymbol{\varphi}_0[s]$, so we have

$$\bar{\mathbf{u}}_{0,s} = \mathbf{R}[\boldsymbol{\varphi}_0]^T (\mathbf{u}_{0,s} + \mathbf{e}_1) - \mathbf{e}_1, \quad \mathbf{W}_{0,s} = \mathbf{R}[\boldsymbol{\varphi}_0]^T \mathbf{R}_{,s}[\boldsymbol{\varphi}_0] \quad (5.9)$$

5.5 The quadratic strain model

The use of a quadratic expression for the Biot's strain (3.18b), make possible to taking into account the effect of the pointwise nonzero section rotation collected in the vector $\mathbf{w} = \frac{1}{2}(\bar{\boldsymbol{\gamma}} - \nabla w)$. The definition of the internal work (5.4b), in this case give the following expression for $\bar{\boldsymbol{\varepsilon}}_\sigma$ and $\bar{\boldsymbol{\varepsilon}}_\tau$:

$$\begin{cases} \boldsymbol{\varepsilon}_\sigma := \bar{\boldsymbol{\varepsilon}}_\sigma + \int_{\bar{S}} \mathbf{D}_\sigma^T \left\{ \frac{1}{2} \boldsymbol{\gamma}^T \boldsymbol{\gamma} - \frac{1}{8G^2} \boldsymbol{\tau}^T \boldsymbol{\tau} \right\} dA \\ \boldsymbol{\varepsilon}_\tau := \bar{\boldsymbol{\varepsilon}}_\tau + \int_{\bar{S}} \mathbf{D}_\tau^T \boldsymbol{\varepsilon} \left(\boldsymbol{\gamma} - \frac{\boldsymbol{\tau}}{2G} \right) \end{cases} \quad (5.10)$$

Chapter 6

Nonlinear plate model

ICM is now applied in order to recover a nonlinear plate based on Reissner plate model.

6.1 Recovering linear solution

For linear stress $\bar{\sigma}_l$ Reissner plate model assumes that

$$\bar{\sigma}_l[\mathbf{t}] := \begin{bmatrix} N_x + \frac{z}{J}M_y & N_{xy} - \frac{z}{J}M_{xy} & \psi_{,z}T_{xy} \\ \cdot & N_y - \frac{z}{J}M_x & \psi_{,z}T_{yz} \\ \text{sym.} & \cdot & 0 \end{bmatrix} \quad (6.1a)$$

where $J = \frac{h^3}{12}$ being h the thickness, while ψ is the stress function defined as

$$\psi := \frac{3h^2z - 4z^3}{2h^3} \quad , \quad \int_{-h/2}^{h/2} \psi dz = 0 \quad , \quad \int_{-h/2}^{h/2} \psi_{,y} dz = 1 \quad (6.1b)$$

being the in-plane generalized stress $\mathbf{N} := \{N_x, N_y, N_{xy}\}^T$ defined as

$$N_x := \frac{1}{h} \int_{-h/2}^{h/2} \sigma_{xx} dz \quad , \quad N_y := \frac{1}{h} \int_{-h/2}^{h/2} \sigma_{yy} dz \quad , \quad N_{xy} := \frac{1}{h} \int_{-h/2}^{h/2} \sigma_{xy} dz \quad (6.1c)$$

for the shear stress $\mathbf{T} := T_{xz}, T_{yz}^T$

$$T_{xz} := \frac{1}{h} \int_{-h/2}^{h/2} \sigma_{xz} dz \quad , \quad T_{yz} := \frac{1}{h} \int_{-h/2}^{h/2} \sigma_{yz} dz \quad (6.1d)$$

and finally for bending and torsional couples $\mathbf{M} := \{M_x, M_y, M_{xy}\}^T$

$$M_x := \frac{1}{J} \int_{-h/2}^{h/2} z \sigma_{yy} dz \quad , \quad M_y := \frac{1}{J} \int_{-h/2}^{h/2} z \sigma_{xx} dz \quad , \quad M_{xy} := -\frac{1}{J} \int_{-h/2}^{h/2} \sigma_{xy} dz \quad (6.1e)$$

The kinematics of linear plate model gives for the symmetric $\bar{\mathbf{E}}[\bar{\mathbf{d}}]$ and skew-symmetric $\bar{\mathbf{W}}[\bar{\mathbf{d}}]$ part of the gradient of displacement $\nabla \mathbf{u}[\bar{\mathbf{d}}]$:

$$\bar{\mathbf{E}}[\bar{\mathbf{d}}] = \begin{bmatrix} \bar{\varepsilon}_x + z \bar{\chi}_y & \frac{1}{2}(\bar{\varepsilon}_{xy} - \bar{\chi}_{xy}) & \frac{1}{2} \bar{\gamma}_z \\ \cdot & \bar{\varepsilon}_y + z \bar{\chi}_x & \frac{1}{2} \bar{\gamma}_y \\ \text{sym.} & \cdot & 0 \end{bmatrix}, \quad \bar{\mathbf{W}}[\bar{\mathbf{d}}] = \begin{bmatrix} 0 & \cdots & \bar{\varphi}_y - \frac{1}{2} \bar{\gamma}_z \\ \cdot & 0 & -\bar{\varphi}_x - \frac{1}{2} \bar{\gamma}_y \\ \text{skew} & \cdot & 0 \end{bmatrix} \quad (6.2a)$$

being $\bar{\varepsilon}$, $\bar{\gamma}$ and $\bar{\chi}$ the membranal, shear and flexural strain works conjugate with \mathbf{N} , \mathbf{T} and \mathbf{M}

$$\boldsymbol{\varepsilon} := \begin{Bmatrix} \bar{\varepsilon}_x \\ \bar{\varepsilon}_y \\ \bar{\varepsilon}_{xy} \end{Bmatrix}, \quad \boldsymbol{\gamma} := \begin{Bmatrix} \bar{\gamma}_y \\ \bar{\gamma}_z \end{Bmatrix}, \quad \boldsymbol{\chi} := \begin{Bmatrix} \bar{\chi}_x \\ \bar{\chi}_y \\ \bar{\chi}_{xy} \end{Bmatrix} \quad (6.2b)$$

6.2 Galerkin approximation

Riscrivere in formato misto

With the same procedure used for the beam the plate linear model, in case of isotropic material, is defined by the following strain energy Φ :

$$\Phi = \int_A \{ \bar{\boldsymbol{\varepsilon}} \cdot \mathbf{C} \bar{\boldsymbol{\varepsilon}} + \bar{\boldsymbol{\gamma}} \cdot \mathbf{D} \bar{\boldsymbol{\gamma}} + \bar{\boldsymbol{\chi}} \cdot \mathbf{B} \bar{\boldsymbol{\chi}} \} dA$$

and \mathbf{C} , \mathbf{D} and \mathbf{B} the standard matrix of elastic modula. For more general material the same constitutive relationship of the linear model holds then the only modification regards a more general expression of these relationship.

6.3 Kinematics equations

Displacements field $\mathbf{u}[x, y, z]$ can expressed as

$$\mathbf{u} := \mathbf{u}_0 + \mathbf{W}_0(\mathbf{X} - \mathbf{X}_0) \quad (6.3a)$$

being \mathbf{u}_0 and \mathbf{W}_0 the average displacements and rotation of the average plane and the cross-section

$$\mathbf{u}_0[x, y] := \begin{bmatrix} u \\ v \\ w \end{bmatrix}, \quad \mathbf{W}_0[x, y] := \begin{bmatrix} 0 & 0 & \bar{\varphi}_y \\ 0 & 0 & -\bar{\varphi}_z \\ -\bar{\varphi}_y & \bar{\varphi}_z & 0 \end{bmatrix}, \quad \mathbf{X} := \begin{bmatrix} x \\ y \\ z \end{bmatrix}, \quad \mathbf{X}_0 := \begin{bmatrix} 0 \\ 0 \\ z \end{bmatrix} \quad (6.3b)$$

Recalling the definition for local strain (6.2b) and the previous relationships (6.3)

$$\boldsymbol{\varepsilon} = \begin{Bmatrix} \bar{u}_{,x} \\ \bar{v}_{,y} \\ \bar{u}_{,y} + \bar{v}_{,x} \end{Bmatrix}, \quad \boldsymbol{\gamma} = \begin{Bmatrix} \bar{w}_{,x} + \bar{\varphi}_y \\ \bar{w}_{,y} - \bar{\varphi}_x \end{Bmatrix}, \quad \boldsymbol{\chi} = \begin{Bmatrix} -\bar{\varphi}_{y,x} \\ \bar{\varphi}_{x,y} \\ \bar{\varphi}_{x,x} - \bar{\varphi}_{y,y} \end{Bmatrix} \quad (6.4)$$

Using equation (3.18g) and defining CR frame $\mathbf{Q} = \{\mathbf{i}_1, \mathbf{i}_2, \mathbf{i}_3\}$ so that local rotation $\bar{\varphi}_y = 0$ and $\bar{\varphi}_z = 0$:

$$\boldsymbol{\varepsilon} = \left\{ \begin{array}{l} \mathbf{i}_1^T \mathbf{a}_1 - 1 \\ \mathbf{i}_2^T \mathbf{a}_2 - 1 \\ \mathbf{i}_1^T \mathbf{a}_2 + \mathbf{i}_2^T \mathbf{a}_1 \end{array} \right\}, \quad \boldsymbol{\gamma} = \left\{ \begin{array}{l} \mathbf{i}_3^T \mathbf{a}_1 \\ \mathbf{i}_3^T \mathbf{a}_2 \end{array} \right\}, \quad \boldsymbol{\chi} = \left\{ \begin{array}{l} \mathbf{i}_3^T \mathbf{i}_{1,1} \\ \mathbf{i}_3^T \mathbf{i}_{2,2} \\ \mathbf{i}_3^T (\mathbf{i}_{2,1} + \mathbf{i}_{1,2}) \end{array} \right\} \quad (6.5)$$

being

$$\mathbf{a}_1 = \left\{ \begin{array}{l} u_{,1} + 1 \\ v_{,1} \\ w_{,1} \end{array} \right\}, \quad \mathbf{a}_2 = \left\{ \begin{array}{l} u_{,2} \\ v_{,2} + 1 \\ w_{,2} \end{array} \right\} \quad (6.6)$$

Note that the strain measures (6.5) coincide with those of Simo [33].

6.4 Kirchoff's thin plate

A problem that present interest in application and can be easily implemented without any treatments of the rotation is that defined by the Kirchoff plate model, that can be obtained assuming $\boldsymbol{\gamma} = \mathbf{0}$:

$$\left\{ \begin{array}{l} \mathbf{t}_3 \cdot \mathbf{a}_1 = 0 \\ \mathbf{t}_3 \cdot \mathbf{a}_2 = 0 \end{array} \right\} \Rightarrow \mathbf{t}_3 = \frac{\mathbf{a}_1 \wedge \mathbf{a}_2}{|\mathbf{a}_1 \wedge \mathbf{a}_2|}$$

and \mathbf{t}_1 and \mathbf{t}_2 contained in the plane spanned by \mathbf{a}_1 and \mathbf{a}_2 . In particular with an error in the norm of the in plane shear strain with respect to 1 it is possible to assume:

$$\mathbf{t}_\alpha \approx \frac{\mathbf{a}_\alpha}{|\mathbf{a}_\alpha|} \quad \alpha = 1 \cdots 2 \quad (6.7)$$

Using (6.7) we find, that:

$$\mathbf{t}_{\alpha,\beta} = \frac{1}{|\mathbf{a}_\alpha|} \mathbf{a}_{\alpha,\beta} - \frac{\mathbf{a}_\alpha \cdot \mathbf{a}_{\alpha,\beta}}{(\mathbf{a}_\alpha \cdot \mathbf{a}_\alpha)^{\frac{3}{2}}} \mathbf{a}_\alpha \quad \alpha, \beta = 1, 2$$

and that

$$\mathbf{t}_3 \cdot \mathbf{t}_{\alpha,\beta} = \frac{\mathbf{t}_3 \cdot \mathbf{a}_{\alpha,\beta}}{|\mathbf{a}_\alpha|} = \frac{(\mathbf{a}_1 \wedge \mathbf{a}_2) \cdot \mathbf{a}_{\alpha,\beta}}{|\mathbf{a}_\alpha| |\mathbf{a}_1 \wedge \mathbf{a}_2|} \approx (\mathbf{a}_1 \wedge \mathbf{a}_2) \cdot \mathbf{a}_{\alpha,\beta} \quad \text{with } \alpha, \beta = 1, 2$$

With the usual hypothesis of small strain we have, in extended notation:

$$\boldsymbol{\varepsilon}_0 = \left[\begin{array}{l} \frac{1}{2}(\mathbf{a}_1 \cdot \mathbf{a}_1 - 1) \\ \frac{1}{2}(\mathbf{a}_2 \cdot \mathbf{a}_2 - 1) \\ \frac{1}{2}(\mathbf{a}_1 \cdot \mathbf{a}_2 + \mathbf{a}_2 \cdot \mathbf{a}_1) \end{array} \right] = \left\{ \begin{array}{l} u_{01,1} + \frac{1}{2}(u_{01,1}^2 + u_{02,1}^2 + u_{03,1}^2) \\ u_{02,2} + \frac{1}{2}(u_{01,2}^2 + u_{02,2}^2 + u_{03,2}^2) \\ u_{01,2}(1 + u_{01,1}) + u_{02,1}(1 + u_{02,2}) + u_{03,1}u_{03,2} \end{array} \right\} \quad (6.8)$$

$$\bar{\chi} = \begin{bmatrix} (\mathbf{a}_1 \wedge \mathbf{a}_2) \cdot \mathbf{a}_{1,1} \\ (\mathbf{a}_1 \wedge \mathbf{a}_2) \cdot \mathbf{a}_{2,2} \\ (\mathbf{a}_1 \wedge \mathbf{a}_2) \cdot (\mathbf{a}_{1,2} + \mathbf{a}_{2,1}) \end{bmatrix} = \left\{ \begin{array}{l} (-u_{03,1} (1 + u_{02,2}) + u_{02,1} u_{03,2}) u_{01,11} \\ + (u_{03,1} u_{01,2} - (1 + u_{01,1}) u_{03,2}) u_{02,11} \\ + (-u_{02,1} u_{01,2} + (1 + u_{01,1}) (1 + u_{02,2})) u_{03,11} \\ (-u_{03,1} (1 + u_{02,2}) + u_{02,1} u_{03,2}) u_{01,22} \\ + (u_{03,1} u_{01,2} - (1 + u_{01,1}) u_{03,2}) u_{02,22} \\ + (-u_{02,1} u_{01,2} + (1 + u_{01,1}) (1 + u_{02,2})) u_{03,22} \\ 2(-u_{03,1} (1 + u_{02,2}) + u_{02,1} u_{03,2}) u_{01,12} \\ + 2(u_{03,1} u_{01,2} + (-1 - u_{01,1}) u_{03,2}) u_{02,12} \\ + 2(-u_{02,1} u_{01,2} + (1 + u_{01,1}) (1 + u_{02,2})) u_{03,12} \end{array} \right\} \quad (6.9)$$

Note as with these hypothesis the membranal part of the strain coincide with the Green strain tensor reduced to the plate axis while the curvature assume a complex expression with respect to classical technical models [6].

Chapter 7

FEM implementation

The FEM implementation of nonlinear model for beams and plates recovered using ICM can be performed through different strategy. Corotational approach (CR) and Total Lagrangian (TL) will be placed into ICM, Update Lagrangian (UL) approach that in the context of large displacements/rotations small strains is not convenient in its original formulation, is rearranged in a formulation that can be considered a 'frozen' CR approach.

ICM allows to recover the energy of the nonlinear model exploiting the kinematical relationship $\epsilon[\bar{\mathbf{d}}]$ in term of kinematical parameters $\bar{\mathbf{d}}$ into CR frame rotated by \mathbf{Q} :

$$\Phi[\mathbf{t}, \mathbf{e}] = \int_s \left\{ \mathbf{t}^T \epsilon[\bar{\mathbf{d}}] - \frac{1}{2} \mathbf{t}^T \mathbf{K}^{-1} \mathbf{t} \right\} ds \quad (7.1a)$$

or exploiting the kinematical relationship $\epsilon[\mathbf{d}]$ in terms of kinematical parameters \mathbf{d} into global fixed frame

$$\Phi[\mathbf{t}, \mathbf{e}] = \int_s \left\{ \mathbf{t}^T \epsilon[\mathbf{d}] - \frac{1}{2} \mathbf{t}^T \mathbf{K}^{-1} \mathbf{t} \right\} ds \quad (7.1b)$$

through the geometrical relationships between kinematical parameters $\bar{\mathbf{d}}$ in CR and the corresponding in global fixed frame \mathbf{d} :

$$\bar{\mathbf{d}} = \mathbf{g}[\mathbf{d}] \quad (7.1c)$$

being $\mathbf{g}[\mathbf{d}]$ the geometric law defining the CR kinematics relationships.

The mixed format used in deriving the nonlinear model allows to use in natural way a mixed FEM discretization. Assuming an interpolation of generalized stress field

$$\mathbf{t} = \mathbf{D}_t[s] \mathbf{t}_e \quad (7.2)$$

being $\mathbf{D}_t[s]$ the operator collecting the interpolation functions and \mathbf{t}_e the discrete stress defining of the element. The discrete form of complementary

energy can be easily obtained substituting (7.2) into (7.1a) or (7.1b)

$$\Phi_c[\mathbf{t}_e] = \frac{1}{2} \int_s \{\mathbf{t}_e^T \mathbf{K}_e^{-1} \mathbf{t}_e\} ds, \quad \mathbf{K}_e := \int_s \{\mathbf{D}_t^T[s] \mathbf{K} \mathbf{D}_t[s]\} ds \quad (7.3)$$

The discrete form of internal work \mathcal{W} can be obtained through different interpolation of kinematics relationships, the CR and TL will be carry-out:

7.1 Corotational strategy

In this case the discretization is given on kinematical parameters $\bar{\mathbf{d}}$ in CR frame

$$\bar{\mathbf{d}} = \bar{\mathbf{D}}_d[s] \bar{\mathbf{d}}_e \quad (7.4a)$$

Substituting into (7.1c) and performing integration we get the following discrete energy

$$\mathcal{W}[\mathbf{t}_e, \boldsymbol{\varrho}_e] = \mathbf{t}_e^T \boldsymbol{\varrho}_e[\bar{\mathbf{d}}_e], \quad \boldsymbol{\varrho}_e[\bar{\mathbf{d}}_e] := \int_s \{\mathbf{D}_t^T[s] \epsilon[\bar{\mathbf{D}}_d[s] \bar{\mathbf{d}}_e]\} ds \quad (7.4b)$$

The discrete strain measure can maybe expanded using Taylor expansion []

$$\boldsymbol{\varrho}_e[\bar{\mathbf{d}}_e] = \boldsymbol{\varrho}_{1e}[\bar{\mathbf{d}}_e] + \boldsymbol{\varrho}_{2e}[\bar{\mathbf{d}}_e, \bar{\mathbf{d}}_e] + \cdots + \boldsymbol{\varrho}_{ne}[\bar{\mathbf{d}}_e, \bar{\mathbf{d}}_e, \cdots] \quad (7.4c)$$

recalling that the average rigid rotation is filtered by CR frame and that locally simplified kinematics relationship can be used without loss in accuracy. The interpolation is completed exploiting the CR transformation between discrete kinematical parameters $\bar{\mathbf{d}}_e$ in CR frame and the corresponding in global fixed frame \mathbf{d}_e

$$\bar{\mathbf{d}}_e = \mathbf{g}_e[\mathbf{d}_e] \quad (7.4d)$$

In the expression of geometric transformation law $\mathbf{g}_e[\mathbf{d}_e]$, rotation \mathbf{Q} can be handle in two different way. In the first case, CR frame continuously moves with the element and then rotation

$$\mathbf{Q} = \mathbf{Q}[\mathbf{d}_e] \quad (7.4e)$$

is appropriately defined in terms of global discrete kinematics parameters \mathbf{d}_e . In the second case CR frame is 'frozen' and is assumed to be coincided with an appropriate average rigid rotation \mathbf{Q}_a of a known configuration for the element:

$$\mathbf{Q} \equiv \mathbf{Q}_a \quad (7.4f)$$

The previous strategy corresponds to a rearranged in more convenient fashion UL strategy.

7.2 Total–Lagrangian strategy

In this strategy we make discrete the kinematical parameters \mathbf{d} in global fixed frame

$$\mathbf{d} = \mathbf{D}_d[s]\mathbf{d}_e \quad (7.5a)$$

being $\mathbf{D}[s]$ and \mathbf{d}_e the operator contains the interpolation function and \mathbf{d}_e the kinematical parameters defining the element. Energy (7.1b) then becomes:

$$\Phi[\mathbf{t}_e, \boldsymbol{\varrho}_e] = \mathbf{t}_e^T \boldsymbol{\varrho}_e[\mathbf{d}_e], \quad \boldsymbol{\varrho}_e[\mathbf{d}_e] := \int_s \{ \mathbf{D}_t^T[s] \boldsymbol{\epsilon}[\mathbf{D}_d[s]\mathbf{d}_e] \} ds \quad (7.5b)$$

Note that, a TL interpolation can be also obtained from CR interpolation in way consistent, really combining (7.4d) with (7.1c) and (7.5b) we obtain the equivalence

$$\mathbf{g}[\mathbf{d}] = \bar{\mathbf{D}}_d[s]\mathbf{g}_e[\mathbf{d}_e] \quad (7.6)$$

solving \mathbf{d} in terms of \mathbf{d}_e gives a nonlinear interpolation for \mathbf{d} kinematical field in term of \mathbf{d}_e .

7.3 The asymptotic method (Koiter analysis)

The FEM implementation of Koiter’s asymptotic approach is not widely dif-fused within computational mechanics analysis, essentially because its high requirements as regards modeling accuracy. Many papers are however avail-able in literature (e.g. see [4, 5, 11, 6, 7, 3] and references therein), so can be considered well known. A brief overview of method is presented here, for the convenience of the reader and to summarize the main notation and equations involved.

We consider a slender hyperelastic structure subject to conservative loads $\lambda\hat{p}$ increasing with the amplifier factor λ . The equilibrium is expressed by the virtual work equation:

$$\Phi'[u]\delta u - \lambda\hat{p}\delta u = 0, \quad \forall \delta u \in \mathcal{T} \quad (7.7)$$

where $u \in \mathcal{U}$ is the field of configuration variables, $\Phi[u]$ denotes the strain energy, \mathcal{T} is the tangent space of \mathcal{U} at u and a prime is used for expressing the Fréchet derivative with respect to u . We assume that \mathcal{U} will be a linear manifold so that its tangent space \mathcal{T} will be independent from u . Eq.(7.7) defines a curve in the (u, λ) space, the *equilibrium path* of the structure, that can be composed of several branches. We are usually interested in the branch starting from an initial known equilibrium point $\{u_0, \lambda_0\}$ and without any loss of generality we can assume $u_0 = 0, \lambda_0 = 0$. It is worth mentioning that a mixed format is generally convenient to avoid the so called nonlinear

locking phenomena (see [11, 6, 7]), so configuration u usually collects both displacement and stress fields.

The asymptotic method is based on an expansion of the potential energy, in terms of load factor λ and buckling mode amplitudes ξ_i , which is characterized by fourth-order accuracy. It provides an approximation of the equilibrium path by performing the following steps:

1. The *fundamental path* is obtained as a linear extrapolation, from a known equilibrium configuration:

$$u^f[\lambda] := \lambda \hat{u} \quad (7.8)$$

where \hat{u} is the tangent evaluated at $\{0, 0\}$, obtained as a solution of the linear equation

$$\Phi_0'' \hat{u} \delta u = \hat{p} \delta u, \quad \forall \delta u \in \mathcal{T} \quad (7.9)$$

and an index denotes the point along u^f which the quantities are evaluated, that is $\Phi_0'' \equiv \Phi''[u^f[\lambda_0]]$.

2. A cluster of buckling loads $\{\lambda_1 \cdots \lambda_m\}$ and associated buckling modes $(\dot{v}_1 \cdots \dot{v}_m)$ are defined along $u^f[\lambda]$ by the critical condition

$$\Phi''[u^f[\lambda_i]] \dot{v}_i \delta u = 0, \quad \forall \delta u \in \mathcal{T} \quad (7.10)$$

Buckling loads are considered to be sufficiently close to each other to allow the following linearization

$$\Phi_b'' \dot{v}_i \delta u + (\lambda_i - \lambda_b) \Phi_b''' \hat{u} \dot{v}_i \delta u = 0, \quad \forall \delta u \in \mathcal{T} \quad (7.11)$$

λ_b being an appropriate reference value of λ (e.g. the first of λ_i or their mean value). Normalizing we obtain $\Phi_b''' \hat{u} \dot{v}_i \dot{v}_j = -\delta_{ij}$, where δ_{ij} is Kroneker's symbol.

3. The tangent space \mathcal{T} is decomposed into the tangent $\mathcal{V} \equiv \{\dot{v} = \sum_i \xi_i \dot{v}_i\}$ and orthogonal $\mathcal{W} \equiv \{w : \Phi_b''' \hat{u} \dot{v}_i w = 0\}$ subspaces so that $\mathcal{T} = \mathcal{V} \oplus \mathcal{W}$. Making $\xi_0 = \lambda$ and $\dot{v}_0 := \hat{u}$, the asymptotic approximation for the required path is defined by the expansion

$$u[\lambda, \xi_k] \equiv \sum_{i=0}^m \xi \dot{v}_i + \frac{1}{2} \sum_{i,j=0}^m \xi_i \xi_j w_{ij} \quad (7.12)$$

where w_{ij} are quadratic corrections introduced to satisfy the projection of eq.(7.7) onto \mathcal{W} and obtained by the linear *orthogonal equations*

$$\Phi_b'' w_{ij} \delta w = -\Phi_b''' \dot{v}_i \dot{v}_j \delta w, \quad w_{ij}, \delta w \in \mathcal{W} \quad (7.13)$$

where, because of the orthogonality condition, $w_{0i} = 0$.

4. The following energy terms are computed for $i, j, k = 1 \dots m$:

$$\begin{aligned}
\mu_k[\lambda] &= \frac{1}{2} \lambda^2 \Phi_b''' \hat{u}^2 \dot{v}_k + \frac{1}{6} \lambda^2 (\lambda - 3\lambda_b) \Phi_b'''' \hat{u}^3 \dot{v}_k \\
\mathcal{A}_{ijk} &= \Phi_b''' \dot{v}_i \dot{v}_j \dot{v}_k \\
\mathcal{B}_{ijhk} &= \Phi_b'''' \dot{v}_i \dot{v}_j \dot{v}_h \dot{v}_k - \Phi_b'' (w_{ij} w_{hk} + w_{ih} w_{jk} + w_{ik} w_{jh}) \\
\mathcal{B}_{00ik} &= \Phi_b'''' \hat{u}^2 \dot{v}_i \dot{v}_k - \Phi_b'' w_{00} w_{ik} \\
\mathcal{B}_{0ijk} &= \Phi_b'''' \hat{u} \dot{v}_i \dot{v}_j \dot{v}_k \\
\mathcal{C}_{ik} &= \Phi_b'' w_{00} w_{ik}
\end{aligned} \tag{7.14}$$

where the *implicit imperfection factors* μ_k are defined by the 4th order expansion of the unbalanced work on the fundamental path (i.e. $\mu_k[\lambda] := (\lambda \hat{p} - \Phi'[\lambda \hat{u}]) \dot{v}_k$).

5. The equilibrium path is obtained by satisfying the projection of the equilibrium equation (7.7) onto \mathcal{V} . According to eqs, (7.13) and (7.14), we have

$$\begin{aligned}
&(\lambda_k - \lambda) \xi_k - \lambda_b \left(\lambda - \frac{\lambda_b}{2} \right) \sum_{i=1}^m \xi_i \mathcal{C}_{ik} + \frac{1}{2} \sum_{i,j=1}^m \xi_i \xi_j \mathcal{A}_{ijk} + \frac{1}{2} (\lambda - \lambda_b)^2 \sum_{i=1}^m \xi_i \mathcal{B}_{00ik} \\
&+ \frac{1}{2} (\lambda - \lambda_b) \sum_{i,j=1}^m \xi_i \xi_j \mathcal{B}_{0ijk} + \frac{1}{6} \sum_{i,j,h=1}^m \xi_i \xi_j \xi_h \mathcal{B}_{ijhk} + \mu_k[\lambda] = 0, \quad k = 1 \dots m
\end{aligned} \tag{7.15}$$

Equation (7.15) corresponds to a highly nonlinear system in the $m + 1$ unknowns $\lambda - \xi_i$ and can be solved using a standard path-following strategy. It provides the initial post-buckling behavior of the structure, including *modal interactions* and *jumping-after-bifurcation* phenomena.

Once the first analysis has been performed (step 1 to 4), the presence of small additional, load or displacement, imperfections can be taken into account in the postprocessing phase by adding additional coefficients to eq.(7.15), with a negligible computational extra-cost (see [3] for a general discussion about this topic). From eq. (7.15) we can also extract information about the worst imperfection shapes we can use to improve the imperfection sensitivity analysis or for driving more detailed investigation through specialized path-following analysis (see [8, 9] and references therein).

Note that, within a FEM context and standard FEM notations, eqs. (7.9) and (7.10) write

$$\mathbf{K}_0 \hat{\mathbf{u}} = \hat{\mathbf{p}} \quad , \quad \mathbf{K}[\lambda_i] \dot{\mathbf{v}}_i = 0$$

where \mathbf{K}_0 and $\mathbf{K}[\lambda]$ are the tangent stiffness matrix evaluated at the configuration $\mathbf{u} = \mathbf{0}$ and $\mathbf{u} = \lambda_i \hat{\mathbf{u}}$, respectively. Both equations correspond to standard problems, a linear solution and an eigenvalue problem, which are easily solved numerically (see [3]). Eq. (7.11) writes

$$(\mathbf{K}[\lambda_b] + (\lambda_i - \lambda_b)\mathbf{K}_1)\dot{\mathbf{v}}_i \delta \mathbf{u} = 0$$

where $\mathbf{K}_1 := d\mathbf{K}[\lambda]/d\lambda$ at $\lambda = \lambda_b$. It corresponds to a standard local linearization of the eigenvalue equation (7.10). Eq. (7.13) writes

$$\mathbf{K}[\lambda_b]\mathbf{w}_{ij} = \mathbf{p}_{ij}$$

and corresponds to a linear system in \mathbf{w}_{ij} , the right-hand vector \mathbf{p}_{ij} being computed from \mathbf{v}_i and \mathbf{v}_j . Finally coefficients $\mu_k \cdots \mathcal{C}_{ik}$ defined in eq. (7.14) are all scalar quantities which can be computed as integrals of known functions. So the actual implementation of the method as a computational tool is quite easy in practice. We can mention that it can provide very accurate results (see [3] for a discussion and an analytical estimate of the error). However, because of the use of a fourth-order expansion of the strain energy, it requires that a fourth-order accuracy be guaranteed in the structural modeling, which is a heavy and unusual demand in FEM analysis. The corotational approach presented in the sequel intends to give a contribution in this direction.

7.4 The path-following method

In the following a brief sketch of the path-following iterative scheme is reported. Further details can be found in Riks'papers [2] and in [10].

Using an N -variable finite element discretization, the equilibrium path defined in eq.(7.7) $\mathbf{p}[\lambda] := \lambda \hat{\mathbf{p}}$ is defined by the condition:

$$\mathbf{r}[\mathbf{x}] := \mathbf{s}[\mathbf{u}] - \lambda \hat{\mathbf{p}} = \mathbf{0} \quad (7.16)$$

where $\mathbf{r} : \mathfrak{R}^{N+1} \rightarrow \mathfrak{R}^N$ is a nonlinear vectorial function of the vector $\mathbf{x}^T := \{\mathbf{u}^T, \lambda\}^T \in \mathfrak{R}^{N+1}$, collecting the configuration $\mathbf{u} \in \mathfrak{R}^N$ and the load multiplier $\lambda \in \mathfrak{R}$, $\hat{\mathbf{p}} \in \mathfrak{R}^N$ is the nominal load vector. Eq.(7.16) represents an N -equation system with $N + 1$ unknowns and describes the equilibrium path as a curve in \mathfrak{R}^{N+1} . To determine a point on that curve we have to introduce a constraint equation:

$$g[\mathbf{x}] - \xi = 0 \quad (7.17)$$

able to complete eq.(7.16). From a geometrical point of view, eq.(7.17) defines a surface in \mathfrak{R}^{N+1} . If we assign successive values to the control parameter ξ the surface moves to \mathfrak{R}^{N+1} and its intersections with eq.(7.16) define a sequence of points belonging to the equilibrium path.

The conditions for achieving a proper intersection between Eq. (7.16) and (7.17) are extensively described in Riks' papers we recall that Eq. 7.17 will vary according to the curve (*adaptive parameterizations*) in order to provide a proper intersection with the equilibrium path. Constraint surfaces, defined as planes with constant orientation, can simplify the description of the system (7.16, 7.17) but fail to provide solutions for the presence of turning points (i.e. the classic load-controlled process fails near the limit point ($\lambda = 0$) that is a turning point for the particular constraint equation ($g[\mathbf{x}] := \lambda$) used.

7.4.1 The arc-length iterative scheme

By expressing the equilibrium path as a function of the parameter ξ , the extended system collecting the equilibrium equations (7.16) and the constraint equation (7.17) can be rewritten in the form

$$\mathbf{R}[\mathbf{x}, \xi] := \begin{Bmatrix} \mathbf{r}[\mathbf{x}] \\ g[\mathbf{x}] - \xi \end{Bmatrix} = \mathbf{0} \quad \mathbf{R} \in \mathfrak{R}^{N+1} \quad (7.18)$$

Eq.(7.18) represents a nonlinear system of $N + 1$ unknowns which is solved iteratively using a Newton–Raphson scheme and defining a sequence of equilibrium points $\mathbf{x}^{(k)}$. While more complex choices may be possible a suitable expression for the constrained surface is the following hyperplane equation

$$\bar{\mathbf{n}}^T \bar{\mathbf{M}}(\mathbf{x} - \mathbf{x}^{(k)}) = \Delta \xi_k \quad (7.19)$$

$\bar{\mathbf{n}} := (\mathbf{n}, \nu)$ being an appropriate orientation and $\bar{\mathbf{M}} := \text{diag}(\mathbf{M}, \mu)$ a positive definite symmetric matrix which defines a scalar product in the (\mathbf{u}, λ) space suitable for homogenizing variables of different nature. Starting from $\mathbf{x}_0 := \mathbf{x}^{(k)}$, the first estimate (*predictor*) \mathbf{x}_1 can be provided by an extrapolation based on previously computed points. System (7.18) is solved by a Newton–Raphson iteration method (*corrector*) computing a convergent sequence of estimates $\mathbf{x}_j := (\mathbf{u}_j, \lambda_j), j = 2, 3 \dots$:

$$\mathbf{x}_{j+1} = \mathbf{x}_j + \dot{\mathbf{x}}_j \quad (7.20)$$

where the correction $\dot{\mathbf{x}}_j$ is obtained as a solution of

$$\mathbf{J}_0 \dot{\mathbf{x}}_j = -\mathbf{R}_j \quad , \quad \mathbf{R}_j := \begin{bmatrix} \mathbf{r}_j \\ 0 \end{bmatrix} \quad (7.21)$$

\mathbf{J}_0 being the Jacobian matrix of eq.(7.18):

$$\mathbf{J}_0 := \begin{bmatrix} \mathbf{K}_0 & -\hat{\mathbf{p}} \\ \mathbf{n}^T \mathbf{M} & \nu \mu \end{bmatrix} \quad \mathbf{K}_0 := \left\{ \frac{d\mathbf{s}[\mathbf{u}]}{d\mathbf{u}} \right\} \Big|_{\mathbf{u}=\mathbf{u}_0} \quad (7.22)$$

and \mathbf{K}_0 the stiffness matrix that can be updated at each iteration loop $\mathbf{u}_0 := \mathbf{u}_j$ (*Pure Newton* scheme) or evaluated only once at the beginning of the incremental step (*Modified Newton* scheme). The latter usually more convenient from a computational point of view, is widely used.

A suitable choice for Eq.7.17 is to assume $\bar{\mathbf{n}} := (\mathbf{u}_j - \mathbf{u}_0, \lambda_j - \lambda_0)$, i.e., to use as constraint surface $g[\mathbf{u}, \lambda]$ the hyperplane normal, with respect to the orthogonality defined by matrix $\bar{\mathbf{M}}$, to the current step increment . This choice is a good compromise between the need for good adaptive parameterizations and simplicity in its numerical implementation.

System (7.20) is then solved in partitioned form in order to exploit the symmetry and banded structure of the stiffness matrix. By making:

$$\mathbf{v}_j = \mathbf{K}_0^{-1} \mathbf{M} \mathbf{n} \quad (7.23)$$

the solution to system (7.20) is

$$\dot{\lambda}_j = \frac{\mathbf{v}_j^T \mathbf{r}_j}{\mu\nu + \mathbf{v}_j^T \hat{\mathbf{p}}} \quad (7.24)$$

$$\dot{\mathbf{u}}_j = \mathbf{K}_0^{-1} [\dot{\lambda}_j \hat{\mathbf{p}} - \mathbf{r}_j] = -\mathbf{K}_0^{-1} \left[\mathbf{I} - \frac{\hat{\mathbf{p}} \mathbf{v}_j^T}{\mu\nu + \hat{\mathbf{p}}^T \mathbf{v}_j} \right] \mathbf{r}_j \quad (7.25)$$

The algorithm also needs a stepsize criterion to determine a sequence of step-lengths selected according to the nonlinearity of the equilibrium path to minimize the computational work (see [2, 10]).

The convergence of the iterative process (7.23–7.25) has been widely discussed in [10], to which the interested reader is referred. By summarizing the results given there, the convergence speed is essentially related to the relative difference, along directions orthogonal to the path tangent, between the current stiffness matrix $\mathbf{K}_j := \mathbf{K}[\mathbf{u}_j]$ and its estimate \mathbf{K}_0 used as iteration matrix. That is, it depends on how small the step length is but more, on the nonlinearity of the problem representation. Convergence failures usually occur when \mathbf{K}_j tends to stiffen during the iteration process as typically occurs, in compatible formulations, due to the interaction of large axial/flexural stiffness ratios with even small element rotations. The use of a mixed formulation avoids this interaction and noticeably improves the convergence without needing to decrease the step length more than strictly required by an accurate description of the equilibrium path.

Chapter 8

FEM implementation of the Saint Venant nonlinear beam model–Corotational formulation

8.1 3D rotation algebra

The nonlinear analysis of spatial structures depends on 3D rotation algebra. A great amount of work on this topic is available in the literature see [47, 48, 80].

Finite 3D rotations can be directly represented in terms of an orthogonal tensor \mathbf{R} that is a member of the nonlinear manifold $\text{SO}(3)$. In coordinate representation, the rotation tensor \mathbf{R} becomes a 3×3 orthogonal matrix that, by exploiting the orthogonality property $\mathbf{R}^{-1} = \mathbf{R}^T$, is a function of only three parameters. However it may not be convenient to express the configuration changes through variables belonging to a nonlinear manifold due to the complications involved in the successive variations (see [35]). A useful way to express \mathbf{R} in terms of the quantities lying in a vector space is that of Rodrigues [12]:

$$\mathbf{R}[\boldsymbol{\theta}] = \mathbf{I} + \frac{\sin \theta}{\theta} \mathbf{W}[\boldsymbol{\theta}] + \frac{(1 - \cos \theta)}{\theta^2} \mathbf{W}^2[\boldsymbol{\theta}], \quad \mathbf{W}[\boldsymbol{\theta}] \equiv \text{spin}[\boldsymbol{\theta}] = \begin{bmatrix} 0 & -\theta_3 & \theta_2 \\ \theta_3 & 0 & -\theta_1 \\ -\theta_2 & \theta_1 & 0 \end{bmatrix} \quad (8.1)$$

which uses the rotation vectors $\boldsymbol{\theta} = [\theta_1, \theta_2, \theta_3]^T$, $\theta = \sqrt{\theta_1^2 + \theta_2^2 + \theta_3^2}$ being the magnitude of the rotation vector. This representation uses a minimal set of parameters, is singularity free and gives a one-to-one correspondence in the range $0 \leq \theta < 2\pi$ (see [80]). Making $\mathbf{R}_\theta \equiv \mathbf{R}[\boldsymbol{\theta}]$ and $\mathbf{W}_\theta \equiv \mathbf{W}[\boldsymbol{\theta}]$,

equation (8.1) is equivalent to the exponential map

$$\mathbf{R}_\theta = \mathbf{I} + \mathbf{W}_\theta + \frac{\mathbf{W}_\theta^2}{2!} + \dots = \sum_{n=0}^{\infty} \frac{\mathbf{W}_\theta^n}{n!} = \exp(\mathbf{W}_\theta) \quad (8.2)$$

The inverse relation is given by

$$\boldsymbol{\theta} = \frac{\arcsin \omega}{\omega} \boldsymbol{\omega} \quad (8.3a)$$

$\boldsymbol{\omega}$ being the axial vector of the skew-symmetric part of \mathbf{R}_θ , implicitly defined by

$$\mathbf{W}[\boldsymbol{\omega}] = \frac{1}{2}(\mathbf{R}_\theta - \mathbf{R}_\theta^T) \quad (8.3b)$$

and ω the Euclidian norm of $\boldsymbol{\omega}$. By a Taylor expansion we obtain

$$\boldsymbol{\theta} = (1 + \frac{1}{6}\omega^2 + \frac{3}{40}\omega^4 + \dots)\boldsymbol{\omega} \quad (8.3c)$$

The extraction of the rotation vector by the rotation matrix \mathbf{R}_θ , as defined by eqs. (8.3), will from now on be denoted by $\boldsymbol{\theta} \equiv \log[\mathbf{R}_\theta]$.

The most commonly used approach in defining structural models involving 3D rotations is to express the kinematics in terms of the spin variations $\delta\mathbf{W}$ which, as pointed out by Nour-Omid and Rankin [40], are the quantities associated through virtual works with the common accepted definition of moments. In this case, using eq. (8.2), the variation $\delta\mathbf{R}$ of \mathbf{R} could be expressed in terms of the infinitesimal rotations defined by the spin $\delta\mathbf{W}$:

$$\delta\mathbf{R} = \mathbf{R}\delta\mathbf{W} \quad (8.4)$$

If the current rotation \mathbf{R} is known, eq. (8.4) allows for a simple expression of the first variations of the strain energy required by the equilibrium condition (7.7).

Remembering that \mathbf{R} belongs to a nonlinear manifold, the successive variations of the energy quickly become increasingly complicated [35]. This does not however present a real problem in the path-following analysis, which requires the accurate evaluation of the first variations of energy with respect to the configuration variables and exploits the second variations only to define an iteration matrix to be used within a Newton-like scheme. Thus a rough evaluation of these variations, obtained through simplified formulas, can be sufficient for the analysis. The only difficulty in this context is related to the evaluation of the current rotation \mathbf{R} , which requires a rather expensive multiplicative updating process. Consequently, a large amount of research has been devoted to setting up an efficient updating (see [96] for further details on this topic).

The use of the rotation vector $\boldsymbol{\theta}$ to express 3D rotations, as introduced in [47, 48, 80], allows the multiplicative updating to be avoided, but introduces an additional nonlinear relation through eq. (8.1). The main advantage is, however, the possibility of describing the configuration in terms of variables belonging to a linear manifold thereby allowing the strain energy variations to be evaluated accurately through standard directional derivatives. This is particularly useful within asymptotic analysis, where an accurate evaluation of these variations, up to fourth-order, is necessary. It becomes even more necessary when using the standard asymptotic formulation, which requires that the configuration manifold \mathcal{U} be linear. Accordingly, the rotation vector $\boldsymbol{\theta}$ will be assumed as configuration variable in the sequel. It will also be shown that, rather simple general rules can be derived in order to obtain explicit expressions for the energy variations needed by the analysis.

8.2 Corotational formulation

The goal of the corotational approach is to split the element motion into two parts: a rigid and a deformational one, thus providing an easy way to recover an objective structural modeling. The rigid part is defined, on average, as the motion of a corotational frame (CR observer) which translates and rotates with the element from the initial reference configuration to the current one. The deformational part is the local motion seen by the CR observer, within this frame. It can be made small enough with an appropriate mesh refinement, allowing the differences between pointwise and element average rotations to be reduced. Since the strains depend only on the deformational part, which can be assumed to be small, they can be described using simplified kinematical relationships: in particular, a linearized kinematics, as the simplest choice, or a more refined quadratic kinematics, for better accuracy. The former choice allows standard linear finite elements to be reused as recognized by Rankin [40]. The latter choice requires a nonlinear description of the element, while still allowing the usual simplifying "technical" assumptions for the element modeling, due to the assumption of small deformations.

8.2.1 Strain energy in the CR frame

Let's assume a fixed frame with versors $\{\mathbf{e}_1, \mathbf{e}_2, \mathbf{e}_3\}$ and consider the motion described by the point displacement $\mathbf{d}[\mathbf{X}]$ and rotation $\boldsymbol{\varphi}[\mathbf{X}]$ vector fields, \mathbf{X} being the position of the point in the reference configuration with respect to the fixed frame. The corotational versors are defined by

$$\mathbf{i}_k = \mathbf{Q}\mathbf{e}_k \quad \text{with} \quad \mathbf{Q} \equiv \mathbf{R}[\boldsymbol{\alpha}], \quad k = 1 \dots 3. \quad (8.5)$$

where $\boldsymbol{\alpha}$ is the rigid rotation vector and \mathbf{c} the translation vector which defines the CR motion. Using simple geometric considerations and omitting the dependence on \mathbf{X} , for an easy notation, the deformational local part of $\mathbf{d}[\mathbf{X}]$ can be described by the expressions

$$\mathbf{d}_c = \mathbf{Q}^T(\mathbf{X} + \mathbf{d} - \mathbf{c}) - \mathbf{X} \quad (8.6)$$

where \mathbf{d}_c collects the components of the deformational displacement.

Similarly, the rotation vector of the local part of point rotation $\mathbf{R} := \mathbf{R}[\boldsymbol{\varphi}]$ is expressed by

$$\boldsymbol{\varphi}_c = \log(\mathbf{R}_c) \quad \text{with} \quad \mathbf{R}_c = \mathbf{Q}^T \mathbf{R} \quad (8.7)$$

The point strain will be a function of the deformational displacement and rotation:

$$\boldsymbol{\varepsilon} = \boldsymbol{\varepsilon}[\mathbf{d}_c, \boldsymbol{\varphi}_c]$$

Assuming that \mathbf{d}_c and $\boldsymbol{\varphi}_c$ are small, the constitutive laws can be taken as linear. It is then possible to express the finite element strain energy, in mixed form, as

$$\Phi_e[u] := \int_{\Omega_e} \left\{ \boldsymbol{\sigma} \cdot \boldsymbol{\varepsilon}[\mathbf{d}_c, \boldsymbol{\varphi}_c] - \frac{1}{2} \boldsymbol{\sigma} \cdot \mathbf{E}^{-1} \boldsymbol{\sigma} \right\} d\Omega_e \quad (8.8)$$

where $\boldsymbol{\sigma}$ is the stress associated with the elastic tensor \mathbf{E} to the strain and Ω_e is the finite element domain. Exploiting the element interpolation laws, (8.8) can be rewritten, in discrete form, as:

$$\Phi_e[u] = \mathbf{t}_e^T \boldsymbol{\varrho}[\mathbf{d}_{ce}] - \frac{1}{2} \mathbf{t}_e^T \mathbf{K}_c^{-1} \mathbf{t}_e \quad (8.9)$$

\mathbf{t}_e being the vector of the element stress parameters and $\boldsymbol{\varrho}$ the associated vector of the strains, as a function of the displacement element vector \mathbf{d}_{ce} collecting deformational displacements \mathbf{d}_{ck} and rotations $\boldsymbol{\varphi}_{ck}$ of all k -th finite element nodes (or a relevant linear combination of them). Finally \mathbf{K}_c^{-1} is the Clapeyron compliance matrix provided by the complementary energy equivalence

$$\frac{1}{2} \mathbf{t}_e^T \mathbf{K}_c^{-1} \mathbf{t}_e = \frac{1}{2} \int_{\Omega_e} \boldsymbol{\sigma} \cdot \mathbf{E}^{-1} \boldsymbol{\sigma} d\Omega_e \quad , \quad \forall \mathbf{t}_e, \boldsymbol{\sigma}[\mathbf{t}_e]$$

Exploiting the smallness of deformational displacements, we assume that $\boldsymbol{\varrho}$ can have, at most, the following quadratic expression in terms of \mathbf{d}_{ce} :

$$\boldsymbol{\varrho} = \boldsymbol{\varrho}_l[\mathbf{d}_{ce}] + \boldsymbol{\varrho}_q[\mathbf{d}_{ce}, \mathbf{d}_{ce}] \quad (8.10)$$

where $\boldsymbol{\varrho}_l[\mathbf{d}_{ce}] = \mathbf{D} \mathbf{d}_{ce}$ is a linear relationship while the j -th component of the symmetric bilinear quadratic part of $\boldsymbol{\varrho}_q$ is defined as:

$$\varrho_{qj}[\mathbf{d}_{ce}, \mathbf{d}_{ce}] = \frac{1}{2} \mathbf{d}_{ce}^T \boldsymbol{\Psi}_j \mathbf{d}_{ce} \quad , \quad \boldsymbol{\Psi}_j = \boldsymbol{\Psi}_j^T$$

with $j = 1 \dots n_\rho$, n_ρ being the dimension of vector $\boldsymbol{\varrho}$.

The discrete expression of the strain energy (8.9) becomes

$$\Phi_e[u] = \mathbf{t}_e^T \mathbf{D} \mathbf{d}_{ce} + \frac{1}{2} \mathbf{d}_{ce}^T \boldsymbol{\Psi}[\mathbf{t}_e] \mathbf{d}_{ce} - \frac{1}{2} \mathbf{t}_e^T \mathbf{K}_c^{-1} \mathbf{t}_e \quad (8.11a)$$

where $\boldsymbol{\Psi}[\mathbf{t}_e] = \sum_j t_{ej} \boldsymbol{\Psi}_j$. Using a linear strain measure ($\boldsymbol{\varrho}_q \approx 0$), it reduces to the common expression of the linear elastic case

$$\Phi_e[u] = \mathbf{t}_e^T \mathbf{D} \mathbf{d}_{ce} - \frac{1}{2} \mathbf{t}_e^T \mathbf{K}_c^{-1} \mathbf{t}_e \quad (8.11b)$$

8.2.2 A remark on the corotational description

Letting $\boldsymbol{\alpha}_e$ be the CR rotation vector associated to the average rigid rotation of the element and

$$\mathbf{Q}_e = \mathbf{R}[\boldsymbol{\alpha}_e] \quad (8.12)$$

the CR formulation is based on two fundamental steps:

- a) the definition of kinematical relationships (8.6) and (8.7) that express a purely *geometric nonlinear relation*

$$\mathbf{d}_{ce} = \mathbf{d}_{0e} + \mathbf{d}_g[\boldsymbol{\alpha}_e, \mathbf{d}_e] \quad (8.13)$$

between the element displacement vector in the CR (\mathbf{d}_{ce}) and fixed frames (\mathbf{d}_e). We assume that $\mathbf{d}_g[\boldsymbol{\alpha}_e, \mathbf{0}] = \mathbf{0}$, so that \mathbf{d}_{0e} will be the initial deformational displacement vector for $\mathbf{d}_e = \mathbf{0}$. The additive rule in (8.13) is possible thanks to the assumption that both \mathbf{d}_{0e} and \mathbf{d}_g are small.

- b) a *local modeling* of the mechanical behavior of the structures, which is an implicitly defined expression of the strain energy of the element in terms of local CR finite element parameters, which is written in the simplified form (8.11), because of the assumption of small local displacements.

Note that the geometrical nonlinearities are essentially contained in eq. (8.13), while the local modeling only implies standard finite element procedures and, if using expression (8.11b), corresponds to a linear FEM modeling. The corotational approach then leads to an efficient way of reusing standard FEM technology in a nonlinear context.

8.2.3 Strain energy in the fixed frame

The CR rotation vector $\boldsymbol{\alpha}_e$ will be a function of the current displacement vector \mathbf{d}_e :

$$\boldsymbol{\alpha}_e := \boldsymbol{\alpha}_e[\mathbf{d}_e] \quad (8.14)$$

The explicit expression of this function will depend on the particular element which is used and is based on the best compromise between algebraic simplicity and accuracy, the latter being essentially related to the smallness of the deformational part of the motion. By substituting eq. (8.14) into (8.13), we can express \mathbf{d}_{ce} as a function of \mathbf{d}_e alone:

$$\mathbf{d}_{ce} = \mathbf{d}_{0e} + \mathbf{g}[\mathbf{d}_e] \quad (8.15)$$

The combination of eqs. (8.11) and (8.13) allows the element energy to be expressed in terms of the element vector

$$\mathbf{u}_e := \{\mathbf{t}_e, \mathbf{d}_e\}^T \quad (8.16)$$

which collects all parameters defining the element configuration in a single vector and can be related to the global vector \mathbf{u} , expressing the overall configuration of the assemblage, through the known relation

$$\mathbf{u}_e = \mathbf{A}_e \mathbf{u} \quad (8.17)$$

where matrix \mathbf{A}_e implicitly contains the link constraints between elements. This allows the energy to be expressed as an algebraic nonlinear function of \mathbf{u} :

$$\Phi[u] := \sum_e \Phi_e[u]$$

The asymptotic approach requires the evaluation of the 2nd, 3rd and 4th variations of the energy by correspondence to a configuration which can be either the initial u_0 or the bifurcation one u_b . In both cases, through an appropriate configuration updating process, we refer to a configuration characterized by $\mathbf{d}_e = \mathbf{0}$, the initial stresses and (small) deformational displacements being described by the element vectors \mathbf{t}_{0e} and \mathbf{d}_{0e} .

To express the strain energy variations, it is convenient to refer to the fourth order Taylor expansion of $\mathbf{g}[\mathbf{d}_e]$ starting from a configuration characterized by $\mathbf{d}_e = \mathbf{0}$:

$$\mathbf{g}[\mathbf{d}_e] = \mathbf{g}_1[\mathbf{d}_e] + \frac{1}{2}\mathbf{g}_2[\mathbf{d}_e, \mathbf{d}_e] + \frac{1}{6}\mathbf{g}_3[\mathbf{d}_e, \mathbf{d}_e, \mathbf{d}_e] + \frac{1}{24}\mathbf{g}_4[\mathbf{d}_e, \mathbf{d}_e, \mathbf{d}_e, \mathbf{d}_e] + \dots \quad (8.18)$$

where \mathbf{g}_n , $n = 1 \dots 4$ are n -multilinear symmetric forms which express the n th Fréchet variations of function $\mathbf{g}[\mathbf{d}_e]$.

The relevant strain energy variations are reported here, for the simpler case of *linear local modeling* defined by eq. (8.11b), and then extended to the *quadratic local modeling* defined by eq. (8.11a).

We will denote with u_i ($i = 1 \dots 4$) a generic variation of the configuration field u , with \mathbf{u}_i the corresponding global configuration vector in the FEM

discretization and with $\mathbf{u}_{ie} = \mathbf{A}_e \mathbf{u}_i$ the finite element configuration vector collecting both displacement and stress element vectors: $\mathbf{u}_{ie} = \{\mathbf{t}_{ie}, \mathbf{d}_{ie}\}^T$. With the same notation \mathbf{u}_0 and \mathbf{u}_{0e} are the global and element reference configuration vectors.

Second order variations using linear local modeling

Second order energy variations are used in the evaluation of the fundamental mode \hat{u} (through eq. (7.9)) and of the bifurcation modes \hat{v}_i (through eq. (7.10)). In both cases, using expansion (8.18) and the energy expression (8.11a), the contribution of the element to the energy variation can be expressed as

$$\Phi_e'' u_1 u_2 = \mathbf{t}_{1e}^T \boldsymbol{\varrho}_1[\mathbf{d}_{2e}] + \mathbf{t}_{2e}^T \boldsymbol{\varrho}_1[\mathbf{d}_{2e}] - \mathbf{t}_{1e}^T \mathbf{K}_c^{-1} \mathbf{t}_{2e} + \mathbf{t}_{0e}^T \boldsymbol{\varrho}_2[\mathbf{d}_{1e}, \mathbf{d}_{2e}] \quad (8.19a)$$

where $\boldsymbol{\varrho}_1$ and $\boldsymbol{\varrho}_2$ are defined by

$$\boldsymbol{\varrho}_1[\mathbf{d}_{je}] = \mathbf{D} \mathbf{g}_1[\mathbf{d}_{je}] \quad \boldsymbol{\varrho}_2[\mathbf{d}_{1e}, \mathbf{d}_{2e}] = \mathbf{D} \mathbf{g}_2[\mathbf{d}_{1e}, \mathbf{d}_{2e}] \quad j = 1, 2 \quad (8.19b)$$

Introducing the matrices \mathbf{L}_1 and $\mathbf{G}[\mathbf{t}_e]$ through the following equivalences

$$\mathbf{L}_1 \mathbf{d}_{je} = \mathbf{g}_1[\mathbf{d}_{je}] \quad , \quad \mathbf{d}_{1e}^T \mathbf{G}[\mathbf{t}_{0e}] \mathbf{d}_{2e} = \mathbf{t}_{0e}^T \boldsymbol{\varrho}_2[\mathbf{d}_{1e}, \mathbf{d}_{2e}] \quad (8.20)$$

eq. (8.19) can be rearranged in a more convenient compact form:

$$\Phi_e'' u_1 u_2 = \mathbf{u}_{1e}^T \mathbf{H}_e \mathbf{u}_{2e} \quad , \quad \mathbf{H}_e = \begin{bmatrix} -\mathbf{K}_c^{-1} & \mathbf{D} \mathbf{L}_1 \\ \mathbf{L}_1^T \mathbf{D}^T & \mathbf{G}[\mathbf{t}_{0e}] \end{bmatrix} \quad (8.21)$$

The mixed tangent matrix of the element \mathbf{H}_e can be directly used, through a standard assemblage process, to obtain the overall Hessian matrix \mathbf{H} :

$$\Phi'' u_1 u_2 = \mathbf{u}_1^T \mathbf{H} \mathbf{u}_2 \quad , \quad \mathbf{H} := \sum_e \mathbf{A}_e^T \mathbf{H}_e \mathbf{A}_e \quad (8.22)$$

allowing eqs. (7.9) and (7.10) to be rewritten in matrix form.

Third order variations using linear modeling

Third order energy variations are used in eq. (7.14) for evaluating the third-order coefficients \mathcal{A}_{ijk} and the third-order terms of the factors μ_k , which are scalar quantities obtained as variations with respect to known fields \hat{u} and \hat{v}_i . They are also used in eq. (7.13) for evaluating the right-side of the equation which implicitly defines the quadratic modes w_{ij} . In this case we have to evaluate secondary force vector $\mathbf{s}[\mathbf{u}_1, \mathbf{u}_2]$ defined by the equivalence

$$\delta \mathbf{u}^T \mathbf{s}[\mathbf{u}_1, \mathbf{u}_2] = \Phi''' u_1 u_2 \delta u \quad (8.23)$$

δu being a generic virtual variation and $\delta \mathbf{u}$ its corresponding discrete representation. The element contribution to the scalar expressions is easily evaluated using the general formula

$$\Phi_e''' u_1 u_2 u_3 = \mathbf{t}_{1e}^T \boldsymbol{\varrho}_2[\mathbf{d}_{2e}, \mathbf{d}_{3e}] + \mathbf{t}_{2e}^T \boldsymbol{\varrho}_2[\mathbf{d}_{3e}, \mathbf{d}_{1e}] + \mathbf{t}_{3e}^T \boldsymbol{\varrho}_2[\mathbf{d}_{1e}, \mathbf{d}_{2e}] + \mathbf{t}_{0e}^T \boldsymbol{\varrho}_3[\mathbf{d}_{1e}, \mathbf{d}_{2e}, \mathbf{d}_{3e}] \quad (8.24a)$$

where $\boldsymbol{\varrho}_2[\cdot, \cdot]$ is defined by (8.19b) and $\boldsymbol{\varrho}_3[\cdot \cdot \cdot]$ is obtained by

$$\boldsymbol{\varrho}_3[\mathbf{d}_{1e}, \mathbf{d}_{2e}, \mathbf{d}_{3e}] = \mathbf{D} \mathbf{g}_3[\mathbf{d}_{1e}, \mathbf{d}_{2e}, \mathbf{d}_{3e}] \quad (8.24b)$$

When the vectorial expression (8.23) is needed, making $u_3 = \delta u$, eq. (8.24a) can be rearranged in the form

$$\Phi_e''' u_1 u_2 \delta u := \delta \mathbf{u}_e^T \mathbf{s}_e = \begin{bmatrix} \delta \mathbf{t}_e \\ \delta \mathbf{d}_e \end{bmatrix}^T \begin{bmatrix} \mathbf{s}_{et} \\ \mathbf{s}_{ed} \end{bmatrix} \quad (8.25)$$

where $\mathbf{s}_{et} := \boldsymbol{\varrho}_2[\mathbf{d}_{1e}, \mathbf{d}_{2e}]$ and \mathbf{s}_{ed} is defined by the equivalence

$$\delta \mathbf{d}_e^T \mathbf{s}_{ed} = \delta \mathbf{d}_e^T (\mathbf{G}[\mathbf{t}_{1e}] \mathbf{d}_{2e} + \mathbf{G}[\mathbf{t}_{2e}] \mathbf{d}_{1e}) + \mathbf{t}_{0e}^T \boldsymbol{\varrho}_3[\mathbf{d}_{1e}, \mathbf{d}_{2e}, \delta \mathbf{d}_e] \quad (8.26)$$

The overall vector \mathbf{s} is then obtained by a standard assemblage

$$\mathbf{s}[\mathbf{u}_1, \mathbf{u}_2] = \sum_e \mathbf{A}_e^T \mathbf{s}_e[\mathbf{u}_{1e}, \mathbf{u}_{2e}]$$

Fourth order variations using linear local modeling

Fourth order energy variations are used in eq. (7.14) for evaluating the fourth-order coefficients \mathcal{B}_{ijhk} and the fourth-order terms in μ_k . The following general formula for the element contributions can be used.

$$\begin{aligned} \Phi_e'''' u_1 u_2 u_3 u_4 &= \mathbf{t}_{1e}^T \boldsymbol{\varrho}_3[\mathbf{d}_{2e}, \mathbf{d}_{3e}, \mathbf{d}_{4e}] + \mathbf{t}_{2e}^T \boldsymbol{\varrho}_3[\mathbf{d}_{3e}, \mathbf{d}_{4e}, \mathbf{d}_{1e}] \\ &+ \mathbf{t}_{3e}^T \boldsymbol{\varrho}_3[\mathbf{d}_{4e}, \mathbf{d}_{1e}, \mathbf{d}_{2e}] + \mathbf{t}_{4e}^T \boldsymbol{\varrho}_3[\mathbf{d}_{1e}, \mathbf{d}_{2e}, \mathbf{d}_{3e}] \\ &+ \mathbf{t}_{0e}^T \boldsymbol{\varrho}_4[\mathbf{d}_{1e}, \mathbf{d}_{2e}, \mathbf{d}_{3e}, \mathbf{d}_{4e}] \end{aligned} \quad (8.27)$$

where function $\boldsymbol{\varrho}_4[\cdot]$ is obtained by

$$\boldsymbol{\varrho}_4[\mathbf{d}_{1e}, \mathbf{d}_{2e}, \mathbf{d}_{3e}, \mathbf{d}_{4e}] = \mathbf{D} \mathbf{g}_4[\mathbf{d}_{1e}, \mathbf{d}_{2e}, \mathbf{d}_{3e}, \mathbf{d}_{4e}].$$

Energy variations using quadratic local modeling

When using quadratic local modeling we only need to redefine the expressions for $\boldsymbol{\varrho}_2[\cdot]$, $\boldsymbol{\varrho}_3[\cdot]$ and $\boldsymbol{\varrho}_4[\cdot]$ which appear in the energy variations. By substituting eq. (8.11a) in eq. (8.11b) we obtain

$$\boldsymbol{\varrho}_2[\mathbf{d}_{1e}, \mathbf{d}_{2e}] = \mathbf{D} \mathbf{g}_{2(1,2)} + \boldsymbol{\varrho}_q[\mathbf{g}_{1(1)}, \mathbf{g}_{1(2)}] + \boldsymbol{\varrho}_q[\mathbf{d}_{0e}, \mathbf{g}_{2(1,2)}] \quad (8.28a)$$

$$\begin{aligned} \boldsymbol{\varrho}_3[\mathbf{d}_{1e}, \mathbf{d}_{2e}, \mathbf{d}_{3e}] = & \mathbf{D}\mathbf{g}_{3(1,2,3)} + \boldsymbol{\varrho}_q[\mathbf{g}_{1(1)}, \mathbf{g}_{2(2,3)}] + \boldsymbol{\varrho}_q[\mathbf{g}_{1(2)}, \mathbf{g}_{2(1,3)}] \\ & + \boldsymbol{\varrho}_q[\mathbf{g}_{1(3)}, \mathbf{g}_{2(1,2)}] + \boldsymbol{\varrho}_q[\mathbf{d}_{0e}, \mathbf{g}_{3(1,2,3)}] \end{aligned} \quad (8.28b)$$

$$\begin{aligned} \boldsymbol{\varrho}_4[\mathbf{d}_{1e}, \mathbf{d}_{2e}, \mathbf{d}_{3e}, \mathbf{d}_{4e}] = & \mathbf{D}\mathbf{g}_{4(1,2,3,4)} + \boldsymbol{\varrho}_q[\mathbf{g}_{1(1)}, \mathbf{g}_{3(2,3,4)}] + \boldsymbol{\varrho}_q[\mathbf{g}_{1(2)}, \mathbf{g}_{3(1,3,4)}] \\ & + \boldsymbol{\varrho}_q[\mathbf{g}_{1(3)}, \mathbf{g}_{3(1,2,4)}] + \boldsymbol{\varrho}_q[\mathbf{g}_{1(4)}, \mathbf{g}_{3(1,2,3)}] \\ & + \boldsymbol{\varrho}_q[\mathbf{g}_{2(1,2)}, \mathbf{g}_{2(3,4)}] + \boldsymbol{\varrho}_q[\mathbf{g}_{2(1,3)}, \mathbf{g}_{2(2,4)}] \\ & + \boldsymbol{\varrho}_q[\mathbf{g}_{2(1,4)}, \mathbf{g}_{2(2,3)}] + \boldsymbol{\varrho}_q[\mathbf{d}_{0e}, \mathbf{g}_{4(1,2,3,4)}]. \end{aligned} \quad (8.28c)$$

where the synthetic notation $\mathbf{g}_{k,(i,j,\dots)} \equiv \mathbf{g}_k[\mathbf{u}_{ie}, \mathbf{u}_{je}, \dots]$, $k, i, j = 1, \dots, 4$ has been used, for an easier writing.

Note that when using quadratic local modeling, the expressions for $\boldsymbol{\varrho}_2$, $\boldsymbol{\varrho}_3$ and $\boldsymbol{\varrho}_4$ also depend on the initial local displacement \mathbf{d}_{0e} which does not affect the linear model at all. Its influence is, however, very small and can be neglected.

8.3 Local beam modeling

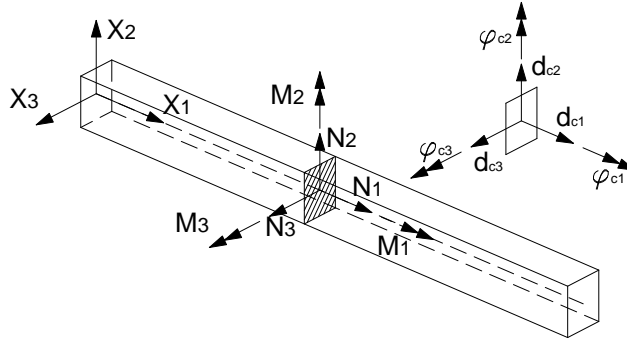


Fig. 8.1: Static and kinematic quantities in CR frame for the beam.

The corotational description presented above, is now applied to a 3D beam element. We assume that the reference configuration of the beam is straight, the initial curvatures being taken into account through a nonzero initial displacement. The local Cartesian reference frame $\{X_1, X_2, X_3\}$, with versors $\{\mathbf{e}_1, \mathbf{e}_2, \mathbf{e}_3\}$, is aligned to the beam axis (\mathbf{e}_1) and to the principal inertia axis of the cross section (\mathbf{e}_2 and \mathbf{e}_3), as shown in fig. 8.1, so that the section position $\mathbf{X} = s \mathbf{e}_1$ is identified by the real abscissa $s \in [0 \dots \ell]$, ℓ being the beam length.

8.3.1 Linear local modeling for the beam

The local beam modeling is taken from that presented in [93], directly derived from Saint Venant general rod theory. We will denote by $\mathbf{N}[s]$ and $\mathbf{M}[s]$ the stress resultants over the section and by $\boldsymbol{\varepsilon}[s]$ and $\boldsymbol{\chi}[s]$ the corresponding work-conjugated section strains. The latter collect axial and shear elongations and torsional and flexural curvatures, respectively and are related to the displacements $\mathbf{d}[s]$ and rotations $\boldsymbol{\varphi}[s]$ of the section by the linear kinematics relationship

$$\begin{cases} \boldsymbol{\varepsilon} = \mathbf{d}_{c,s} + \mathbf{e}_1 \times \boldsymbol{\varphi}_c \\ \boldsymbol{\chi} = \boldsymbol{\varphi}_{c,s} \end{cases} \quad (8.29)$$

As shown in [?] we have

$$\begin{Bmatrix} \boldsymbol{\varepsilon} \\ \boldsymbol{\chi} \end{Bmatrix} = \mathbf{H} \begin{Bmatrix} \mathbf{N} \\ \mathbf{M} \end{Bmatrix} \quad (8.30)$$

where the symmetric and positive defined compliance matrix \mathbf{H} is easily obtained, as a function of E and G elastic modula and section geometry, through a numerical strategy. The element strain energy (8.8) can then be rewritten

$$\Phi[u] = \int_0^\ell \left\{ \mathbf{N}^T \boldsymbol{\varepsilon} + \mathbf{M}^T \boldsymbol{\chi} - \frac{1}{2} \begin{Bmatrix} \mathbf{N} \\ \mathbf{M} \end{Bmatrix}^T \mathbf{H} \begin{Bmatrix} \mathbf{N} \\ \mathbf{M} \end{Bmatrix} \right\} ds \quad (8.31)$$

The assumption of zero body forces implies both \mathbf{N} and the torsional component M_1 of \mathbf{M} be constant while the flexural components \mathbf{M}_2 and \mathbf{M}_3 vary linearly along the beam axis, according to the value shear components N_2 and N_3 . In this way we obtain the following stress interpolation law

$$\begin{cases} N_1[s] = n \\ N_2[s] = -m_{3e}/\ell \\ N_3[s] = m_{2e}/\ell \end{cases}, \quad \begin{cases} M_1[s] = -\frac{1}{2} m_{1s} \\ M_2[s] = -\frac{1}{2} m_{2s} + \left(\frac{1}{2} - \frac{s}{\ell}\right) m_{e2} \\ M_3[s] = -\frac{1}{2} m_{3s} + \left(\frac{1}{2} - \frac{s}{\ell}\right) m_{e3} \end{cases} \quad (8.32a)$$

depending on six stress parameters we can collect in the element stress element vector

$$\mathbf{t}_e := [n_e, m_{2e}, m_{3e}, m_{1s}, m_{2s}, m_{3s}]^T \quad (8.32b)$$

The complementary energy in (8.31) can then be rewritten in the form

$$\int_0^\ell \left\{ \begin{Bmatrix} \mathbf{N} \\ \mathbf{M} \end{Bmatrix}^T \mathbf{H} \begin{Bmatrix} \mathbf{N} \\ \mathbf{M} \end{Bmatrix} \right\} ds = \mathbf{t}_e^T \mathbf{K}_c^{-1} \mathbf{t}_e \quad (8.33)$$

\mathbf{K}_e being the so called element stiffness matrix. Note that, when the flexural and shear of the section coincide, matrix \mathbf{K}_e simplifies in the usual diagonal form

$$\mathbf{K}_e = \text{diag} \left[EA\ell, \frac{12EJ_2}{\ell(1+\beta_3)}, \frac{12EJ_3}{\ell(1+\beta_2)}, \frac{4GJ_t^*}{\ell}, \frac{4EJ_2}{\ell}, \frac{4EJ_3}{\ell} \right]$$

where A , J_2 and J_3 are the area and flexural inertia of section, J_t^* the torsional inertia, and $\beta_2 = 12EJ_3/GA_2\ell^2$ and $\beta_3 = 12EJ_2/GA_3\ell^2$ the so called shear factors, A_2^* and A_3^* being the shear areas.

The strain work in (8.31), using interpolation (8.32), becomes

$$\int_0^\ell \{ \mathbf{N}^T \boldsymbol{\varepsilon} + \mathbf{M}^T \boldsymbol{\chi} \} ds = \mathbf{M}_j^T \boldsymbol{\varphi}_j - \mathbf{M}_i^T \boldsymbol{\varphi}_i + \mathbf{N}^T (\mathbf{d}_j - \mathbf{d}_i) = \mathbf{t}_e^T \mathbf{D} \mathbf{d}_{ce} \quad (8.34a)$$

where i and j denote quantities evaluated for $s = 0$ and $s = \ell$ and where

$$\mathbf{D} = \begin{bmatrix} 1 & \cdot & \cdot & \cdot & \cdot & \cdot & \cdot & \cdot & \cdot \\ \cdot & \cdot & -1 & \cdot & 1 & \cdot & \cdot & \cdot & \cdot \\ \cdot & 1 & \cdot & \cdot & \cdot & 1 & \cdot & \cdot & \cdot \\ \cdot & \cdot & \cdot & \cdot & \cdot & \cdot & 1 & \cdot & \cdot \\ \cdot & \cdot & \cdot & \cdot & \cdot & \cdot & \cdot & 1 & \cdot \\ \cdot & \cdot & \cdot & \cdot & \cdot & \cdot & \cdot & \cdot & 1 \end{bmatrix}, \quad \mathbf{d}_{ce} = \begin{Bmatrix} \phi_{cr} \\ \phi_{ce} \\ \phi_{cs} \end{Bmatrix} \quad (8.34b)$$

ϕ_{cr} , ϕ_{ce} and ϕ_{cs} being the *natural modes* of the element [?]:

$$\phi_{cr} = \frac{\mathbf{d}_{cj} - \mathbf{d}_{ci}}{\ell}, \quad \phi_{cs} = \frac{\varphi_{ci} - \varphi_{cj}}{2}, \quad \phi_{ce} = \frac{\varphi_{ci} + \varphi_{cj}}{2} \quad (8.34c)$$

8.3.2 The CR transformation for the beam

Beam kinematics will be governed by their displacements by reference to the initial configuration, collected in the nine dimensional vector

$$\mathbf{d}_e := \{ \phi_r, \phi_e, \phi_s \}^T \quad (8.35)$$

where

$$\phi_r = \frac{\mathbf{d}_j - \mathbf{d}_i}{\ell}, \quad \phi_e = \frac{\varphi_i + \varphi_j}{2}, \quad \phi_s = \frac{\varphi_i - \varphi_j}{2}$$

The relation (8.15), relating these displacements with the analogous ones referred to the current configuration and defined in eq. (8.34), becomes

$$\mathbf{g}_e[\mathbf{d}_e] = \{ \mathbf{g}_r, \mathbf{g}_e, \mathbf{g}_s \}^T \quad (8.36)$$

where

$$\mathbf{g}_r = \mathbf{Q}_e^T (\mathbf{e}_1 + \phi_r) - \mathbf{e}_1, \quad \mathbf{g}_e = \frac{\mathbf{g}_i + \mathbf{g}_j}{2}, \quad \mathbf{g}_s = \frac{\mathbf{g}_i - \mathbf{g}_j}{2}$$

and \mathbf{g}_i and \mathbf{g}_j express the relation between the deformational and global rotations of nodes i and j of the element. From eq. (8.3c) we have

$$\mathbf{g}_i := \log [\mathbf{Q}_e^T \mathbf{R}[\varphi_i]] \quad , \quad \mathbf{g}_j := \log [\mathbf{Q}_e^T \mathbf{R}[\varphi_j]]$$

After some algebra, we obtain the following fourth-order Taylor expansion

$$\begin{aligned} \mathbf{g}_k &= \varphi_k - \boldsymbol{\alpha}_e - \frac{1}{2} \mathbf{W}[\boldsymbol{\alpha}_e] \varphi_k + \frac{1}{12} (\mathbf{W}[\boldsymbol{\alpha}_e]^2 \varphi_k - \mathbf{W}[\varphi_k]^2 \boldsymbol{\alpha}_e) \\ &\quad - \frac{1}{24} \mathbf{W}[\varphi_k] \mathbf{W}^2[\boldsymbol{\alpha}_e] \varphi_k + \dots \quad , \quad k = i, j \end{aligned} \quad (8.37)$$

Eqs.(8.37) are unaffected by the CR translation \mathbf{c} and are fully defined once the relation between the element CR rotation vector $\boldsymbol{\alpha}_e$ and the displacement vector \mathbf{d}_e has been stated. A possible choice is that of defining the rotation $\mathbf{Q}_e = [\mathbf{i}_1, \mathbf{i}_2, \mathbf{i}_3]$ according to the so called secant rule, i.e. by selecting \mathbf{i}_1 along the line connecting beam nodes and \mathbf{i}_2 and \mathbf{i}_3 in an appropriate fashion to eliminate the torsional rigid motion:

$$\mathbf{i}_1 := \frac{\mathbf{e}_1 + \boldsymbol{\phi}_r}{\|\mathbf{e}_1 + \boldsymbol{\phi}_r\|} \quad , \quad \mathbf{i}_3 := \frac{\mathbf{i}_1 \times \mathbf{q}}{\|\mathbf{i}_1 \times \mathbf{q}\|} \quad , \quad \mathbf{i}_2 := \mathbf{i}_3 \times \mathbf{i}_1 \quad (8.38)$$

where

$$\mathbf{q} := \mathbf{R}[\varphi_m] \mathbf{R}_i \mathbf{e}_2 \quad , \quad \varphi_m := \frac{1}{2} \log [\mathbf{R}_j \mathbf{R}_i^T]$$

This choice gives good accuracy even if it results in a strongly nonlinear expression between the rigid rotation vector $\boldsymbol{\alpha}_e$ and \mathbf{d}_e . A notable simplification is obtained by defining $\mathbf{Q}_e := \mathbf{R}[\varphi_m] \mathbf{R}_i$, we obtain

$$\boldsymbol{\alpha}_e = \boldsymbol{\phi}_e - \frac{1}{12} \mathbf{W}[\boldsymbol{\phi}_s]^2 \boldsymbol{\phi}_e \quad (8.39)$$

However several other choices are possible the simplest one being obtained by defining the CR rotation vector $\boldsymbol{\alpha}_e$ as a simple average of nodal rotations

$$\boldsymbol{\alpha}_e := \frac{1}{2} (\varphi_i + \varphi_j) = \boldsymbol{\phi}_e \quad (8.40)$$

This choice, which can also be viewed as a simplification of (8.39), gives accurate results and could be the best compromise. The analytical expressions of the strain variations in this simple case are reported here in explicit form. The analogous expressions, corresponding to the other possible choices for $\mathbf{Q}[\mathbf{d}_e]$, are noticeably more complex and are not given here. In fact, their derivation can be easily performed with the aid of symbolic algebraic manipulation software, see [104].

Strain energy variations for linear local beam modeling

Making $\mathbf{W}_e := \mathbf{W}[\phi_e]$ and assuming that $\boldsymbol{\alpha}_e$ is defined by eq. (8.40), we have

$$\begin{aligned}
\mathbf{g}_r[\mathbf{d}_e] &= \phi_r + \mathbf{W}_1 \phi_e + \frac{1}{2} (\mathbf{W}_e^2 \mathbf{e}_1 - 2\mathbf{W}_e \phi_r) + \frac{1}{6} (3\mathbf{W}_e^2 \phi_r - \mathbf{W}_e^3 \mathbf{e}_1) \\
&\quad + \frac{1}{24} (\mathbf{W}_e^4 \mathbf{e}_1 - 4\mathbf{W}_e^3 \phi_r) \\
\mathbf{g}_e[\mathbf{d}_e] &= -\frac{1}{12} \mathbf{W}_s^2 \phi_e - \frac{1}{24} \mathbf{W}_s \mathbf{W}_e^2 \phi_s \\
\mathbf{g}_s[\mathbf{d}_e] &= \phi_s - \frac{\mathbf{W}_e}{2} \phi_s + \frac{\mathbf{W}_e^2}{6} \phi_s - \frac{\mathbf{W}_e^3}{24} \phi_s
\end{aligned} \tag{8.41}$$

being $\mathbf{W}_1 := \text{spin}[\mathbf{e}_1]$. We then obtain

$$\mathbf{g}_{1r}[\mathbf{d}_{1e}] = \phi_{1r} + \mathbf{W}_1 \phi_{1e} \quad , \quad \mathbf{g}_{1e}[\mathbf{d}_{1e}] = \mathbf{0} \quad , \quad \mathbf{g}_{1s}[\mathbf{d}_{1e}] = \phi_{1s}$$

which, through eq.(8.20), provides

$$\mathbf{L}_1 = \begin{bmatrix} \mathbf{I}_3 & \mathbf{W}_1 & \mathbf{0}_3 \\ \mathbf{0}_3 & \mathbf{0}_3 & \mathbf{0}_3 \\ \mathbf{0}_3 & \mathbf{0}_3 & \mathbf{I}_3 \end{bmatrix}$$

Introducing $\mathbf{W}_{ie} := \mathbf{W}[\phi_{ie}]$ and $\mathbf{W}_{is} := \mathbf{W}[\phi_{is}]$, we also obtain

$$\begin{aligned}
\mathbf{g}_{2r}[\mathbf{d}_{1e}, \mathbf{d}_{2e}] &= \frac{1}{2} (\mathbf{W}_{2e} \mathbf{W}_{1e} + \mathbf{W}_{1e} \mathbf{W}_{2e}) \mathbf{e}_1 - (\mathbf{W}_{2e} \phi_{1r} + \mathbf{W}_{1e} \phi_{2r}) \\
\mathbf{g}_{2e}[\mathbf{d}_{1e}, \mathbf{d}_{2e}] &= \mathbf{0} \\
\mathbf{g}_{2s}[\mathbf{d}_{1e}, \mathbf{d}_{2e}] &= \frac{1}{2} (\mathbf{W}_{2s} \phi_{1e} + \mathbf{W}_{1s} \phi_{2e})
\end{aligned}$$

The previous equation allows the explicit evaluation of $\boldsymbol{\varrho}_1[\mathbf{d}_1]$ and $\boldsymbol{\varrho}_2[\mathbf{d}_1, \mathbf{d}_2]$. Introducing the symmetric matrix

$$\mathbf{W}_2[\phi_i, \phi_j] = \frac{1}{6} (\mathbf{W}[\phi_i] \mathbf{W}[\phi_j] + \mathbf{W}[\phi_j] \mathbf{W}[\phi_i])$$

which satisfies the condition

$$\mathbf{n}^T \mathbf{W}_2[\phi_i, \delta\phi] \phi_j = \delta\phi^T \mathbf{W}_2[\mathbf{n}, \phi_j] \phi_i$$

for any $\mathbf{n}, \delta\phi \in \mathbb{R}^3$, matrix $\mathbf{G}[\mathbf{t}_{0e}]$, defined by the equivalence (8.20), becomes

$$\mathbf{G}_l[\mathbf{t}_{0e}] = \begin{bmatrix} \mathbf{0}_3 & \mathbf{W}[\mathbf{n}_{e0}] & \mathbf{0}_3 \\ -\mathbf{W}[\mathbf{n}_{e0}] & 3\mathbf{W}_2[\mathbf{n}_{e0}, \mathbf{e}_1] & -\mathbf{W}[\mathbf{m}_{s0}]/2 \\ \mathbf{0}_3 & \mathbf{W}[\mathbf{m}_{s0}]/2 & \mathbf{0}_3 \end{bmatrix} \tag{8.42}$$

where $\mathbf{n}_e := [n_e, -m_{e3}/l, m_{e2}/l]^T$, $\mathbf{m}_s = [m_{s1}, m_{s2}, m_{s3}]^T$ and $\mathbf{m}_e = [0, m_{e2}, m_{e3}]^T$, when referring to the local linear model (8.11b). The third variation of eq (8.41) is:

$$\begin{aligned} \mathbf{g}_{3r}[\mathbf{d}_{1e}, \mathbf{d}_{2e}, \mathbf{d}_{3e}] &= \mathbf{W}_2[\phi_{2e}, \phi_{3e}](3\phi_{1r} + \mathbf{W}_1\phi_{1e}) + \mathbf{W}_2[\phi_{1e}, \phi_{3e}](3\phi_{2r} + \mathbf{W}_1\phi_{2e}) \\ &\quad + \mathbf{W}_2[\phi_{1e}, \phi_{2e}](3\phi_{3r} + \mathbf{W}_1\phi_{3e}) \\ \mathbf{g}_{3e}[\mathbf{d}_{1e}, \mathbf{d}_{2e}, \mathbf{d}_{3e}] &= -\frac{1}{2}(\mathbf{W}_2[\phi_{2s}, \phi_{3s}]\phi_{1e} + \mathbf{W}_2[\phi_{1s}, \phi_{3s}]\phi_{2e} + \mathbf{W}_2[\phi_{1s}, \phi_{2s}]\phi_{3e}) \\ \mathbf{g}_{3s}[\mathbf{d}_{1e}, \mathbf{d}_{2e}, \mathbf{d}_{3e}] &= \mathbf{W}_2[\phi_{2e}, \phi_{3e}]\phi_{1s} + \mathbf{W}_2[\phi_{1e}, \phi_{3e}]\phi_{2s} + \mathbf{W}_2[\phi_{1e}, \phi_{2e}]\phi_{3s} \end{aligned}$$

thus allowing the evaluation of $\boldsymbol{\rho}_3[\mathbf{d}_{1e}, \mathbf{d}_{2e}, \mathbf{d}_{3e}]$ and of the third energy variations in scalar form, through eq. (8.24a). To recover their vectorial form (8.25), we need vector \mathbf{s}_{ed} defined in eq.(8.26). This can be expressed as

$$\mathbf{s}_{ed} = \mathbf{G}[\mathbf{t}_{1e}]\mathbf{d}_{2e} + \mathbf{G}[\mathbf{t}_{2e}]\mathbf{d}_{1e} + \mathbf{s}_0 \quad (8.43)$$

\mathbf{s}_0 being defined by the equivalence

$$\delta \mathbf{d}_e^T \mathbf{s}_e = \mathbf{t}_{0e}^T \boldsymbol{\rho}_3[\mathbf{d}_{1e}, \mathbf{d}_{2e}, \delta \mathbf{d}_e]$$

After some algebra, we obtain

$$\begin{aligned} \mathbf{s}_{0r} &= 3\mathbf{W}_2[\phi_{1e}, \phi_{2e}]\mathbf{n}_{e0} \\ \mathbf{s}_{0e} &= (\mathbf{W}_2[\omega_1, \mathbf{n}_0] + \mathbf{W}_2[\phi_{1s}, \mathbf{m}_{s0}])\phi_{2e} + (\mathbf{W}_2[\omega_2, \mathbf{n}_0] + \mathbf{W}_2[\phi_{2s}, \mathbf{m}_{s0}])\phi_{1e} \\ &\quad - \frac{1}{2}\mathbf{W}_2[\phi_{1s}, \phi_{2s}]\mathbf{m}_{e0} - \mathbf{W}_1\mathbf{W}_2[\phi_{1e}, \phi_{2e}]\mathbf{n}_{e0} \\ \mathbf{s}_{0s} &= -\frac{1}{2}(\mathbf{W}_2[\phi_{1e}, \mathbf{m}_{e0}]\phi_{2s} + \mathbf{W}_2[\phi_{2e}, \mathbf{m}_{e0}]\phi_{1s}) + \mathbf{W}_2[\phi_{1e}, \phi_{2e}]\mathbf{m}_{s0} \end{aligned}$$

where

$$\omega_1 = 3\phi_{1r} + \mathbf{W}_1\phi_{1e} \quad , \quad \omega_2 = 3\phi_{2r} + \mathbf{W}_1\phi_{2e}$$

Finally, introducing the following symmetric cubic form,

$$\mathbf{W}_3[\phi_i, \phi_j, \phi_k] = \frac{1}{4}(\mathbf{W}[\phi_i]\mathbf{W}_2[\phi_j, \phi_k] + \mathbf{W}[\phi_j]\mathbf{W}_2[\phi_k, \phi_i] + \mathbf{W}[\phi_k]\mathbf{W}_2[\phi_i, \phi_j])$$

the expressions for the fourth-order variations of $\mathbf{g}[\mathbf{d}_e]$ are:

$$\begin{aligned} \mathbf{g}_{4r}[\dots] &= -\mathbf{W}_3[\phi_{4e}, \phi_{3e}, \phi_{2e}](4\phi_{1r} + \mathbf{W}_1\phi_{1e}) - \mathbf{W}_3[\phi_{4e}, \phi_{3e}, \phi_{1e}](4\phi_{2r} + \mathbf{W}_1\phi_{2e}) \\ &\quad - \mathbf{W}_3[\phi_{4e}, \phi_{2e}, \phi_{1e}](4\phi_{3r} + \mathbf{W}_1\phi_{3e}) - \mathbf{W}_3[\phi_{3e}, \phi_{2e}, \phi_{1e}](4\phi_{4r} + \mathbf{W}_1\phi_{4e}) \\ \mathbf{g}_{4e}[\dots] &= -\mathbf{W}_3[\phi_{4s}, \phi_{3e}, \phi_{2e}]\phi_{1s} - \mathbf{W}_3[\phi_{4s}, \phi_{3e}, \phi_{1e}]\phi_{2s} \\ &\quad - \mathbf{W}_3[\phi_{4s}, \phi_{2e}, \phi_{1e}]\phi_{3s} - \mathbf{W}_3[\phi_{3s}, \phi_{2e}, \phi_{1e}]\phi_{4s} \\ \mathbf{g}_{4s}[\dots] &= -\mathbf{W}_3[\phi_{4e}, \phi_{3e}, \phi_{2e}]\phi_{1s} - \mathbf{W}_3[\phi_{4e}, \phi_{3e}, \phi_{1e}]\phi_{2s} \\ &\quad - \mathbf{W}_3[\phi_{4e}, \phi_{2e}, \phi_{1e}]\phi_{3s} - \mathbf{W}_3[\phi_{3e}, \phi_{2e}, \phi_{1e}]\phi_{4s} \end{aligned}$$

8.3.3 The assemblage matrix

The assemblage matrix \mathbf{A}_e connects the element vector $\mathbf{u}_e := \{\mathbf{t}_e, \mathbf{d}_e\}^T$ to the global configuration vector $\mathbf{u} := \{\mathbf{t}_g, \mathbf{d}_g\}^T$, taking into account the different format and the different reference frames used by the two vectors.

In particular, the vector \mathbf{u} will collect, in its first part (denoted as \mathbf{t}_g), the stress parameters \mathbf{t}_e , of all elements ($e = 1 \cdots n_e$) and, in its second part (denoted as \mathbf{d}_g), the nodal displacements \mathbf{d}_{gk} and rotations φ_{gk} , for all the nodes ($k = 1 \cdots n_n$), displacements and rotations being expressed within a fixed global frame $\{\mathbf{E}_1, \mathbf{E}_2, \mathbf{E}_3\}$. Conversely, vector \mathbf{u}_e collects, in its first part, the stress parameters of the element \mathbf{t}_e and, in its second part, its natural modes ϕ_r, ϕ_e and ϕ_s , the latter being expressed within a fixed local reference frame $\{\mathbf{e}_1, \mathbf{e}_2, \mathbf{e}_3\}$, chosen according to our assumption that the reference configuration be described by $\mathbf{d}_e = \mathbf{0}$. Denoting the rotation matrix between the global and local reference frames by \mathbf{R}_{ge} , eq. (8.17) becomes

$$\mathbf{u}_e := \begin{bmatrix} \mathbf{I}_6 & \mathbf{0}_3 & \mathbf{0}_3 & \mathbf{0}_3 & \mathbf{0}_3 \\ \mathbf{0}_3 & -\frac{\mathbf{R}_{e0}}{\ell} & \mathbf{0}_3 & \frac{\mathbf{R}_{e0}}{\ell} & \mathbf{0}_3 \\ \mathbf{0}_3 & \mathbf{0}_3 & \frac{1}{2}\mathbf{R}_{e0} & \mathbf{0}_3 & \frac{1}{2}\mathbf{R}_{e0} \\ \mathbf{0}_3 & \mathbf{0}_3 & \frac{1}{2}\mathbf{R}_{e0} & \mathbf{0}_3 & -\frac{1}{2}\mathbf{R}_{e0} \end{bmatrix} \begin{bmatrix} \mathbf{t}_e \\ \mathbf{d}_{gi} \\ \varphi_{gi} \\ \mathbf{d}_{gj} \\ \varphi_{gj} \end{bmatrix} \quad (8.44)$$

Matrix \mathbf{R}_{ge} is conveniently obtained by the secant rule (8.54). With this choice, the initial deformational displacement \mathbf{d}_{e0} of the element will be defined by $\phi_{r0} = \mathbf{0}$, ϕ_{e0} and ϕ_{s0} being obtained through

$$\varphi_{i0} = \log [\mathbf{R}_{ge}^T \mathbf{R}[\varphi_{gi}]] \quad , \quad \varphi_{j0} = \log [\mathbf{R}_{ge}^T \mathbf{R}[\varphi_{gj}]] \quad (8.45)$$

where φ_{gi} and φ_{gj} are the rotation vectors of the nodes of the element in the reference configuration.

8.3.4 The quadratic local modeling for the beam

The quadratic local model is defined by substituting eq.(8.29) with the strain measure obtained as a coherent second-order expansion of the Reissner-Antman strain measure [35]

$$\begin{cases} \boldsymbol{\epsilon} = \mathbf{d}_{c,s} - \mathbf{W}_c(\mathbf{e}_1 + \mathbf{d}_{c,s}) + \frac{1}{2}\mathbf{W}_c^2\mathbf{e}_1 \\ \boldsymbol{\chi} = \varphi_{c,s} - \frac{1}{2}\mathbf{W}_c\varphi_{c,s} \end{cases} \quad (8.46)$$

with $\mathbf{W}_c = \text{spin}[\varphi_c]$.

With respect to the linear local modeling we only need to evaluate eq.(8.9) now using eq.(8.46) instead of eq. (8.29). However, it is necessary,

to explicitly assume an interpolation for displacements and rotations. We will use the classic polynomial interpolation of the first order beam theory

$$\mathbf{d}_{c,s} = \mathbf{W}_c \mathbf{e}_1 + \phi_{cr1} \mathbf{e}_1 \quad , \quad \boldsymbol{\varphi}_c[s] = \boldsymbol{\omega}_{cr} + f_s[s] \boldsymbol{\phi}_{cs} + f_e[s] (\boldsymbol{\phi}_{ce} - \boldsymbol{\omega}_{cr}) \quad (8.47)$$

where vector $\boldsymbol{\omega}_{cr}$ is defined as

$$\boldsymbol{\omega}_{cr} = \mathbf{W}_1 \boldsymbol{\phi}_{cr} + \phi_{ce1} \mathbf{e}_1$$

and

$$f_s[s] = f_m[s] \quad , \quad f_e[s] = 1 - 6\frac{s}{\ell} + 6\frac{s^2}{\ell^2} \quad , \quad \int_0^\ell f_s[s] ds = \int_0^\ell f_e[s] ds = \int_0^\ell f_s[s] f_e[s] ds = 0$$

After some algebra we obtain

$$\int_0^\ell \{ \mathbf{N}^T \boldsymbol{\epsilon} + \mathbf{M}^T \boldsymbol{\chi} \} ds = \mathbf{t}_e^T \boldsymbol{\varrho}_l + \frac{1}{2} \mathbf{d}_{ce}^T \boldsymbol{\Psi}[\mathbf{t}_e] \mathbf{d}_{ce} \quad (8.48)$$

$\boldsymbol{\varrho}_l$ being defined by eq. (8.34) and

$$\boldsymbol{\Psi}[\mathbf{t}_e] = \sum_{j=1}^6 t_{ej} \boldsymbol{\Psi}_j \quad (8.49)$$

where $\boldsymbol{\Psi}_j, j = 1 \dots 6$ are given by

$$\begin{aligned} \boldsymbol{\Psi}_1 &= - \begin{bmatrix} 6\frac{\mathbf{W}_1^2}{5} & -\frac{\mathbf{W}_1}{5} & \mathbf{0}_3 \\ \frac{\mathbf{W}_1}{5} & \frac{\mathbf{W}_1^2}{5} & \mathbf{0}_3 \\ \mathbf{0}_3 & \mathbf{0}_3 & \frac{\mathbf{W}_1^2}{3} \end{bmatrix} & \boldsymbol{\Psi}_2 &= \begin{bmatrix} -\mathbf{P}_{13} & -\mathbf{d}_{21} & \mathbf{0}_3 \\ -\mathbf{d}_{12} & \frac{\mathbf{P}_{13}}{2} & \mathbf{0}_3 \\ \mathbf{0}_3 & \mathbf{0}_3 & -\frac{\mathbf{P}_{13}}{6} \end{bmatrix} & \boldsymbol{\Psi}_3 &= \begin{bmatrix} \mathbf{P}_{12} & -\mathbf{d}_{31} & \mathbf{0}_3 \\ -\mathbf{d}_{13} & -\frac{\mathbf{P}_{12}}{2} & \mathbf{0}_3 \\ \mathbf{0}_3 & \mathbf{0}_3 & \frac{\mathbf{P}_{12}}{6} \end{bmatrix} \\ \boldsymbol{\Psi}_4 &= \begin{bmatrix} \mathbf{0}_3 & \mathbf{0}_3 & -\frac{\mathbf{W}_1^2}{2} \\ \mathbf{0}_3 & \mathbf{0}_3 & -\frac{\mathbf{W}_1}{2} \\ -\mathbf{W}_1^2 & \frac{\mathbf{W}_1}{2} & \mathbf{0}_3 \end{bmatrix} & \boldsymbol{\Psi}_5 &= \begin{bmatrix} \mathbf{0}_3 & \mathbf{0}_3 & -\mathbf{d}_{21} \\ \mathbf{0}_3 & \mathbf{0}_3 & \frac{\mathbf{P}_{13}}{2} \\ -\mathbf{d}_{12} & \frac{\mathbf{P}_{13}}{2} & \mathbf{0}_3 \end{bmatrix} & \boldsymbol{\Psi}_6 &= - \begin{bmatrix} \mathbf{0}_3 & \mathbf{0}_3 & \mathbf{d}_{31} \\ \mathbf{0}_3 & \mathbf{0}_3 & \frac{\mathbf{P}_{12}}{2} \\ \mathbf{d}_{13} & \frac{\mathbf{P}_{12}}{2} & \mathbf{0}_3 \end{bmatrix} \end{aligned}$$

where $\mathbf{d}_{hk} = \mathbf{e}_h \mathbf{e}_k^T = \mathbf{d}_{kh}^T$ and $\mathbf{P}_{hk} = \mathbf{d}_{hk} + \mathbf{d}_{kh}$.

The evaluation of strain energy variations, require only the redefinition of $\boldsymbol{\varrho}_2[\cdot], \boldsymbol{\varrho}_3[\cdot]$ and $\boldsymbol{\varrho}_4[\cdot]$, following eqs. (8.28) using expression of $\boldsymbol{\Psi}[\mathbf{t}_e]$ given by eq. (8.49). In this case the geometric matrix becomes:

$$\mathbf{G}_q[\mathbf{t}_{0e}] = \mathbf{G}_l[\mathbf{t}_{0e}] + \mathbf{L}_1^T \boldsymbol{\Psi}[\mathbf{t}_{0e}] \mathbf{L}_1 \quad (8.50)$$

$\mathbf{G}_l[\mathbf{t}_{0e}]$ being provided by eq. (8.42). The expression of geometric matrix $\mathbf{G}_q[\mathbf{t}_{0e}]$ in scalar components given in table 8.1, for the case $\mathbf{d}_{e0} = \mathbf{0}$.

$$\mathbf{G}[t_e] = \begin{bmatrix} 0 & m_{e3} & -m_{e2} & 0 & 0 & 0 & 0 & 0 & 0 \\ m_{e3} & \frac{6n_a}{5} & 0 & -m_{e2} & 0 & -\frac{n_a}{5} & -m_{s2} & m_{s1} & 0 \\ -m_{e2} & 0 & \frac{6n_a}{5} & -m_{e3} & \frac{n_a}{5} & 0 & -m_{s3} & 0 & m_{s1} \\ 0 & -m_{e2} & -m_{e3} & 0 & -\frac{m_{e3}}{2} & \frac{m_{e2}}{2} & 0 & -\frac{m_{s3}}{2} & \frac{m_{s2}}{2} \\ 0 & 0 & \frac{n_a}{5} & -\frac{m_{e3}}{2} & \frac{n_a}{5} & 0 & -\frac{m_{s3}}{2} & 0 & \frac{m_{s1}}{2} \\ 0 & -\frac{n_a}{5} & 0 & \frac{m_{s2}}{2} & 0 & \frac{n_a}{5} & \frac{m_{s2}}{2} & -\frac{m_{s1}}{2} & 0 \\ 0 & -m_{s2} & -m_{s3} & 0 & -\frac{m_{s3}}{2} & \frac{m_{s2}}{2} & 0 & \frac{m_{e3}}{6} & -\frac{m_{e2}}{6} \\ 0 & m_{s1} & 0 & -\frac{m_{s3}}{2} & 0 & -\frac{m_{s1}}{2} & \frac{m_{e3}}{6} & \frac{n_a}{3} & 0 \\ 0 & 0 & m_{s1} & \frac{m_{s2}}{2} & \frac{m_{s1}}{2} & 0 & -\frac{m_{e2}}{6} & 0 & \frac{n_a}{3} \end{bmatrix}$$

Tab. 8.1: Geometric matrix $\mathbf{G}[t_e]$ for the quadratic local model, assuming $\mathbf{d}_{0e} = \mathbf{0}$.

8.4 Some further detail for Riks analysis

8.4.1 Updated scheme

The relation defined by equation (8.6) and (8.7)

$$\begin{cases} \mathbf{d}_c = \mathbf{Q}^T(\mathbf{X} + \mathbf{d} - \mathbf{c}) - \mathbf{X} \\ \mathbf{R}_c = \mathbf{Q}^T \mathbf{R} \end{cases} \quad (8.51)$$

define the kinematics relationship between a fixed and corotational frame. The fixed frame $\{\mathbf{e}_1, \mathbf{e}_2, \mathbf{e}_3\}$ can be assumed coincident with the initial local frame of the beam $\mathbf{Q}_0^g = \{\mathbf{e}_1^g, \mathbf{e}_2^g, \mathbf{e}_3^g\}$ or with the frame defining the rigid body motion associate to the last equilibrium configuration $\mathbf{Q}^s = \{\mathbf{e}_1^s, \mathbf{e}_2^s, \mathbf{e}_3^s\}$. This last assumption [48], corresponds to use as configurations variable the local increments \mathbf{d}_c and $\boldsymbol{\varphi}_c$. In the last equilibrium configuration the description is a standard corotational formulation. Moreover, the stage between two successive configuration could be described using linearized corotational relationship. In particular while the finite quantity could be evaluated using exact corotational relationship, for the evaluation of first and second variation we use a Taylor expansion of corotational expression. This allows to obtain in easy way the structural response e tangent stiffness matrix. Obviously in the incremental variable $\mathbf{u}_c, \boldsymbol{\varphi}_c$ the tangent stiffness is symmetric. Really the formulation with regarding the rotation variable is additive. With respect to initial configuration the global quantities are evaluated using the following relationships:

$$\mathbf{Q}^g = \mathbf{Q}^s \mathbf{Q} \quad \mathbf{d}^g = \mathbf{Q}^g(\mathbf{d}_c + \mathbf{X}) - \mathbf{X} + \mathbf{c}^g \quad \boldsymbol{\varphi}^g = \log(\mathbf{Q}^s \mathbf{R}_c)$$

8.4.2 The CR transformation for the beam

Let be \mathbf{d}_e the nine dimensional vector

$$\mathbf{d}_e := \{\phi_r, \phi_e, \phi_s\}^T \quad (8.52)$$

where

$$\phi_r = \frac{\mathbf{d}_j - \mathbf{d}_i}{\ell}, \quad \phi_e = \frac{\varphi_i + \varphi_j}{2}, \quad \phi_s = \frac{\varphi_i - \varphi_j}{2}$$

are the *natural modes* of the element [24]. The relation (8.15) that defines $\mathbf{g}[\mathbf{d}_e]$ then becomes

$$\mathbf{g}_e[\mathbf{d}_e] = \{\mathbf{g}_r, \mathbf{g}_e, \mathbf{g}_s\}^T \quad (8.53)$$

where

$$\mathbf{g}_r = \mathbf{Q}_e^T(\mathbf{e}_1 + \phi_r) - \mathbf{e}_1, \quad \mathbf{g}_e = \frac{\mathbf{g}_i + \mathbf{g}_j}{2}, \quad \mathbf{g}_s = \frac{\mathbf{g}_i - \mathbf{g}_j}{2}$$

and \mathbf{g}_i and \mathbf{g}_j define the relation between the deformational and global node rotations by means of eq. (8.3c):

$$\mathbf{g}_i := \log [\mathbf{Q}_e^T \mathbf{R}[\varphi_i]] \quad , \quad \mathbf{g}_j := \log [\mathbf{Q}_e^T \mathbf{R}[\varphi_j]]$$

A possible choice is that of defining the rotation $\mathbf{Q}_e = [\mathbf{i}_1, \mathbf{i}_2, \mathbf{i}_3]$ according to the so called secant rule, i.e. by selecting \mathbf{i}_1 along the line connecting beam nodes and \mathbf{i}_2 and \mathbf{i}_3 in an appropriate fashion to eliminate the torsional rigid motion:

$$\mathbf{i}_1 := \frac{\mathbf{e}_1 + \phi_r}{\|\mathbf{e}_1 + \phi_r\|}, \quad \mathbf{i}_3 := \frac{\mathbf{i}_1 \times \mathbf{q}}{\|\mathbf{i}_1 \times \mathbf{q}\|}, \quad \mathbf{i}_2 := \mathbf{i}_3 \times \mathbf{i}_1 \quad (8.54)$$

where

$$\mathbf{q} := \mathbf{R}[\varphi_m] \mathbf{R}_i \mathbf{e}_2 \quad , \quad \varphi_m := \frac{1}{2} \log [\mathbf{R}_j \mathbf{R}_i^T]$$

This choice gives good accuracy even if it results in a strongly nonlinear expression between the rigid rotation vector $\boldsymbol{\alpha}_e$ and \mathbf{d}_e . The transformation law in this case is

$$\begin{aligned} \mathbf{g}_r[\mathbf{d}_e] &= \mathbf{L}_{1r} \mathbf{d}_e + \sum_{i=1}^3 (\mathbf{d}_e^T \mathbf{L}_{2ir} \mathbf{d}_e) \mathbf{e}_i \\ \mathbf{g}_e[\mathbf{d}_e] &= \mathbf{L}_{1e} \mathbf{d}_e + \sum_{i=1}^3 (\mathbf{d}_e^T \mathbf{L}_{2ie} \mathbf{d}_e) \mathbf{e}_i \\ \mathbf{g}_s[\mathbf{d}_e] &= \mathbf{L}_{1s} \mathbf{d}_e + \sum_{i=1}^3 (\mathbf{d}_e^T \mathbf{L}_{2is} \mathbf{d}_e) \mathbf{e}_i \end{aligned}$$

where

$$\begin{aligned}\mathbf{L}_{1r} &= [\mathbf{d}_{11} \quad \mathbf{0}_3 \quad \mathbf{0}_3] \\ \mathbf{L}_{1e} &= [\mathbf{W}_1 \quad \mathbf{d}_{22} + \mathbf{d}_{33} \quad \mathbf{0}_3] \\ \mathbf{L}_{1s} &= [\mathbf{0}_3 \quad \mathbf{0}_3 \quad \mathbf{I}_3]\end{aligned}$$

and

$$\begin{aligned}\mathbf{L}_{2r1} &= \begin{bmatrix} \mathbf{d}_{22} + \mathbf{d}_{33} & \mathbf{0}_3 & \mathbf{0}_3 \\ \mathbf{0}_3 & \mathbf{0}_3 & \mathbf{0}_3 \\ \mathbf{0}_3 & \mathbf{0}_3 & \mathbf{0}_3 \end{bmatrix} \\ \mathbf{L}_{2r2} &= \begin{bmatrix} \mathbf{0}_3 & \mathbf{0}_3 & \mathbf{0}_3 \\ \mathbf{0}_3 & \mathbf{0}_3 & \mathbf{0}_3 \\ \mathbf{0}_3 & \mathbf{0}_3 & \mathbf{0}_3 \end{bmatrix} \\ \mathbf{L}_{2r3} &= \begin{bmatrix} \mathbf{0}_3 & \mathbf{0}_3 & \mathbf{0}_3 \\ \mathbf{0}_3 & \mathbf{0}_3 & \mathbf{0}_3 \\ \mathbf{0}_3 & \mathbf{0}_3 & \mathbf{0}_3 \end{bmatrix} \\ \mathbf{L}_{2e1} &= \frac{1}{2} \begin{bmatrix} \mathbf{P}_{23} & \mathbf{d}_{22} - \mathbf{d}_{33} & \mathbf{0}_3 \\ \mathbf{d}_{22} - \mathbf{d}_{33} & -\mathbf{P}_{23} & \mathbf{0}_3 \\ \mathbf{0}_3 & \mathbf{0}_3 & \mathbf{0}_3 \end{bmatrix} \\ \mathbf{L}_{2e2} &= \begin{bmatrix} -\mathbf{P}_{13} & -\mathbf{d}_{21} & \mathbf{0}_3 \\ -\mathbf{d}_{12} & \frac{1}{2}\mathbf{P}_{13} & \mathbf{0}_3 \\ \mathbf{0}_3 & \mathbf{0}_3 & \mathbf{0}_3 \end{bmatrix} \\ \mathbf{L}_{2e3} &= \begin{bmatrix} \mathbf{P}_{12} & -\mathbf{d}_{32} & \mathbf{0}_3 \\ -\mathbf{d}_{23} & -\frac{1}{2}\mathbf{P}_{12} & \mathbf{0}_3 \\ \mathbf{0}_3 & \mathbf{0}_3 & \mathbf{0}_3 \end{bmatrix} \\ \mathbf{L}_{2s1} &= \frac{1}{2} \begin{bmatrix} \mathbf{0}_3 & \mathbf{0}_3 & \mathbf{d}_{22} + \mathbf{d}_{33} \\ \mathbf{0}_3 & \mathbf{0}_3 & \mathbf{0}_3 \\ \mathbf{d}_{22} + \mathbf{d}_{33} & \mathbf{0}_3 & \mathbf{0}_3 \end{bmatrix} \\ \mathbf{L}_{2s2} &= \frac{1}{2} \begin{bmatrix} \mathbf{0}_3 & \mathbf{0}_3 & -\mathbf{d}_{21} \\ \mathbf{0}_3 & \mathbf{0}_3 & \mathbf{d}_{13} \\ -\mathbf{d}_{12} & \mathbf{d}_{31} & \mathbf{0}_3 \end{bmatrix} \\ \mathbf{L}_{2s3} &= \frac{1}{2} \begin{bmatrix} \mathbf{0}_3 & \mathbf{0}_3 & -\mathbf{d}_{31} \\ \mathbf{0}_3 & \mathbf{0}_3 & \mathbf{d}_{12} \\ -\mathbf{d}_{13} & \mathbf{d}_{21} & \mathbf{0}_3 \end{bmatrix}\end{aligned}$$

8.4.3 Expressions for the strain variations for linear model

In case of secant frame (8.54) and linear local model, the structural response can be written as:

$$\mathbf{s}_e = \{\mathbf{s}_{te}, \mathbf{s}_{de}\}^T$$

whit

$$\begin{aligned}\mathbf{s}_{te} &= \boldsymbol{\varrho}[\mathbf{d}_e] - \mathbf{K}_c^{-1} \mathbf{t}_e \\ \mathbf{s}_{de} &= \{\mathbf{s}_{re}, \mathbf{s}_{ee}, \mathbf{s}_{se}\}^T\end{aligned}$$

and

$$\begin{aligned}\mathbf{s}_{re} &= (\mathbf{L}_{1r}^T + \sum_{i=1}^3 (\mathbf{L}_{2ir} \mathbf{d}_e) \mathbf{e}_i^T) \mathbf{D}^T \mathbf{t}_e \\ \mathbf{s}_{ee} &= (\mathbf{L}_{1e}^T + \sum_{i=1}^3 (\mathbf{L}_{2ie} \mathbf{d}_e) \mathbf{e}_i^T) \mathbf{D}^T \mathbf{t}_e \\ \mathbf{s}_{se} &= (\mathbf{L}_{1s}^T + \sum_{i=1}^3 (\mathbf{L}_{2is} \mathbf{d}_e) \mathbf{e}_i^T) \mathbf{D}^T \mathbf{t}_e\end{aligned}$$

For the definition of the Hessian, the evaluation of matrix \mathbf{L} give:

$$\mathbf{L} = \begin{bmatrix} \mathbf{L}_{1r} + \sum_{i=1}^3 \mathbf{e}_i \mathbf{d}_e^T \mathbf{L}_{2ir} \\ \mathbf{L}_{1e} + \sum_{i=1}^3 \mathbf{e}_i \mathbf{d}_e^T \mathbf{L}_{2ie} \\ \mathbf{L}_{1s} + \sum_{i=1}^3 \mathbf{e}_i \mathbf{d}_e^T \mathbf{L}_{2is} \end{bmatrix}$$

while for the matrix $\mathbf{G}[\mathbf{t}_e]$, assuming $\mathbf{D} = [\mathbf{D}_r, \mathbf{D}_e, \mathbf{D}_s]$, we have that

$$\mathbf{G}[\mathbf{t}_e] = \sum_{i=1}^3 (\mathbf{t}_e^T \mathbf{D}_r \mathbf{e}_i \mathbf{L}_{2ir} + \mathbf{t}_e^T \mathbf{D}_e \mathbf{e}_i \mathbf{L}_{2ie} + \mathbf{t}_e^T \mathbf{D}_s \mathbf{e}_i \mathbf{L}_{2is})$$

8.4.4 Computational remarks

The use of quaternion algebra are more efficient from computationally point of view The four components defining a quaternion $\mathbf{p} = [p_0, \bar{\mathbf{p}}]^T = [p_0, p_1, p_2, p_3]^T$ is defined as

$$p_0 = \cos \frac{\theta}{2} \quad p_i = \frac{\theta_i}{\theta} \sin \frac{\theta}{2} \quad i = 1..3$$

The evaluation of rotation vector $\boldsymbol{\theta}$ starting from a matrix $\mathbf{R}[\boldsymbol{\theta}]$ defined by eq.(8.3), can be done using the Spurrier [96] algorithm. Choose the largest between $\text{tr}(\mathbf{R}[\boldsymbol{\theta}]) = \sum_{i=1}^3 R_{ii}$ and R_{ii} , $i = 1..3$,

If $\text{tr}(\mathbf{R}[\boldsymbol{\theta}]) \geq R_{ii}$

$$p_0 = \frac{1}{2} \sqrt{1 + \text{tr} \mathbf{R}[\boldsymbol{\theta}]} \quad p_i = \frac{1}{4} (R_{kj} - R_{jk} / p_0)$$

being j and k the cyclic permutation of i .

Otherwise if $\text{tr}(\mathbf{R}[\boldsymbol{\theta}]) \geq R_{ii}$

$$\begin{aligned}p_i &= \frac{1}{2} \sqrt{\frac{1}{2} + \frac{1}{4} (1 - \text{tr}(\mathbf{R}[\boldsymbol{\theta}]))} \quad p_0 = \frac{1}{4} (R_{kj} - R_{jk} / p_i) \\ p_m &= \frac{1}{4} (R_{mi} + R_{im}) / p_i \quad m = j, k\end{aligned}$$

Once evaluated \mathbf{p} is easy to evaluate $\boldsymbol{\theta}$.

The use of quaternion is also convenient in the evaluation of rotation vector $\boldsymbol{\theta}_{12}$ associate to the rotation $\mathbf{R}[\boldsymbol{\theta}_{12}]$ defined as $\mathbf{R}[\boldsymbol{\theta}_{12}] = \mathbf{R}[\boldsymbol{\theta}_1]\mathbf{R}[\boldsymbol{\theta}_2]$. In particular defining $\mathbf{p}_1, \mathbf{p}_2$ and \mathbf{p}_{12} the quaternion associate to the rotation vectors $\boldsymbol{\theta}_1, \boldsymbol{\theta}_2, \boldsymbol{\theta}_{12}$ the following formula holds :

$$\mathbf{p}_{12} = \begin{bmatrix} p_{01}p_{02} - \bar{\mathbf{p}}_1^T \bar{\mathbf{p}}_2 \\ p_{01}\bar{\mathbf{p}}_2 + p_{02}\bar{\mathbf{p}}_1 - \bar{\mathbf{p}}_1 \wedge \bar{\mathbf{p}}_2 \end{bmatrix}$$

8.5 Numerical results

Some numerical tests have been performed to investigate the accuracy of the proposed approach, the convergence behavior at mesh refining and the influence of different choices in the local modeling, i.e. linear or quadratic, as well as in the definition of the CR rotation vector $\boldsymbol{\alpha}_e$, i.e. according to the secant frame (8.54) (*Sec*) or to the average rotation (8.40) (*Mid*) strategies.

The results are reported here, including the graph of the equilibrium path and the relevant quantities of the asymptotic analysis, i.e. the buckling multiplier λ_b , the initial postbuckling slope $\mathcal{A} := \mathcal{A}_{111}$ and the initial postbuckling curvature $\mathcal{B} := \mathcal{B}_{1111}$. The path is always compared with the one obtained through a careful path-following analysis using the commercial code **ABAQUS**; the synthetic scalar results are compared with the "exact" analytical ones, when these are possible.

A more complex test, referring to a problem with modal interaction, is also reported to show the reliability of the proposed strategy in large scale analyses.

8.5.1 Planar beams

The first test is the classical Euler beam for which geometry and loads are reported in fig. 8.2 and the analytical solution gives $\lambda_b = 0.987$ and $\mathcal{B} = 1.480$. In this simple case the choice of the CR frame has some influence on the coarser mesh. As expected the quadratic model is more accurate than the linear one, providing, the exact value of the buckling load. The results for both λ_b and \mathcal{B} are practically the same using 4 finite elements and the quadratic model with secant frame. Nonetheless, the linear model performs well, the error being inferior to 1.30% for both λ_b and \mathcal{B} using 8-element discretization.

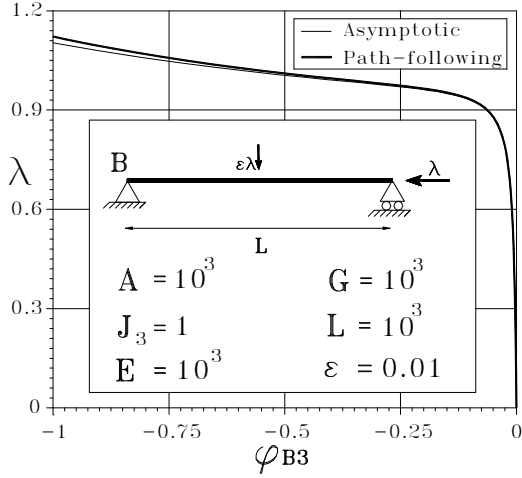


Fig. 8.2: Euler beam: geometry and equilibrium path. Rotation φ_3 of node B

The second example refers to the planar frame shown in fig. 8.3. This frame exhibits a strongly nonlinear precritical behavior, therefore it is suitable in testing the accuracy of the asymptotic analysis in this context. The results are reported in table 8.3 and fig. 8.3. We obtain a fast convergence to the "exact" analytical solution and, also in this case, the *Sec* strategy is slightly more accurate than *Mid* one, for rough meshes.

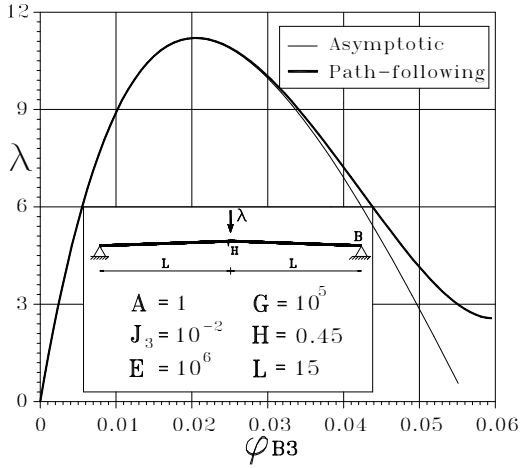


Fig. 8.3: Shallow frame: geometry and equilibrium path. Rotation φ_3 of node B

		<i>linear</i>			<i>quadr</i>	
loc. mod.		4e	8e	16e	4e	8e
λ_b	Sec	1.039	1.000	0.990	0.987	0.987
	Mid	1.042	1.000	0.990	0.987	0.987
$\mathcal{B} \cdot 10^3$	Sec	15.58	15.00	14.85	14.80	14.80
	Mid	15.47	14.99	14.85	14.65	14.70

Tab. 8.2: Euler beam: relevant asymptotic quantities

		<i>linear</i>		<i>quadratic</i>	
loc. mod.		8e	16e	8e	16e
λ_b	Sec	22.27	22.04	22.10	22.00
	Mid	22.42	22.08	22.23	22.03
\mathcal{A}	Sec	-48.71	-48.51	-48.51	-48.47
	Mid	-48.77	-48.54	-48.58	-48.49
\mathcal{B}	Sec	8.104	8.329	8.321	8.395
	Mid	7.954	8.308	8.241	8.379

Tab. 8.3: Planar shallow-frame: relevant asymptotic quantities

8.5.2 Spatial beams

The accuracy of the proposed approach is tested on some 3D spatial tests, which will be referred to as: the narrow cantilever beam test, the hinged right angle frame test and the cable hocking test. In all cases, the fundamental path is characterized by uniform stress (shear, bending or torsion) that generates a buckling mode exploiting bending-torsional coupling. For the narrow cantilever beam (fig. 8.4) and the hinged right angle frame (fig. 8.5.3) the analytical solution for the buckling load [105] gives $\lambda_b = 4\sqrt{\frac{EI_2GJ_1}{L^2}} = 3.280$ and $\lambda_b = \frac{\pi\sqrt{EI_2GJ_1}}{L} = 622.2$, respectively.

The results, reported in tabs. 8.4, 8.5 and 8.6, are accurate also in the case of coarse meshes. The results of a 64 element mesh denoted as (*ref.*) are also reported and can be considered exact, remaining unchanged even for successive mesh refinements and unaffected by the local model which is used.

For all tests, the quadratic model using *Sec* or *Mid* CR frame with 8 elements gives an error less than 1% on all quantities with respect to the 64 finite element mesh solution. Moreover in these cases, the quadratic model and the *Sec* frame are more accurate than the linear and *Mid* ones. The accuracy of local quadratic modeling is comparable with the ABAQUS beam elements library. Really, using coarse mesh (4–8 finite elements for each beam) the result, with respect to the buckling load and in recovering equilibrium path, are in practice comparable with the "exact" ones. The asymptotic equilibrium path is also accurate for very large displacements and rotations. Finally, note that the stress distribution on the cross section is very accurate along the equilibrium path (see fig. 8.7).

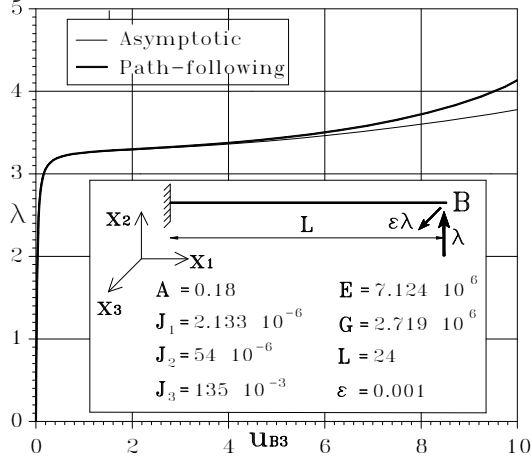


Fig. 8.4: Narrow cantilever beam: geometry and equilibrium path. Displacement u_3 of B node

	loc. mod.	<i>linear</i>			<i>quadratic</i>	
		4e	8e	16e	4e	8e
λ_b	Sec	3.416	3.321	3.298	3.341	3.303
	Mid	3.414	3.321	3.298	3.341	3.303
$\mathcal{B} \cdot 10^2$	Sec	44.59	43.16	42.80	44.05	43.03
	Mid	44.42	43.16	42.81	44.18	43.03

Tab. 8.4: Narrow cantilever beam: relevant asymptotic quantities

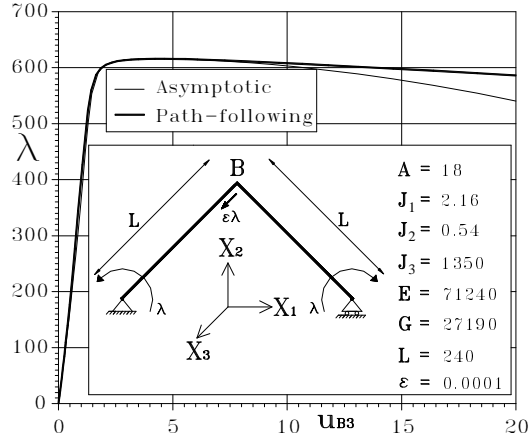


Fig. 8.5: Hinged right angle frame: geometry and equilibrium path. Displacement u_3 of B node

	loc. mod.	<i>linear</i>		<i>quadratic</i>	
		8e	16e	8e	16e
λ_b	Sec	651.7	629.3	638.3	626.2
	Mid	656.3	630.3	638.3	626.2
\mathcal{B}	Sec	-348.7	-294.36	-313.5	-286.6
	Mid	-340.96	-292.35	-311.7	-286.5

Tab. 8.5: Hinged right angle frame: relevant asymptotic quantities

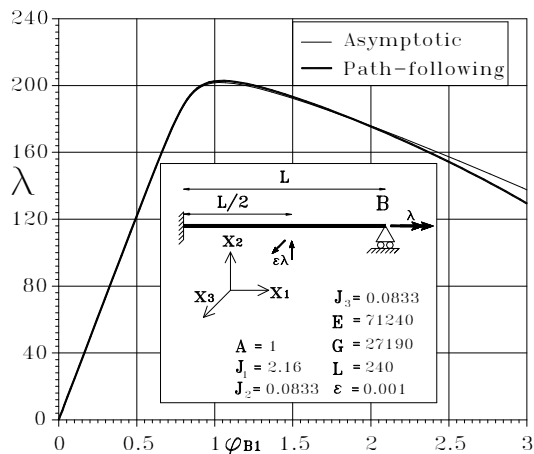


Fig. 8.6: Cable hocking problem: geometry and equilibrium path. Rotation φ_1 of B node

loc. mod.	<i>linear</i>		<i>quadratic</i>		
	$8e$	$16e$	$8e$	$16e$	
λ_b	Sec	241.1	226.7	222.7	222.2
	Mid	248.8	228.2	229.0	222.2
\mathcal{B}	Sec	-126.69	-100.40	-93.65	-92.97
	Mid	-130.53	-100.86	-86.40	-92.49

Tab. 8.6: Cable hocking problem: comparison of relevant asymptotic quantities

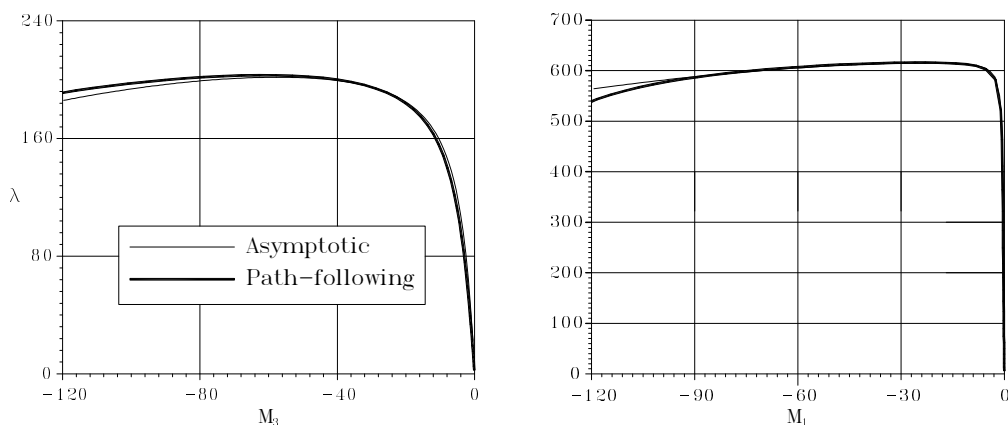


Fig. 8.7: Hinged right angle, torsional moment M_1 at middle. Cable hocking problem bending couple M_3 at middle

Channel-section beam subjected to axial

The method is also tested in a context where shear and bending centers are not coincident. The proposed test is an asymmetric-channel, see fig. 8.8, under axial force. The evaluation of compliance operator \mathbf{H} needed for the recovery of the complementary energy (8.33) has been done through FEM technique in the cross section domain (for further details see [93]).

The equilibrium path recover for different relevant displacement component agrees with the results proposed in the papers [106] and with the results made using ABAQUS (see fig. 8.8).

8.5.3 Modal interaction test: 3D tower

The final test refers to the 3D tower, for which the geometry is shown in fig.8.9. The structure exhibits 10 near coincident buckling modes, reported in fig. 8.11 along with the corresponding buckling loads. The interaction between global and local modes produces a strong instability in the equilibrium path. In fig. 8.12, the interaction between second and seventh buckling mode is shown. The equilibrium path is recovered using 16-finite elements for each beam for the asymptotic and path-following analysis. The accuracy of the asymptotic formulation in particular in the evaluation of the limit load is clear in comparison with the equilibrium path recovered using ABAQUS(see fig. 8.10).

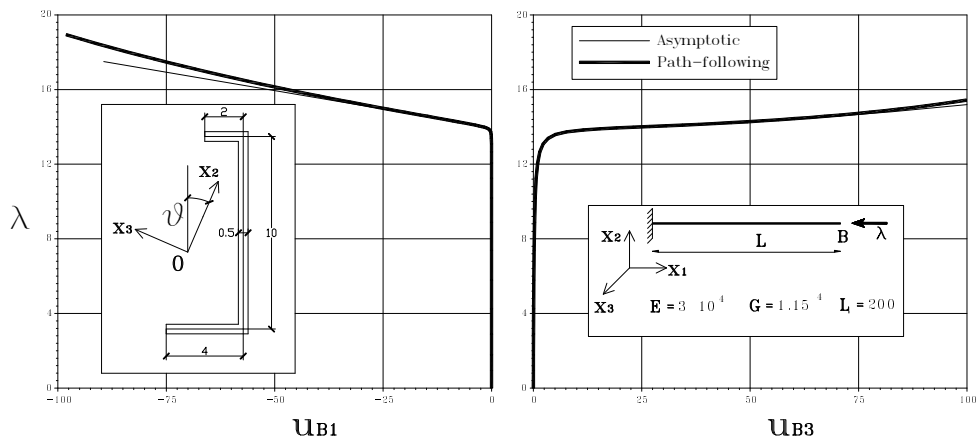


Fig. 8.8: Channel-section beam subjected to axial force. Geometry and equilibrium paths. Displacements u_{B1} and u_{B3}

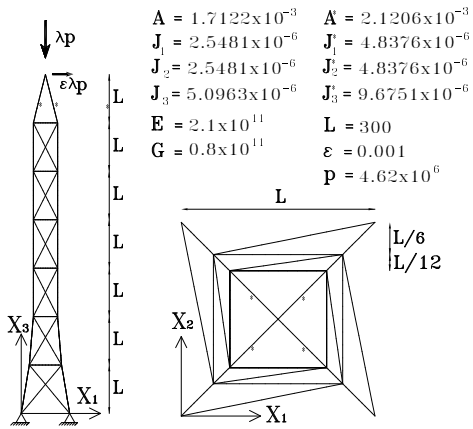


Fig. 8.9: 3D tower: geometry

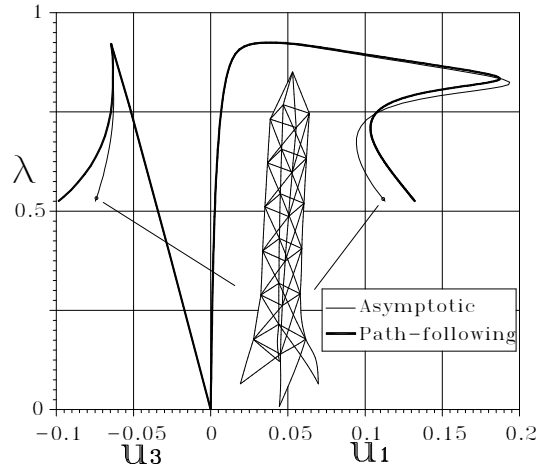


Fig. 8.10: 3D tower: equilibrium path $\lambda - \mathbf{u}_A$

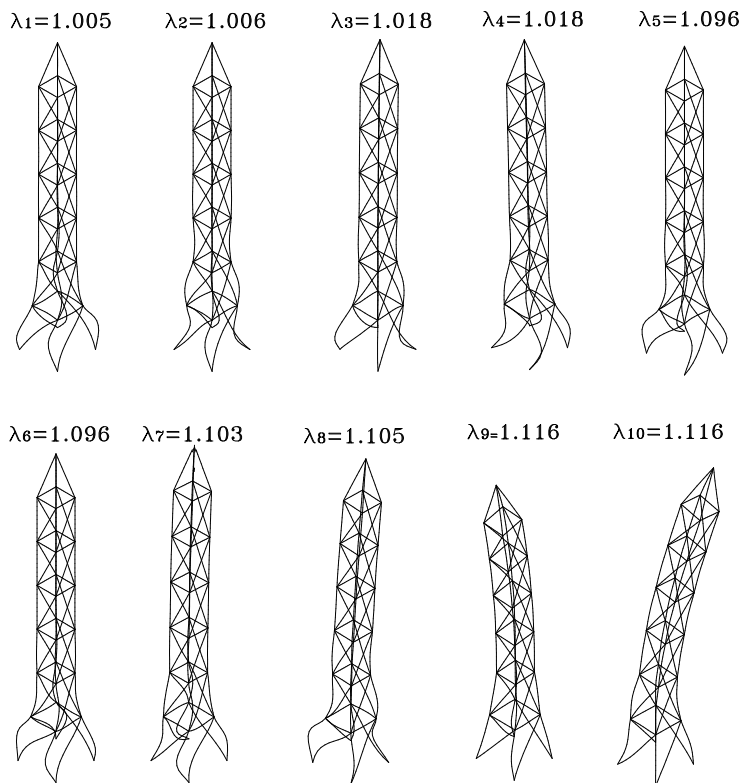


Fig. 8.11: 3D tower: modal shapes

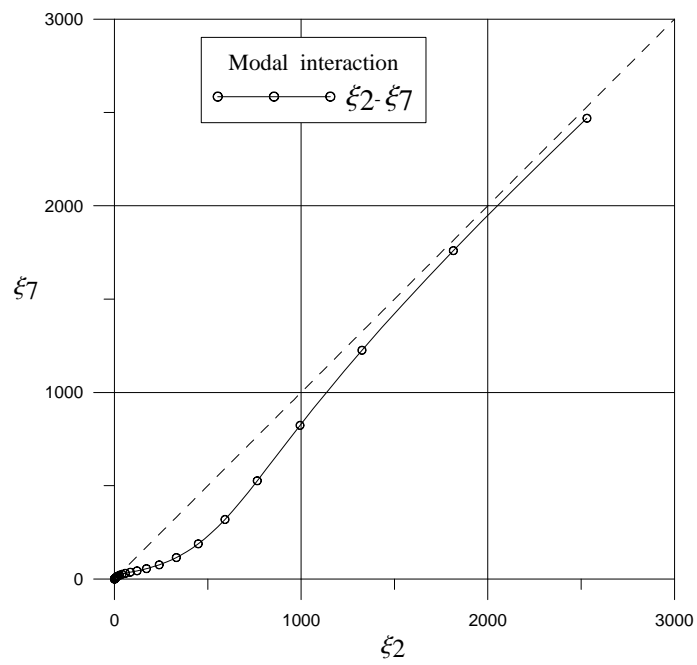


Fig. 8.12: 3D tower: interaction between 2nd and 7th buckling modes

Chapter 9

FEM implementation of the Saint Venant nonlinear beam model-Total Lagrangian formulation

A FEM implementation of 3D Saint Venant nonlinear beam model recovered using ICM and completely defined by eqs. (5.6) is proposed to test the accuracy and the reliability into the frame of Koiter's asymptotic analysis (see [1, 3] and related references). Obviously, being the asymptotic approach based on a fourth order Taylor expansion of strain energy, it represents a restrictive context for checking the objectivity and the accuracy of the beam model more than path-following approach that require only second order expansion of the strain energy. The implementation is carry out following the scheme, the notation and choices presented in the paper [102] at which the reader can refer for furthers details.

9.1 Mixed strain energy

Let be l the length of the beam, the strain energy $\Phi_e[u]$ for the beam element, recalling (5.6), is:

$$\Phi_e[u] := \int_0^l \{ \mathbf{t}^T \boldsymbol{\epsilon} + \frac{1}{2} \boldsymbol{\epsilon}^T \boldsymbol{\Psi}[\mathbf{t} \boldsymbol{\epsilon}] \} dA - \frac{1}{2} \int_0^l \{ \mathbf{t}^T \mathbf{H} \mathbf{t} \} dA \quad (9.1a)$$

where generalized stress and strain are defined as

$$\mathbf{t} := \begin{Bmatrix} \mathbf{N} \\ \mathbf{M} \end{Bmatrix}, \quad \boldsymbol{\epsilon} := \begin{Bmatrix} \boldsymbol{\varepsilon} \\ \boldsymbol{\chi} \end{Bmatrix} \quad (9.1b)$$

being $\mathbf{N} = [N_1, N_2, N_3]^T$ the vector collecting axial and shear forces, $\mathbf{M} = [M_1, M_2, M_3]^T$ the vector collecting torsional and bending couples. The formulation will be developed for linear local deformation (5.4), however the outlines for quadratic local model will be given, then:

$$\boldsymbol{\varepsilon} = \mathbf{R}_0^T(\mathbf{u}_{0,s} + \mathbf{e}_1) - \mathbf{e}_1, \quad \boldsymbol{\chi} = \mathbf{R}_0^T \mathbf{R}_{0,s} \quad (9.1c)$$

In the further develops we will assume a spatial representation for $\boldsymbol{\varepsilon}$, then

$$\boldsymbol{\varepsilon} = \mathbf{u}_{0,s} + (\mathbf{I} - \mathbf{R}_0)\mathbf{e}_1$$

while for curvature we will use a material representation for curvature $\boldsymbol{\chi}$. Using a vector like parametrization for rotations [48], matrix rotation can be expressed in terms of $\boldsymbol{\varphi}$ through Rodriguez formula as:

$$\mathbf{R}_0 = \mathbf{I} + \frac{\sin \varphi}{\varphi} \mathbf{W}[\boldsymbol{\varphi}] + \frac{1 - \cos \varphi}{\varphi^2} \mathbf{W}[\boldsymbol{\varphi}]^2 \quad \text{with} \quad \varphi^2 = \boldsymbol{\varphi}^T \boldsymbol{\varphi} \quad (9.1d)$$

being $\mathbf{W}[\boldsymbol{\varphi}] = \text{spin}[\boldsymbol{\varphi}]$ the skew-symmetric matrix associate to axial vector $\boldsymbol{\varphi}$. Previous choice (9.1d) allows to simplify noticeably the expression of curvatures:

$$\boldsymbol{\chi} = \mathbf{R}_0^T \mathbf{R}_{0,s} = \mathbf{T}^T \boldsymbol{\varphi}_{,s}, \quad \mathbf{T} = \mathbf{I} + \frac{1 - \cos \varphi}{\varphi^2} \mathbf{W}[\boldsymbol{\varphi}] + \frac{\varphi - \sin \varphi}{\varphi^3} \mathbf{W}[\boldsymbol{\varphi}]^2 \quad (9.1e)$$

For an easy evaluation of 4th order Frechét derivative of strain energy, the strain $\boldsymbol{\varepsilon}$ is expanded as:

$$\boldsymbol{\varepsilon} = \boldsymbol{\varepsilon}_1[\delta \mathbf{d}_1] + \boldsymbol{\varepsilon}_2[\delta \mathbf{d}_2] + \boldsymbol{\varepsilon}_3[\delta \mathbf{d}_3] + \boldsymbol{\varepsilon}_4[\delta \mathbf{d}_4] + \dots \quad (9.2a)$$

being the set $\delta \mathbf{d}_n$ defined as

$$\delta \mathbf{d}_n = \{\mathbf{d}_1, \mathbf{d}_2, \dots, \mathbf{d}_n\} \quad (9.2b)$$

and

$$\boldsymbol{\varepsilon}_1[\delta \mathbf{d}_1] = \left\{ \begin{array}{l} \boldsymbol{\varepsilon}_1[\delta \mathbf{d}_1] \\ \boldsymbol{\chi}_1[\delta \mathbf{d}_1] \end{array} \right\}, \quad \boldsymbol{\varepsilon}_2[\delta \mathbf{d}_2] = \left\{ \begin{array}{l} \boldsymbol{\varepsilon}_2[\delta \mathbf{d}_2] \\ \boldsymbol{\chi}_2[\delta \mathbf{d}_2] \end{array} \right\}, \quad \boldsymbol{\varepsilon}_3[\delta \mathbf{d}_3] = \dots \quad (9.2c)$$

where $\boldsymbol{\varepsilon}_n = \{\boldsymbol{\varepsilon}_n, \boldsymbol{\chi}_n\}$, with $n = 1..4$ are n -multilinear symmetric forms which express the n^{th} Frechét variations of function $\boldsymbol{\varepsilon}$, $\boldsymbol{\varepsilon}$ and $\boldsymbol{\chi}$ respectively, with respect to configuration parameters $\mathbf{u} = \{\mathbf{t}, \mathbf{d}\}$, being $\mathbf{d} = \{\mathbf{u}, \boldsymbol{\varphi}\}$ the vector collecting the displacements/rotations parameters. For the deformation $\boldsymbol{\varepsilon}$ we have than:

$$\boldsymbol{\varepsilon}_1[\delta \mathbf{d}_1] = \mathbf{u}_{1,s} - \boldsymbol{\Omega}_1[\delta \boldsymbol{\varphi}_1] \mathbf{e}_1, \quad \boldsymbol{\varepsilon}_n[\delta \mathbf{d}_n] = -\frac{1}{n!} \boldsymbol{\Omega}_n[\delta \mathbf{d}_n] \mathbf{e}_1, \quad n > 2 \quad (9.2d)$$

while for curvature χ holds:

$$\chi_n[\delta \mathbf{d}_n] = \frac{(-1)^{n+1}}{n!} \Omega_{n-1}[\delta \varphi_{nk}] \varphi_{k,s} , \quad k = 1..n \quad (9.2e)$$

being the set $\delta \mathbf{d}_{nk}$ defined as

$$\delta \varphi_{nk} = \{\varphi_1, \varphi_2, \dots, \varphi_n\} \setminus \{\varphi_k\} \quad (9.2f)$$

and $\Omega_n[\delta \varphi_n]$ the Frechét derivative of $\mathbf{W}^n[\varphi]$ and implicitly assuming the summation on repeated index.

9.2 Finite element

The proposed finite element is based on three nodes: the edges and the middle beam points. From now the quantities evaluated on the edge $s = 0$ and $s = l$, will be denoted with the pedex i and j , while these evaluated in the middle point $s = \frac{l}{2}$ will be denoted with the pedex m . The axial-shear forces, according to the equilibrium equations in absence of distributed loads-couples, are assumed constant on the element while the couples are assumed linear:

$$\mathbf{N} = \frac{\mathbf{n}_e}{l} , \quad \mathbf{M} = \mathbf{m}_s + f_s \mathbf{m}_e , \quad \begin{cases} f_s = 1 - \frac{2s}{l} \\ f_e = 1 - \frac{4s}{l} + \frac{4s^2}{l^2} \end{cases} \quad (9.3a)$$

being

$$\mathbf{m}_s := -(\mathbf{M}_j + \mathbf{M}_i) , \quad \mathbf{m}_e = (\mathbf{M}_j - \mathbf{M}_i) \quad (9.3b)$$

symmetric and skew-symmetric couples. Introducing the vector $\mathbf{t}_e = \{\mathbf{n}_e, \mathbf{m}_s, \mathbf{m}_e\}$ collecting the *natural stress*, the stress interpolation is rewritten as:

$$\mathbf{N} = \mathbf{D}_n^T \mathbf{t}_e , \quad \mathbf{M} = \mathbf{D}_m^T \mathbf{t}_e , \quad \mathbf{D}_n = \begin{bmatrix} \frac{1}{l} \mathbf{I}_3 \\ \mathbf{0}_3 \\ \mathbf{0}_3 \end{bmatrix} , \quad \mathbf{D}_m = \begin{bmatrix} \mathbf{0}_3 \\ \frac{1}{2} \mathbf{I}_3 \\ -\frac{f_s}{2} \mathbf{I}_3 \end{bmatrix} \quad (9.3c)$$

with \mathbf{I}_3 and $\mathbf{0}_3$ the identity and zero matrix $\in \mathbb{R}^3$. As regards to kinematic, displacements and rotation vector field are assumed to be linear and quadratic on the element. In particular defining the vector $\mathbf{d}_e = \{\phi_m, \phi_s, \phi_e, \phi_r\}$, collecting the *natural modes*:

$$\varphi_m := \varphi|_{s=l/2} , \quad \phi_s := \frac{\varphi_i - \varphi_j}{2} , \quad \phi_e := \frac{\varphi_i + \varphi_j}{2} , \quad \phi_r := \frac{\mathbf{u}_j - \mathbf{u}_i}{l} \quad (9.4a)$$

the interpolation becomes:

$$\mathbf{u}_{,s} = \mathbf{D}_u^T \mathbf{d}_e \quad , \quad \boldsymbol{\varphi} = \mathbf{D}_\varphi^T \mathbf{d}_e \quad , \quad \mathbf{D}_u = \begin{bmatrix} \mathbf{0}_3 \\ \mathbf{0}_3 \\ \mathbf{0}_3 \\ \frac{1}{l} \mathbf{I}_3 \end{bmatrix} , \quad \mathbf{D}_\varphi = \begin{bmatrix} (1-f_e) \mathbf{I}_3 \\ f_s \mathbf{I}_3 \\ f_e \mathbf{I}_3 \\ \mathbf{0}_3 \end{bmatrix} \quad (9.4b)$$

9.2.1 Energy derivatives

In more compact form the 2^{nd} order Frechét derivative of the strain energy (9.1) is expressed as:

- 2^{nd}

$$\begin{aligned} \Phi_e''[\mathbf{u}_1, \mathbf{u}_2] = & \int_0^l \{ \mathbf{N}_1 \boldsymbol{\varepsilon}_1[\mathbf{d}_2] + \mathbf{N}_2 \boldsymbol{\varepsilon}_1[\mathbf{d}_1] + \mathbf{N} \boldsymbol{\varepsilon}_2[\mathbf{d}_1, \mathbf{d}_2] \\ & + \mathbf{M}_1 \boldsymbol{\chi}_1[\mathbf{d}_2] + \mathbf{M}_2 \boldsymbol{\chi}_1[\mathbf{d}_1] + \mathbf{M} \boldsymbol{\chi}_2[\mathbf{d}_1, \mathbf{d}_2] \} ds \quad (9.5a) \\ & - \int_0^l \{ \mathbf{N}_1 \mathbf{C} \mathbf{N}_2 + \mathbf{M}_1 \mathbf{D} \mathbf{M}_2 \} ds \end{aligned}$$

- n^{th} order with $n > 2$

$$\Phi_e^n[\delta \mathbf{u}_n] = \int_0^l \{ \mathbf{N}_k^T \boldsymbol{\varepsilon}_{n-1}[\delta \mathbf{d}_{nk}] + \mathbf{N}^T \boldsymbol{\varepsilon}_n[\delta \mathbf{d}_n] + \mathbf{M}_k^T \boldsymbol{\chi}_{n-1}[\mathbf{d}_{nk}] + \mathbf{M}^T \boldsymbol{\chi}_n[\delta \mathbf{d}_n] \} ds \quad (9.5b)$$

being $k = 2..n - 1$

9.2.2 Discrete energy derivatives

Using interpolation (9.3) and (9.4), energy derivative (9.1) can be expressed in discrete forms as:

- 2^{nd}

$$\Phi_e''[\mathbf{u}_1, \mathbf{u}_2] = \mathbf{t}_{1e}^T \boldsymbol{\varrho}_1[\mathbf{d}_{2e}] + \mathbf{t}_{2e}^T \boldsymbol{\varrho}_1[\mathbf{d}_{1e}] + \mathbf{t}_e^T \boldsymbol{\varrho}_2[\mathbf{d}_{1e}, \mathbf{d}_{2e}] \quad (9.6a)$$

- n^{th} order with $n > 2$

$$\Phi_e^n[\mathbf{u}_1, \mathbf{u}_2, \dots, \mathbf{u}_n] = \int_0^l \{ \mathbf{t}_{ek}^T \boldsymbol{\varrho}_{n-1}[\{\mathbf{d}_1, \mathbf{d}_2, \dots, \mathbf{d}_n\} \setminus \mathbf{d}_k] + \mathbf{t}^T \boldsymbol{\varrho}_n[\mathbf{d}_1, \mathbf{d}_2, \dots, \mathbf{d}_n] \} ds \quad (9.6b)$$

being

$$\boldsymbol{\varrho}_n[\mathbf{d}_{1e}, \mathbf{d}_{2e}, \dots, \mathbf{d}_{ne}] = \int_0^l \{ \mathbf{D}_n \boldsymbol{\varepsilon}_n[\mathbf{d}_{1e}, \mathbf{d}_{2e}, \dots, \mathbf{d}_{ne}] + \mathbf{D}_m \boldsymbol{\chi}_n[\mathbf{d}_{1e}, \mathbf{d}_{2e}, \dots, \mathbf{d}_{ne}] \} ds \quad (9.6c)$$

and (definizione della matrice di rigidità)

9.2.3 Energy equivalences

Following the framework proposed into [102], for the implementation of asymptotic analysis we had to define the following equivalences:

$$\begin{aligned} \mathbf{d}_{ie}^T \mathbf{s}_1[\mathbf{t}_{je}] &= \mathbf{t}_{je}^T \boldsymbol{\varrho}_1[\mathbf{d}_{ie}] \\ \mathbf{d}_{ie}^T \mathbf{s}_2[\mathbf{d}_{je}, \mathbf{t}_{he}] &= \mathbf{t}_{he}^T \boldsymbol{\varrho}_2[\mathbf{d}_{ie}, \mathbf{d}_{je}] \\ \mathbf{d}_{ie}^T \mathbf{s}_3[\mathbf{d}_{je}, \mathbf{d}_{he}, \mathbf{t}_{ke}] &= \mathbf{t}_{ke}^T \boldsymbol{\varrho}_3[\mathbf{d}_{ie}, \mathbf{d}_{je}, \mathbf{d}_{he}] \end{aligned} \quad (9.7a)$$

in particular

$$\mathbf{s}_1[\mathbf{t}_{je}] = \begin{bmatrix} -\frac{2}{3}(\mathbf{m}_{je} + \mathbf{e}_1 \times \mathbf{n}_{je}) \\ \mathbf{m}_{js} \\ \frac{2}{3}(\mathbf{m}_{je} + \frac{1}{2}\mathbf{e}_1 \times \mathbf{n}_{je}) \\ n_{j1}\mathbf{e}_1 + \mathbf{e}_1 \times \mathbf{n}_{je} \end{bmatrix} \quad \mathbf{s}_2[\mathbf{d}_{je}, \mathbf{t}_{he}] = \mathbf{G}[\mathbf{t}_{he}]\mathbf{d}_{je} \quad (9.7b)$$

For the definition of the Hessian needing

$$\begin{aligned} \mathbf{d}_{ie}^T \mathbf{L}^T \mathbf{t}_{je} &= \mathbf{d}_{ie}^T \mathbf{s}_1[\mathbf{t}_{je}] \\ \mathbf{d}_{ie}^T \mathbf{G}[\mathbf{t}_{he}]\mathbf{d}_{je} &= \mathbf{d}_{ie}^T \mathbf{s}_2[\mathbf{d}_{je}, \mathbf{t}_{he}] \end{aligned} \quad (9.7c)$$

With some algebra

$$\mathbf{L} = \begin{bmatrix} \frac{2}{3}\mathbf{W}[\mathbf{e}_1] & \mathbf{0}_3 & \frac{1}{3}\mathbf{W}[\mathbf{e}_1] & \mathbf{e}_1 \mathbf{e}_1^T \mathbf{W}[\mathbf{e}_1] \\ \mathbf{0}_3 & \mathbf{I}_3 & \mathbf{0} & \mathbf{0} \\ -\frac{2}{3}\mathbf{I}_3 & \mathbf{0}_3 & \frac{2}{3}\mathbf{I}_3 & \mathbf{0} \end{bmatrix} \quad (9.7d)$$

$$\mathbf{G}[\mathbf{t}_{he}] = \begin{bmatrix} \frac{4}{15}\mathbf{G}_n & \frac{2}{3}\mathbf{W}[\mathbf{m}_{hs}] & \frac{1}{3}\mathbf{W}[\mathbf{m}_{he}] + \frac{1}{15}\mathbf{G}_n & \mathbf{0} \\ \frac{2}{3}\mathbf{W}[\mathbf{m}_{hs}] & \frac{1}{6}\mathbf{G}_n & \frac{1}{6}\mathbf{W}[\mathbf{m}_{hs}] & \mathbf{0} \\ \frac{1}{3}\mathbf{W}[\mathbf{m}_{he}] + \frac{1}{15}\mathbf{G}_n & \frac{1}{6}\mathbf{W}[\mathbf{m}_{hs}] & \frac{1}{10}\mathbf{G}_n & \mathbf{0} \\ \mathbf{0} & \mathbf{0} & \mathbf{0} & \mathbf{0} \end{bmatrix} \quad (9.7e)$$

where $\mathbf{G}_n = \mathbf{W}[\mathbf{e}_1 \times \mathbf{n}_h] - 2n_1\mathbf{W}^2[\mathbf{e}_1]$. In To simplify the expression of $\mathbf{s}_3[\mathbf{d}_{je}, \mathbf{d}_{he}, \mathbf{t}_{ke}]$, it is convenient defines:

$$\mathbf{d}_{ie}^T \mathbf{s}_3[\mathbf{d}_{je}, \mathbf{d}_{he}, \mathbf{t}_{ke}] = \mathbf{d}_{ie}^T \mathbf{G}[\mathbf{d}_{je}, \mathbf{t}_{ke}]\mathbf{d}_{he} \quad \rightarrow \quad \mathbf{s}_3[\mathbf{d}_{je}, \mathbf{d}_{he}, \mathbf{t}_{ke}] = \mathbf{G}[\mathbf{d}_{je}, \mathbf{t}_{ke}]\mathbf{d}_{he} \quad (9.7f)$$

In particular

$$\mathbf{G}[\mathbf{d}_{je}, \mathbf{t}_{ke}] = \begin{bmatrix} \mathbf{G}_{11} & \mathbf{G}_{12} & \mathbf{G}_{13} & \mathbf{0}_3 \\ \mathbf{G}_{12}^T & \mathbf{G}_{22} & \mathbf{G}_{23} & \mathbf{0}_3 \\ \mathbf{G}_{13}^T & \mathbf{G}_{23}^T & \mathbf{G}_{33} & \mathbf{0}_3 \\ \mathbf{0}_3 & \mathbf{0}_3 & \mathbf{0}_3 & \mathbf{0}_3 \end{bmatrix} \quad (9.7g)$$

begin:

$$\begin{aligned}
\mathbf{G}_{11} &= \frac{8}{35}(\mathbf{e}_1 \times \mathbf{n})^T (2\boldsymbol{\varphi}_m + \frac{1}{3}\boldsymbol{\varphi}_e) \mathbf{I}_3 \\
&+ \frac{16}{105}(\mathbf{W}[\mathbf{e}_1 \times \mathbf{n}] \mathbf{W}[\boldsymbol{\varphi}_m] + \mathbf{W}[\boldsymbol{\varphi}_m] \mathbf{W}[\mathbf{e}_1 \times \mathbf{n}]) \\
&+ \frac{8}{305}(\mathbf{W}[\mathbf{e}_1 \times \mathbf{n}] \mathbf{W}[\boldsymbol{\varphi}_e] + \mathbf{W}[\boldsymbol{\varphi}_m] \mathbf{W}[\mathbf{e}_1 \times \mathbf{n}]) \quad (9.7h) \\
&+ \frac{2}{15}(\mathbf{W}[\mathbf{m}_s] \mathbf{W}[\boldsymbol{\varphi}_s] + \mathbf{W}[\boldsymbol{\varphi}_s] \mathbf{W}[\mathbf{m}_s]) \\
&+ \frac{2}{45}(\mathbf{W}[\mathbf{m}_e] \mathbf{W}[\boldsymbol{\varphi}_e] + \mathbf{W}[\boldsymbol{\varphi}_e] \mathbf{W}[\mathbf{m}_e])
\end{aligned}$$

$$\begin{aligned}
\mathbf{G}_{22} &= \frac{1}{5}(\mathbf{e}_1 \times \mathbf{n})^T (\frac{2}{3}\boldsymbol{\varphi}_m + \boldsymbol{\varphi}_e) \mathbf{I}_3 \\
&+ \frac{2}{45}(\mathbf{W}[\mathbf{e}_1 \times \mathbf{n}] \mathbf{W}[\boldsymbol{\varphi}_m] + \mathbf{W}[\boldsymbol{\varphi}_m] \mathbf{W}[\mathbf{e}_1 \times \mathbf{n}]) \\
&+ \frac{1}{15}(\mathbf{W}[\mathbf{e}_1 \times \mathbf{n}] \mathbf{W}[\boldsymbol{\varphi}_e] + \mathbf{W}[\boldsymbol{\varphi}_m] \mathbf{W}[\mathbf{e}_1 \times \mathbf{n}]) \quad (9.7i) \\
&- \frac{4}{45}(\mathbf{W}[\mathbf{m}_e] \mathbf{W}[\boldsymbol{\varphi}_m] + \mathbf{W}[\boldsymbol{\varphi}_e] \mathbf{W}[\mathbf{m}_m]) \\
&+ \frac{1}{30}(\mathbf{W}[\mathbf{m}_e] \mathbf{W}[\boldsymbol{\varphi}_e] + \mathbf{W}[\boldsymbol{\varphi}_e] \mathbf{W}[\mathbf{m}_e])
\end{aligned}$$

$$\begin{aligned}
\mathbf{G}_{33} &= \frac{1}{7}(\mathbf{e}_1 \times \mathbf{n})^T (\frac{2}{5}\boldsymbol{\varphi}_m + \boldsymbol{\varphi}_e) \mathbf{I}_3 \\
&+ \frac{2}{105}(\mathbf{W}[\mathbf{e}_1 \times \mathbf{n}] \mathbf{W}[\boldsymbol{\varphi}_m] + \mathbf{W}[\boldsymbol{\varphi}_m] \mathbf{W}[\mathbf{e}_1 \times \mathbf{n}]) \\
&+ \frac{1}{21}(\mathbf{W}[\mathbf{e}_1 \times \mathbf{n}] \mathbf{W}[\boldsymbol{\varphi}_e] + \mathbf{W}[\boldsymbol{\varphi}_m] \mathbf{W}[\mathbf{e}_1 \times \mathbf{n}]) \quad (9.7j) \\
&- \frac{1}{30}(\mathbf{W}[\mathbf{m}_s] \mathbf{W}[\boldsymbol{\varphi}_s] + \mathbf{W}[\boldsymbol{\varphi}_s] \mathbf{W}[\mathbf{m}_s]) \\
&- \frac{1}{15}(\mathbf{W}[\mathbf{m}_e] \mathbf{W}[\boldsymbol{\varphi}_m] + \mathbf{W}[\boldsymbol{\varphi}_m] \mathbf{W}[\mathbf{m}_e])
\end{aligned}$$

Chapter 10

FEM implementation of nonlinear plate model

The shear undeformable plate model obtained in the previous section was implemented in KASP code [4]–[6] in order to perform an asymptotic Koiter analysis of plate assemblages. The sensitivity of Koiter approach to the geometric exactness of the kinematical model is useful to test the accuracy of the proposed plate model. The use of a formulation that can be easily implemented without use finite rotations give the possibility to concentrate the attentions only on the theoretical aspects discussed in the paper and to reuse the KASP code base on HC finite element interpolation.

In this section we shortly recall the asymptotic method and the finite element formulation for plate assemblages. A complete insight on this arguments can be found in previous cited reference and in [3].

10.1 The finite element of the plate

The FEM discretization is based on the HC finite element with a four Gauss point integration scheme, already used in [4, 5, 6, 7].

Each panel of the structures is discretized by a rectangular mesh. Continuity is assumed at the inter–element boundaries for both displacements (u, v, w) and their derivatives. Each element is described as a Von Karman flat plate and is referred to a separate local system. This, as will be shown in the sequel, allows rigid displacement to be filtered from the kinematical relationships and, due to the small size of the elements, makes the approximations implied by the Karman theory acceptable.

10.1.1 Displacements interpolation

Each component of the displacement \mathbf{d} is interpolated through quadratic splines. That is, $\mathbf{d}[x, y]$ is expressed on the element by

$$\mathbf{d}[\xi, \eta] = \sum_{i,j=1}^3 h_i[\xi]h_j[\eta]\mathbf{d}_{ij}, \quad \xi = \frac{x - \bar{x}}{\ell_x}, \eta = \frac{y - \bar{y}}{\ell_y}, \quad (\xi, \eta) \in \left[-\frac{1}{2}, \frac{1}{2}\right] \quad (10.1)$$

where:

$$h_1[\xi] = \frac{1}{8} - \frac{1}{2}\xi + \frac{1}{2}\xi^2 \quad h_2[\xi] = \frac{3}{4} - \xi^2 \quad h_3[\xi] = \frac{1}{8} + \frac{1}{2}\xi + \frac{1}{2}\xi^2$$

\bar{x} , \bar{y} are the coordinates of the center of the element, ℓ_x , ℓ_y the element dimensions, and the nodal displacements $\mathbf{d}_{ij} = \{\mathbf{u}_{ij}, \mathbf{v}_{ij}, \mathbf{w}_{ij}\}$ are defined as the displacements of control nodes initially located in the center of the element which define, by the geometric construction, the deformed shape of the element. A C^1 continuity is obtained with a minimal number of parameters, approximately one node (three parameters) per element.

By collecting all 9 nodal displacements, pertaining to the element, in the element vector $\mathbf{d}_e = \{\mathbf{d}_{11}, \mathbf{d}_{12}, \dots, \mathbf{d}_{33}\}$, Eq.(10.1) can be rewritten in matrix form as:

$$\mathbf{d}[\xi, \eta] := \mathbf{H}[\xi, \eta]\mathbf{d}_e \quad (10.2)$$

where $\mathbf{H}[\xi, \eta]$ is the $[3 \times 27]$ HC interpolation matrix

$$\mathbf{H} := \begin{bmatrix} h_1h_1 & 0 & 0 & h_1h_2 & 0 & 0 & \dots & h_3h_3 & 0 & 0 \\ 0 & h_1h_1 & 0 & 0 & h_1h_2 & 0 & \dots & 0 & h_3h_3 & 0 \\ 0 & 0 & h_1h_1 & 0 & 0 & h_1h_2 & \dots & 0 & 0 & h_3h_3 \end{bmatrix}$$

10.1.2 Numerical integration

A 2×2 Gauss scheme has been used to integrate all the energy terms required by the analysis. Let (x^g, y^g) be the position of the Gauss point g within the element e , the components of the displacement gradient are evaluated in matrix form as:

$$\mathbf{u}_{,x}[x^g, y^g] := \sum_{i,j=1}^3 h_i[\xi^g]_{,x} h_j[\eta^g] \mathbf{u}_{ij} = \mathbf{H}_{ux}^g \mathbf{d}_e \quad (10.3)$$

where

$$\mathbf{H}_{ux}^g := [h_1[\xi^g]_{,x} h_1[\eta^g], 0, 0, h_2[\xi^g]_{,x} h_1[\eta^g], 0, 0, \dots, h_3[\xi^g]_{,x} h_3[\eta^g], 0, 0]$$

is a $[1 \times 27]$ row matrix associated to the Gauss point. In the same manner we define:

$$\mathbf{u}_{,y}^g = \mathbf{H}_{uy}^g \mathbf{d}_e, \quad \mathbf{u}_{,xx}^g = \mathbf{H}_{uxx}^g \mathbf{d}_e, \quad \dots, \quad \mathbf{w}_{,yy}^g = \mathbf{H}_{wyy}^g \mathbf{d}_e \quad (10.4)$$

Eqs. (10.3, 10.4) and (??), provide the Gauss–point strains $\boldsymbol{\varepsilon}^g$ and $\boldsymbol{\chi}^g$ associated to nodal displacements \mathbf{d}_e . By denoting by \mathbf{n}_g the plane stress associated to the Gauss–point and by A_g its influence area, the element energy is evaluated by Gauss quadrature:

$$\begin{aligned}\Phi_e[u] &:= \sum_g \Phi_{eg}[u] \quad , \quad \Phi_{eg}[u] := \frac{1}{2} \{ \mathbf{n}_g^T (\boldsymbol{\varepsilon}_g - \mathbf{F} \mathbf{n}_g) + \boldsymbol{\varepsilon}_g^T \mathbf{n}_g + \boldsymbol{\chi}_g^T \mathbf{D} \boldsymbol{\chi}_g \} A_g \\ \Phi'_e[u] \delta u &:= \sum_g \Phi'_{eg}[u] \delta u \quad , \quad \Phi'_{eg}[u] \delta u = \{ \delta \mathbf{n}^T (\boldsymbol{\varepsilon} - \mathbf{F} \mathbf{n}) + \mathbf{n}^T \delta \boldsymbol{\varepsilon} + \boldsymbol{\chi}^T \mathbf{D} \delta \boldsymbol{\chi} \} A_g \quad (10.5) \\ \Phi''_e[u] \dot{u} \delta u &:= \sum_g \Phi''_{eg}[u] \dot{u} \delta u \quad , \quad \Phi''_{eg}[u] \dot{u} \delta u = \{ \mathbf{n}^T \delta \dot{\boldsymbol{\varepsilon}} + \dot{\mathbf{n}}^T (\delta \boldsymbol{\varepsilon} - \mathbf{F} \delta \mathbf{n}) + \delta \mathbf{n}^T \dot{\boldsymbol{\varepsilon}} + \dot{\boldsymbol{\chi}}^T \mathbf{D} \delta \boldsymbol{\chi} \} A_g\end{aligned}$$

where $\mathbf{n}_g := \{N_x^g, N_y^g, N_{xy}^g\}$ are the local in–plane stresses associated to the Gauss point g .

Note that the proposed integration scheme implies a constant piecewise interpolation of the in–plain element stresses and strains on the influence area of each Gauss–point. While the proposed formulation could allow analytical integrations and more sophisticated interpolations, this choice was made because: i) it is the simplest from both the computational and implementation point of view; ii) it provides an exact correspondence with the available results by allowing to focalize the attention on the approach differences without introducing any disturbing discretization improvement.

It is also worth mentioning that, in the actual computation of expression (10.5), it could be convenient to evaluate separately each quadratic and cubic terms through

$$\int_{A_e} u_{,x} u_{,x} dA := \sum_g u_{,x}^g u_{,x}^g A_g = \sum_g A_g (\mathbf{H}_{ux}^g \mathbf{d}_e) (\mathbf{H}_{ux}^g \mathbf{d}_e) \quad (10.6)$$

...

$$\int_{A_e} u_{,x} w_{,x} w_{,x} dA := \sum_g A_g (\mathbf{H}_{ux}^g \mathbf{d}_e) (\mathbf{H}_{wx}^g \mathbf{d}_e) (\mathbf{H}_{wx}^g \mathbf{d}_e) \quad (10.7)$$

...

and the corresponding analogous ones.

10.2 Numerical results

The numerical results refer to Koiter’s asymptotic analysis of plate assemblages. The proposed simplified Kirchoff plate model (*PM*) has been implemented in a code called KASP [6]. The results are compared with those obtained by the same code using the technical model *complete Green–Lagrange (LC)* and the *simplified Green–Lagrange (LS)*, previously implemented.

The results are compared with analytical solutions, path-following analysis and 2D-3D beam model when possible.

Further details regarding the implementation of the Koiter's asymptotic method and the technical strain models can be found in [6, 4, 5]

10.2.1 The Eulero beam and Roorda Frame

The results obtained by the *LC*, *LS* and *PM* are compared with the analytical solutions, available for these easy tests. In particular the critical load λ_b , postcritical slope $\dot{\lambda}_b$ and postcritical curvature $\ddot{\lambda}_b$ are been considered.

Finally the equilibrium paths are compared with those obtained by path-following analysis using 2D-beam and plate models.

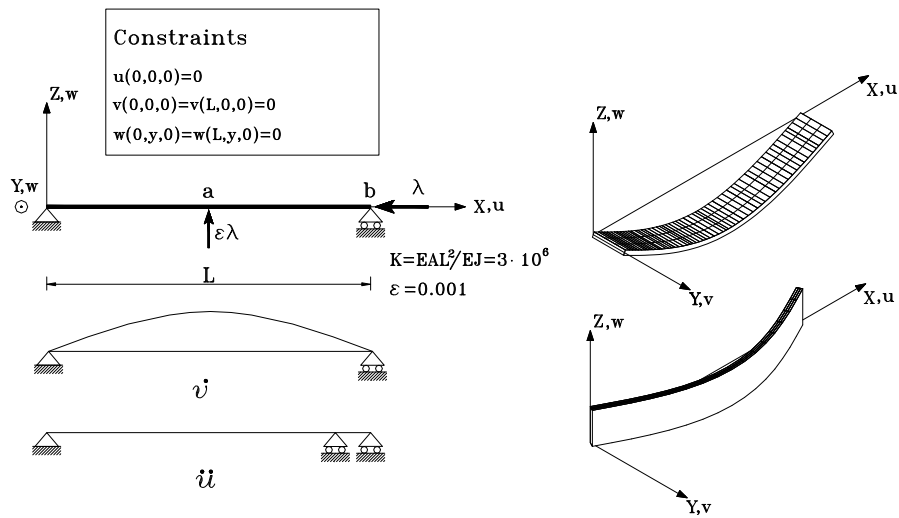


Fig. 10.1: Euler beam

	<i>Out plane</i>			<i>In plane</i>			<i>Beam</i> ^(*)	
	<i>N.elem.</i>	<i>LC</i>	<i>LS</i>	<i>PM</i>	<i>LC</i>	<i>LS</i>		<i>PM</i>
λ_b	16	9.901	9.901	9.901	9.918	9.918	9.918	
	32	9.877	9.877	9.877	9.870	9.870	9.870	9.870
	64	9.872	9.872	9.871	9.867	9.870	9.870	
$\frac{\dot{\lambda}_b}{2\lambda_b}$	16	-0.354	0.020	0.145	0.166	1.03	0.166	
	32	-0.375	0.000	0.125	0.126	1.00	0.126	0.125
	64	-0.375	0.000	0.125	0.125	1.00	0.125	

(*) Solution obtained by Antman model and exact interpolation functions

Tab. 10.1: Euler beam out plane: asymptotic quantity.

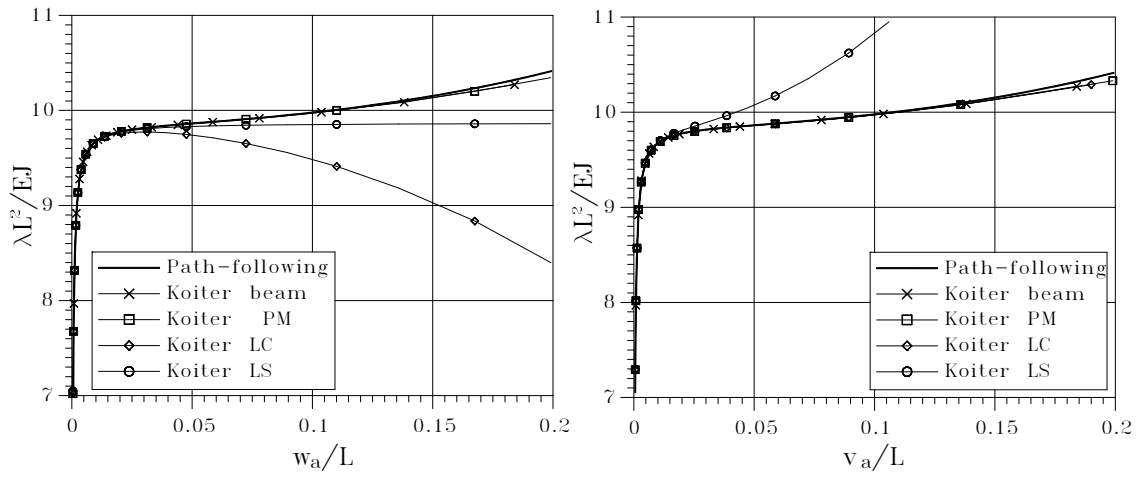


Fig. 10.2: Euler beam: out-plane and in-plane equilibrium path.

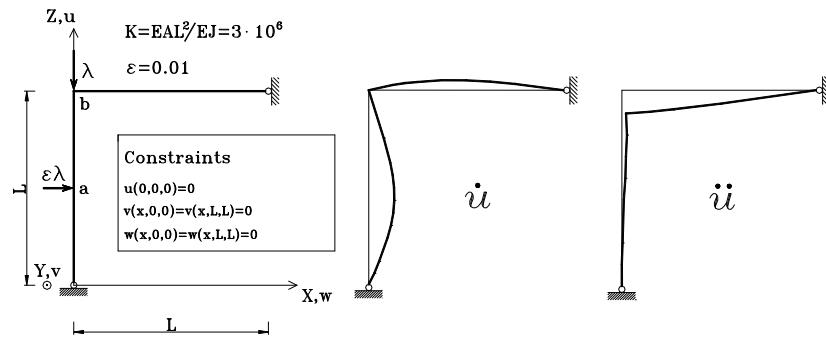


Fig. 10.3: Roorda frame

	<i>elem.nř</i>	<i>LC</i>	<i>LS</i>	<i>PM</i>	<i>Beam</i> ^(*)
λ_b	16	13.954	13.954	13.954	
	32	13.903	13.903	13.903	13.886
	64	13.890	13.890	13.890	
$\frac{\dot{\lambda}_b}{\lambda_b}$	16	0.3815	0.3815	0.3815	
	32	0.3808	0.3808	0.3807	0.3805
	64	0.3806	0.3806	0.3805	
$\ddot{\lambda}_b/2\lambda_b$	16	-0.6421	0.2178	0.4535	
	32	-0.7165	0.1434	0.3797	0.3787
	64	-0.7176	0.1422	0.3785	

^(*)Solution obtained by Antman model and exact interpolation functions

Tab. 10.2: Roorda frame: asymptotic quantity.

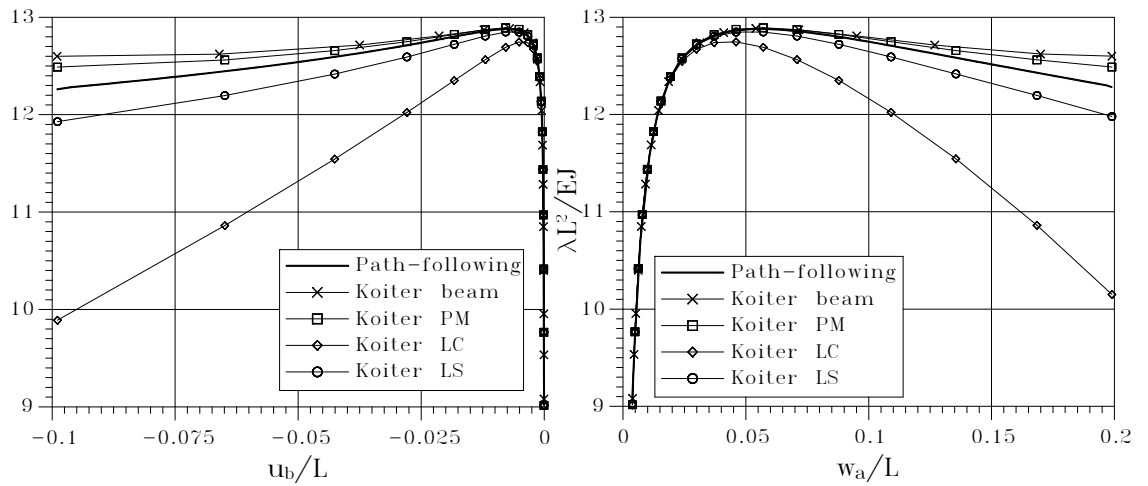


Fig. 10.4: Roorda frame: equilibrium paths.

10.2.2 C section beam

In the numerical analysis of the C section beam reported in fig.10.5 the good agreements between the numerical results obtained by the *PM* model in comparison with the path-following analysis performed by a co-rotational formulation proposed in [7] which is insensitive to the exactness of the strain measures can be observed. As the critical mode is a torsional buckling the behavior of the plate assemblages is practically the same as a 3D beam. The buckling mode it is not followed by stress redistribution and the postcritical curvature becomes very sensitive to the exactness of the strain model [7], as shown in fig. 10.6.

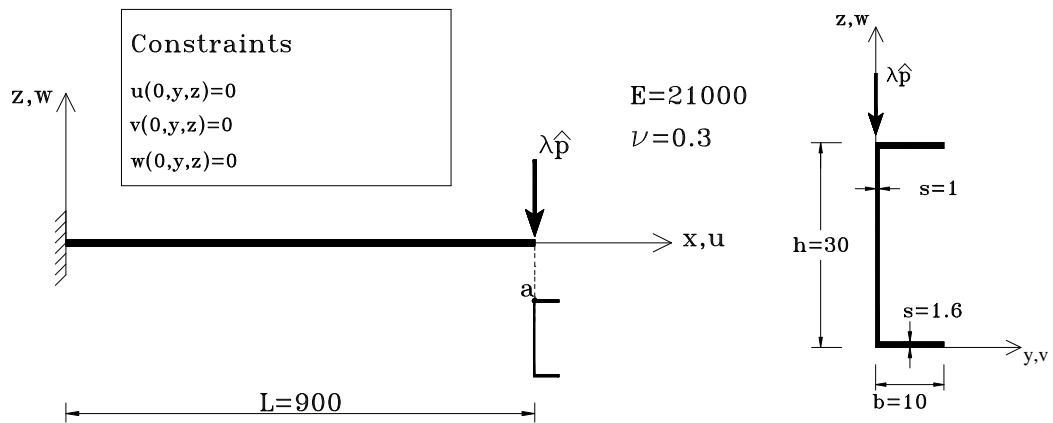


Fig. 10.5: C section beam.

10.2.3 C section with stress redistribution

In this case, whose geometry is reported in fig. 10.7, we have stress redistribution following the multimodal buckling. The structure is analyzed with flexural positive imperfections. In this case the results are unaffected by the strain model used and in practise the technical model also give exact results. More details can be found in [6].

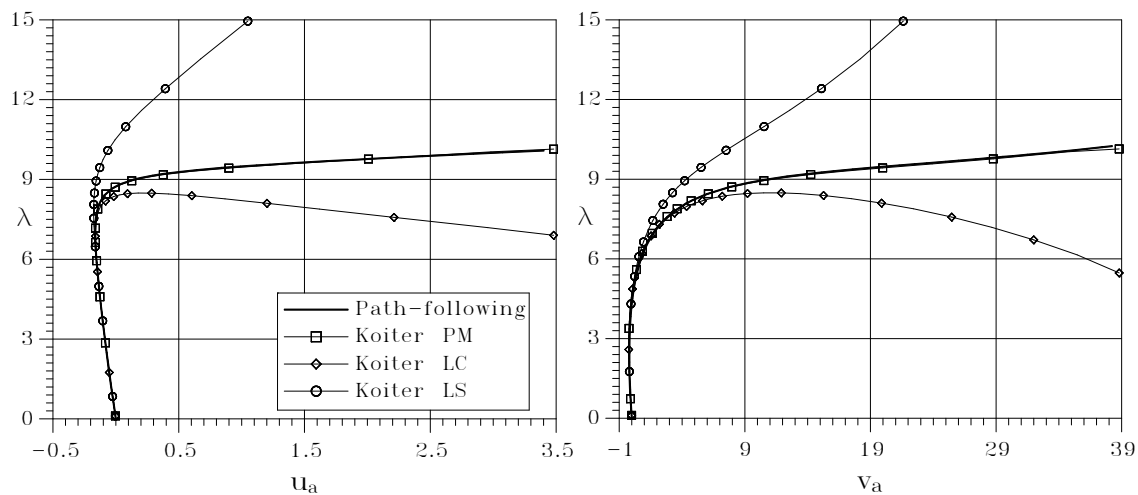


Fig. 10.6: Cantilever C section beam: equilibrium paths.

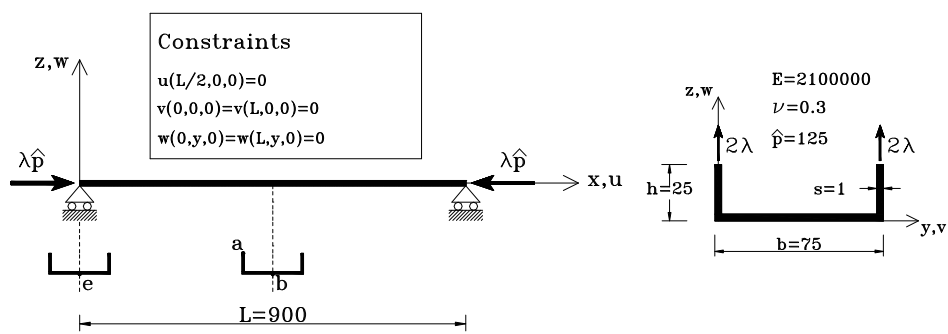


Fig. 10.7: Compressed C section beam.

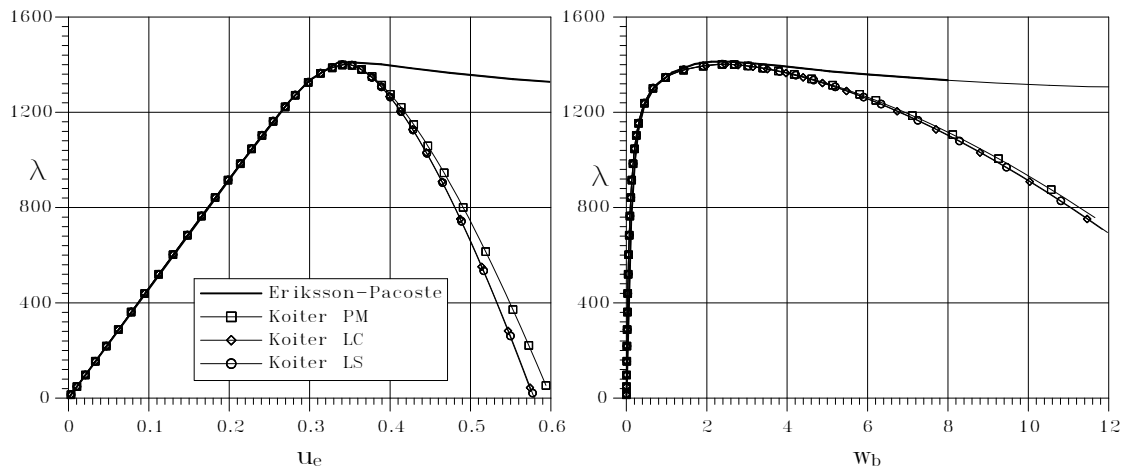


Fig. 10.8: C section beam: equilibrium paths.

Chapter 11

Concluding remarks

A method that allows us to obtain, in a simple and automatic way, exact strain measures for structures undergoing large displacements and small strain, is described. As the displacement field is in the corotational frame infinitesimal, linearized kinematical models for beams, plates and shells can usefully be employed. Since linearized models are always available even for complex structural models (plates or shells) it is easy to obtain the corresponding rational strain measures using this approach.

Geometrically exact strain measures for beams and plates have been obtained. In the case of the beam the correctness of such measures is evident in comparison with those available in literature [33]. An application to shear undeformable beam is also presented. For thin plates the strain measures were obtained for cases of both von Karman and Kirchoff models.

The strength of the method is that it makes it possible obtain, exact strain measures for complex structural models, starting always from linear, first order, theory. For example the extension to other complicated beam models (i.e. including section warping) becomes trivial.

The measures obtained, both for beams and plates, have been used in numerical analysis based on Koiter's asymptotic approach. In this analysis context, which is dramatically sensitive to the strain measure, the results again show once more the correctness of the proposed approach.

Bibliography

- [1] W.T.Koiter, 'On the stability of elastic equilibrium'. Thesis, Delft, 1945. English transl. NASA TT-F10, 883 (1967) and AFFDL\TR70-25 (1970).
- [2] E. Riks, 'An incremental approach to the solution of snapping and buckling problems', *Int. Journal of Solids & Structures*, **15**, pp. 529-551 (1979).
- [3] R. Casciaro, 'Computational Asymptotic Post-Buckling Analysis of Slender Elastic Structures', CISM Courses and Lectures NO. 470, SpringerWien, New-York, (2005).
- [4] A.D. Lanzo, G. Garcea, R. Casciaro, 'Koiter's post-buckling analysis of elastic plates', *Int. Journal for Numerical Methods in Engineering*, **38**, pp. 2325-2345, (1995).
- [5] A.D. Lanzo, G. Garcea, 'Koiter's analysis of thin-walled structures by a finite element approach', *Int. Journal for Numerical Methods in Engineering*, **39**, pp. 3007-3031, (1996).
- [6] G. Garcea, 'Mixed formulation in Koiter analysis of thin-walled beam', *Computer Methods in Applied Mechanics and Engineering*, **190**, pp. 3369-3399, (2001).
- [7] G. Garcea, G.A. Trunfio, R. Casciaro, 'Path-following analysis of thin-walled structures and comparison with asymptotic post-critical solutions', *Int. Journal for Numerical Methods in Engineering*, **55**, pp. 73-100, (2002).
- [8] G. Salerno, R. Casciaro, 'Mode jumping and attractive paths in multi-mode elastic buckling', *Int. Journal for Numerical Methods in Engineering*, **40**, pp. 833-861, (1997).
- [9] G. Salerno, G. Uva, 'Ho's theorem in global-local mode interaction of pin-jointed bar structures', *International Journal of Non-Linear Mechanics*, **41** (3), pp. 359-376, (2006).

- [10] G. Garcea, G.A.Trunfio, R. Casciaro, 'Mixed formulation and locking in path following nonlinear analysis', *Computer Methods in Applied Mechanics and Engineering*, **165** 1-4, pp.247-272, (1998).
- [11] G. Garcea, G. Salerno, R. Casciaro, 'Extrapolation locking and its sanitization in Koiter's asymptotic analysis', *Computer Methods in Applied Mechanics and Engineering*, **180** 1-2, pp. 137-167. (1999).
- [12] Rodrigues O., Des lois géométriques qui régissent les déplacements d'un système solide dans l'espace ..., *Journal de Mathématiques Pures et Appliquées*,**5**, pp. 380-440, (1840).
- [13] Barré de Saint Venant A., 'Mémoire sur la torsion des prismes, avec des considérations sur la flexion',..., *Mémoires des savant étrangers*, **14**, p. 233 (1855).
- [14] M. Jourawsky, 'Sur la résistance d'un corps prismatique et d'une pièce composée en bois ou en tole de fer à une force perpendiculaire à leur longueur, *Annales des Ponts et Chaussées*', (1856).
- [15] E. Cosserat, F. Cosserat, 'Théorie des corps déformables', Hermann et fils, Paris, (1909).
- [16] H. Wagner, 'Torsion and buckling of open section', NACA TM 807. (1936).
- [17] V.Z. Vlasov, 'Thin walled elastic bars', Fizmatgiz, Mosca, (1959).
- [18] L. Malvern, 'Introduction to the Mechanics of a Continuous Medium', Prentice Hall, (1969), New-York.
- [19] S.S. Antmann, 'The theory of rods', Springer Verlag, (1972).
- [20] E. Reissner, 'On one-dimensional finite strain beam theory: the plane problem', *J. Appl. Math. Phys*, **23**, pp. 795-804, (1972).
- [21] T. Belytschko, B.J. Hsieh, 'Non linear transient finite element analysis with convected coordinates', *Int. Journal for Numerical Methods in Engineering*, **7**, pp. 255-271, (1973).
- [22] T. Belytschko, L. Schwer, M.J.Klein, 'Large displacements, transient analysis of space frames', *Int. Journal for Numerical Methods in Engineering*, **11**, pp. 65-84, (1977).
- [23] T. Belytschko, L. Glaum, 'Application of high order corotational stretch theory to nonlinear finite elements analysis', *Computer & Structures*, **10**, pp. 175-182, (1979).

- [24] J.H. Argyris, H.Balmer, S.St Doltsinis, P.C. Dunne, M. Haase, M.Kleiber, G.A. Malejannakis, H.P. Mlejnek, M. Muller, D.W. Scharpf, 'Finite element method - The natural approach ', Computer Methods in Applied Mechanics and Engineering, **17/18**, pp. 1-106, (1979).
- [25] J.H. Argyris, O. Hilpert, G.A. Malejannakis, D.W. Scharpf, 'The geometrical stiffness of a beam in space V.W. approach', Computer Methods in Applied Mechanics and Engineering, **20** 1-2, pp. 105-131, (1979).
- [26] A. Tatone, A. Di Carlo, 'Analisi numerica della biforcazione dell'equilibrio di travi elastiche 3D', Università dell' Aquila, **35**, (1980).
- [27] E. Reissner, 'On finite deformations of space curved beams', J. Appl. Math. Phys.', **32**, pp. 734-744, (1981).
- [28] J.H. Argyris, 'An excursion into large rotations', Computer Methods in Applied Mechanics and Engineering., **32**, pp. 85-155., (1982).
- [29] M. Pignataro, A. Di Carlo, R. Casciaro, 'On nonlinear beam model from the point of view of computational post-buckling analysis. Int. Journal of Solids & Structures, **18** (4), pp. 327-347 (1982).
- [30] E. Reissner, 'On a simple variational analysis of small finite deformations of prismatical beams', J. Appl. Math. Phys. (ZAMP), pp. 642-648, (1983).
- [31] E. Reissner, 'On some problems of buckling of prismatical beams under the influence of axial and transverse loads', J. Appl. Math. Phys. (ZAMP), pp. 649-667, (1983).
- [32] M.B. Rubin, 'On the theory of a Cosserat point and its application to the numerical solution of continuum problems', (1985).
- [33] J.C. Simo, 'A finite strain beam formulation. The three dimensional dynamics problem'. Part I.
- [34] C.C. Rankin, 'An element independent corotational procedure for the treatment of large rotations', J. of Pressure Vessel Technology, **108**, pp. 165-174, (1986).
- [35] J.C. Simo, 'A three dimensional finite-strain rod model. Part II: Computational aspect', Computer Methods in Applied Mechanics and Engineering, **58**, pp. 79-116, (1986).
- [36] , A. Cardona, M. Geradin, 'A beam finite element non-linear theory with finite rotations', Int. Journal for Numerical Methods in Engineering, **26**, pp. 2403-2438, (1988).

- [37] C.C. Rankin, B. Nour-Omid, 'The use of projectors to improve finite element performance', *Computer & Structures*, **30**, pp. 257-267, (1988).
- [38] M.A. Crisfield, 'A consistent co-rotational formulation for nonlinear, three dimensional, beam-elements', *Computer Methods in Applied Mechanics and Engineering*, **81**, pp. 131-150, (1990).
- [39] J.C. Simo, 'A geometrically-exact rod model incorporating shear and torsion-warping deformation', (1991).
- [40] B. Nour-Omid, C.C. Rankin, Finite rotation analysis and consistent linearization using projectors, *Computer Methods in Applied Mechanics and Engineering*, **93**, pp.353-384, (1991).
- [41] J.C. Simo, 'The symmetric Hessian for geometrically nonlinear models in solid mechanics: Intrinsic definition and geometric interpretation', *Computer Methods in Applied Mechanics and Engineering*, **96**, pp. 189-200, (1992).
- [42] J.H. Argyris, V.F. Poterasu, 'Large rotations revisited application of Lie algebra', *Computer Methods in Applied Mechanics and Engineering*, **103**, pp. 11-42, (1993).
- [43] P. Wriggers, F. Gruntmann, 'Thin shells with finite rotations formulated in Biot stress: theory and finite element formulation', *Int. Journal for Numerical Methods in Engineering*, **36**, pp. 2049-2071, (1993).
- [44] Borri, 'Intrinsic beam models based on a helicoidal approximation-part I'.
- [45] Borri, 'Intrinsic beam models based on a helicoidal approximation-part II'.
- [46] S.S. Antman, 'Nonlinear Problems of Elasticity', Springer- Verlag, New-York, (1995).
- [47] A. Ibrahimbegović, 'On finite element implementation of geometrically nonlinear Reissner's beam theory: three dimensional curved beam elements', *Computer Methods in Applied Mechanics and Engineering*, **122**, pp. 11-26, (1995).
- [48] A. Ibrahimbegović, 'Computational aspects of vector-like parametrization of three dimensional finite rotations'.(1995).
- [49] P.F. Pai, A. Palazotto, 'Polar decomposition theory in nonlinear analysis of solids and structures', *J. of Engineering Mechanics*, (1995).

- [50] M.A. Biot, 'Mechanics of Incremental Deformations'. J. Wiley & Sons, New-York, (1995).
- [51] M.A. Crisfield, G.F. Moita, 'A unified co-rotational framework for solids, shells and beams', *Int. Journal of Solids & Structures*, **33**, pp. 2969-2992, (1996).
- [52] M.Y. Kim, 'Spatial stability of thin-walled space frames', *Int. Journal for Numerical Methods in Engineering*, **39**, pp. 499-525, (1996).
- [53] Mingrui Li, 'The finite deformation theory for beam, plate and shell. part I. The two dimensional beam theory', *Computer Methods in Applied Mechanics and Engineering*, **146**, pp. 53-63, (1997).
- [54] M.A. Crisfield, 'Non-linear Finite Element Analysis of Solids and Structures', John Wiley, (1997).
- [55] C. Pacoste, A. Eriksson, 'Beam element in instability problems', *Computer Methods in Applied Mechanics and Engineering*, **144**, pp. 163-197, (1997).
- [56] A. Ibrahimbegović, 'On the choice of finite rotations parameters', *Computer Methods in Applied Mechanics and Engineering*, **149**, pp. 49-71, (1997).
- [57] P. Betsch, A. Menzel, E. Stein, 'On the parametrization of finite rotations in computational mechanics. A classification of concepts with application to smooth shells', *Computer Methods in Applied Mechanics and Engineering*, **155**, pp. 273-305, (1998).
- [58] M.A. Crisfield, 'Interpolation of rotation variables in nonlinear dynamics of 3D beams', *Int. Journal for Numerical Methods in Engineering*, **43**, pp. 1193-1222, (1998).
- [59] F. Gruttmann, R. Sauer, W. Wagner, 'A geometrical nonlinear eccentric 3D-beam element with arbitrary cross sections', *Computer Methods in Applied Mechanics and Engineering*, **160**, pp. 383-400, (1998).
- [60] P. Ladevèze, J. Simmonds, 'New concept for linear beam theory with arbitrary geometry and loading', *Eur. J. Mech. A/Solids*, **17**, pp. 377-402, (1998).
- [61] J. Rhim, W. Lee, 'A Vectorial approach to computational modelling of beams undergoing finite rotations', *Int. Journal for Numerical Methods in Engineering*, **41**, pp. 527-540, (1998).

- [62] K.H. Hsiao, R.T. Yang, Lin W.Y., 'A consistent finite element formulation for linear buckling analysis of spatial beams', *Computer Methods in Applied Mechanics and Engineering*, **156**, pp. 259-276, (1998).
- [63] Mingrui Li, 'The finite deformation theory for beam, plate and shell. part II. The kinematic model and the Green-Lagrange strains', *Computer Methods in Applied Mechanics and Engineering*, **156**, pp. 247-257, (1998).
- [64] Mingrui Li, 'The finite deformation theory for beam, plate and shell. part III. The three-dimensional beam theory and the FE formulation', *Computer Methods in Applied Mechanics and Engineering*, **162**, pp. 287-300, (1998).
- [65] P. Pai, A. Palazotto, J.M. Greer, 'Polar decomposition and appropriate strains and stress for nonlinear structural analysis', *Computer & Structures*, **66**, pp. 823-840, (1998).
- [66] E. Petrov, M. Geradin, 'Finite element theory for curved and twisted beams based on exact solutions for three-dimensional solids Part I: Beam concept and geometrically exact nonlinear formulation', *Computer Methods in Applied Mechanics and Engineering*, **165**, pp. 43-92, (1998).
- [67] E. Petrov, M. Geradin, 'Finite element theory for curved and twisted beams based on exact solutions for three-dimensional solids Part II: Anisotropic and advanced beam models', *Computer Methods in Applied Mechanics and Engineering*, **165**, pp. 93-127, (1998).
- [68] G. Jelenić M.A. Crisfield, 'Geometrically exact 3D beam theory: implementation of strain-invariant finite element for statics and dynamics', *Computer Methods in Applied Mechanics and Engineering*, **171**, pp.141-171, (1999).
- [69] Y.Y. Kim, J.H. Kim, 'Thin-walled closed box beam element for static and dynamics analysis', *Int. Journal for Numerical Methods in Engineering*, **45**, pp. 473-490, (1999).
- [70] K.M. Hsiao, W.Y. Lin, 'A co-rotational finite element formulation for buckling and postbuckling analyses of spatial beams', *Computer Methods in Applied Mechanics and Engineering*, **188**, pp. 567-594, (2000).
- [71] Mingrui Li, F. Zhan, 'The finite deformation theory for beam, plate and shell. part IV. The Fe formulation of Mindlin plate and shell based on Green-Lagrangian strain', *Computer Methods in Applied Mechanics and Engineering*, **182**, pp. 187-203, (2000).

- [72] Mingrui Li, F. Zhan, 'The finite deformation theory for beam, plate and shell. part IV. The shell element with drilling degree of freedom based on Biot strain', *Computer Methods in Applied Mechanics and Engineering*, **189**, pp. 743-759, (2000).
- [73] P. Nardinocchi, L. Teresi, A. Tiero, 'A direct theory of affine bodies', *Int. Journal of Engineering Science*, **38**, pp. 865-878, (2000).
- [74] B.A. Izzuddin, 'Conceptual issues in geometrically nonlinear analysis of 3D framed structures', *Computer Methods in Applied Mechanics and Engineering*, **191**, pp. 1029-1053, (2001).
- [75] W.Y. Lin, K.M. Hsiao, 'A co-rotational formulation for geometric non linear analysis of doubly symmetric thin walled beams', *Computer Methods in Applied Mechanics and Engineering*, **190**, pp. 6023-6052.
- [76] Y.L. Pi, M.A. Bradford, 'Effects of approximations in analysis of beams of open thin - walled cross-section-part I: flexural- torsional stability', *Int. Journal for Numerical Methods in Engineering*, **51**, pp. 773-790, (2001).
- [77] Y.L. Pi, M.A. Bradford, 'Effects of approximations in analysis of beams of open thin - walled cross-section-part II: 3D nonlinear behaviour', *Int. Journal for Numerical Methods in Engineering*
- [78] M. Živković, M. Kojić, R. Slavković, 'A general beam finite element with deformable cross section', *Computer Methods in Applied Mechanics and Engineering*, **190**, pp. 2651-2680, (2001).
- [79] P. Betsch, P. Steinmann, 'Frame-indifferent beam finite elements based upon the geometrically exact beam theory', *Int. Journal for Numerical Methods in Engineering*, **54**, pp. 1775-1788, (2002).
- [80] M. Ritto Corrêa, D.Camotin, 'On the differentiation of the Rodrigues formula and its significance for vector for vector like parametrization of Reissner-Simo beam theory', *Int. Journal for Numerical Methods in Engineering*, **55**, pp. 1005-1032, 2002.
- [81] R. El Fatmi, H. Zenzri, 'On the structural behavior and the Saint Venant solution in the exact beam theory. Application to laminated composite beams', *Computer & Structures*, **80**, pp. 1441-1456, (2002).
- [82] W. Yu, D.H. Hodges, V. Volovoi, C.E.S. Cesnik, ' On Timoshenko-like modeling of initially curved and twisted composite beams', *Int. Journal of Solids & Structures*, **39**, pp. 5101-5121, (2002).

- [83] A. Ibrahimbegović, R. L. Taylor, 'On the role of frame-invariance in structural mechanics models at finite rotations', *Computer Methods in Applied Mechanics and Engineering*, **191** pp. 5159-5176, (2002).
- [84] P. Ladezève, 'The exact theory of plate bending', *Journal of Elasticity*, **68**, pp. 37-71, (2002).
- [85] J.M. Battini, C. Pacoste, 'Co-rotational beam elements with warping effects in instability problems', *Computer Methods in Applied Mechanics and Engineering*, **191**, pp. 1755-1789, (2002).
- [86] P. Nardinocchi, L.Teresi, A. Tiero, 'A direct affine rods', *Eur. Journal of Mechanics A/Solids*, **21**, pp. 653-667, (2002).
- [87] P. Nardinocchi, L.Teresi, A. Tiero, 'Constitutive identification of affine rods', *Mechanics Reserch Comuncations*, **30**, pp. 61-68, (2003).
- [88] M.R. Corrêa, D. Camotim, 'Work-conjugacy between rotation-dependent moments and finite rotations', *Int. Journal of Solids & Structures*, **40**, pp. 2851-2873, (2003).
- [89] R.K. Kapania, J. Li, 'On a geometrically exact curved/twisted beam theory under rigid cross-section assumption', *Computational Mechanics*, **30**, 428-443,(2003).
- [90] R.K. Kapania, J. Li, 'A formulation and implementation of geometrically exact curved beam elements incorporating finite strains and finite rotations', *Computational Mechanics*, **30**, 444-459,(2003).
- [91] D. Zupan, M. Saje, 'Finite-element formulation of geometrically exact three-dimensional beam theories based on interpolation of strain measures', *Computer Methods in Applied Mechanics and Engineering*, **192**, pp. 5209-5248, (2003).
- [92] D. Zupan, M. Saje, 'The three-dimensional beam theory: Finite element formulation based on curvature', *Computer & Structures*, **81**, pp. 1875-1888, (2003).
- [93] A.S. Petrolo, R. Casciaro, '3D beam element based on Saint Venánt's rod theory', *Computer & Structures*, **82**, pp. 2471-2481, (2004).
- [94] R. El Fatmi, H. Zenzri, 'A numerical method for the exact elastic beam theory. Applications to homogeneous and composite beams', *Int. Journal of Solids & Structures*, **41**, pp. 2521-2537, (2004).
- [95] Ali H. Nayfeh, P.F. Pai, 'Linear and Nonlinear Structural Mechanics', *Jon Wiley*, (2004.)

- [96] C.A. Felippa, B.Haughen, A unified formulation of small-strain corotational finite elements: I. Theory. *Computer Methods in Applied Mechanics and Engineering*, **194**, pp. 2285-2335, (2005).
- [97] B.A. Izzuddin, 'An enhanced co-rotational approach for large displacement analysis of plates', *Int. Journal for Numerical Methods in Engineering*.
- [98] M.Y. Kim, S. Kim, N. Kim, 'Spatial stability of shear deformable curved beams with non-symmetric thin-walled sections. I: Stability formulation and closed-form solutions', *Computer & Structures*,**83**, pp. 2525-2541, (2005).
- [99] Y.L. Pi, M.A. Bradford, B. Uy, 'Nonlinear analysis of members curved in space with warping and Wagner effects', *Int. Journal of Solids & Structures*, **42**, pp. 3147-3169, (2005).
- [100] H.H. Chen, W.Y. Lin, K.M. Hsiao, 'Co-rotational finite element formulation for thin-walled beams with generic open section', *Computer Methods in Applied Mechanics and Engineering*, **195**, pp. 2334-2370, (2006).
- [101] D. Zupan, M. Saje, 'The linearized three-dimensional beam theory of naturally curved and twisted beams: The strain vectors formulation', *Computer Methods in Applied Mechanics and Engineering*, **195**, pp. 4557-4578, (2006).
- [102] G.Garcea, A. Madeo, G. Zagari, R. Casciaro, 'Asymptotic post-buckling FEM analysis using a corotational formulation', *International Journal of Solids and Structures*, In press.
- [103] G.Garcea, A. Madeo, 'Rational strain measures-The Implicit Corotational Method', Lisbona Portugal 2006.
- [104] G. Garcea, A. Madeo, 2007. Asymptotic postbuckling analysis of 3D beams using corotational formulation, Università della Calabria, Labmec Report.
www.labmec.unical.it/pubblicazioni/collana.php.
- [105] S.P.Timoshenko, J.M. Gere, 1961. *Theory of elastic stability*, 2nd edition, McGraw-Hill.
- [106] H.H. Chen, W.Y. Lin, K.M. Hsiao, 2006. Co-rotational finite element formulation for thin-walled beams with generic open section, *Computer Methods in Applied Mechanics and Engineering* 195, 2334–2370.

Appendix A

Some remarks on polar decomposition

A.1 Recursive evaluation of polar decomposition

For the evaluation of the polar decomposition we assume an exponential representation for the rotation :

$$\mathbf{R} = \mathbf{I} + \mathbf{W} + \frac{1}{2}\mathbf{W}^2 + \frac{1}{6}\mathbf{W}^3 + \frac{1}{24}\mathbf{W}^4 \dots$$

The \mathbf{W} will be a non linear function of gradient $\nabla \mathbf{u}$, in particular we can assume that:

$$\mathbf{W} = \mathbf{W}_1 + \mathbf{W}_2 + \mathbf{W}_3 + \mathbf{W}_4 + \dots$$

being \mathbf{W}_k the term corresponding to a Taylor expansion for \mathbf{W} . Each term can be evaluated using the following recursive rule:

- First order

$$\mathbf{U} = \mathbf{R}^T \mathbf{F} = (\mathbf{I} + \mathbf{W}_1)^T (\mathbf{I} + \nabla \mathbf{u})$$

for the symmetry on the tensor \mathbf{U} , holds

$$(\mathbf{I} + \mathbf{W}_1)^T (\mathbf{I} + \nabla \mathbf{u}) = (\mathbf{I} + \nabla \mathbf{u})^T (\mathbf{I} + \mathbf{W}_1)$$

requiring a first order accuracy for the symmetry of \mathbf{U}

$$\mathbf{I} + \nabla \mathbf{u} + \mathbf{W}_1^T = \mathbf{I} + \nabla \mathbf{u}^T + \mathbf{W}_1$$

thereby

$$\mathbf{W}_1 = \frac{1}{2}(\nabla \mathbf{u} - \nabla \mathbf{u}^T)$$

- Second order

$$\mathbf{U} = \mathbf{R}^T \mathbf{F} = (\mathbf{I} + \mathbf{W}_1 + \mathbf{W}_2 + \frac{1}{2} \mathbf{W}_1 \mathbf{W}_1)^T (\mathbf{I} + \nabla \mathbf{u})$$

for the symmetry on the tensor \mathbf{U} , holds

$$(\mathbf{I} + \mathbf{W}_1 + \mathbf{W}_2 + \frac{1}{2} \mathbf{W}_1 \mathbf{W}_1)^T (\mathbf{I} + \nabla \mathbf{u}) = (\mathbf{I} + \nabla \mathbf{u})^T (\mathbf{I} + \mathbf{W}_1 + \mathbf{W}_2 + \frac{1}{2} \mathbf{W}_1 \mathbf{W}_1)$$

requiring a first order accuracy for the symmetry of \mathbf{U} and remembering the the expression of \mathbf{W}_1

$$\begin{aligned} (\mathbf{I} + \mathbf{W}_1 + \mathbf{W}_2 + \frac{1}{2} \mathbf{W}_1 \mathbf{W}_1)^T (\mathbf{I} + \nabla \mathbf{u}) &= (\mathbf{I} + \nabla \mathbf{u})^T (\mathbf{I} + \mathbf{W}_1 + \mathbf{W}_2 + \frac{1}{2} \mathbf{W}_1 \mathbf{W}_1) \\ \mathbf{W}_1 \nabla \mathbf{u} + \mathbf{W}_2^T &= \nabla \mathbf{u}^T \mathbf{W}_1^T + \mathbf{W}_2 \end{aligned}$$

we have then

$$\mathbf{W}_2 = \frac{1}{2} (\mathbf{W}_1 \nabla \mathbf{u} - \nabla \mathbf{u}^T \mathbf{W}_1^T)$$

- Third order

$$\mathbf{U} = \mathbf{R}^T \mathbf{F} = (\mathbf{I} + \mathbf{W}_1 + \mathbf{W}_2 + \mathbf{W}_3 + \frac{1}{2} \mathbf{W}_1 \mathbf{W}_1 + \frac{1}{6} (\mathbf{W}_1 \mathbf{W}_2 + \mathbf{W}_2 \mathbf{W}_1))^T (\mathbf{I} + \nabla \mathbf{u})$$

using the same approach presented in the first two step, we have that

$$\mathbf{W}_3 = \frac{1}{2} (\mathbf{W}_2 \nabla \mathbf{u} - \nabla \mathbf{u}^T \mathbf{W}_2^T)$$

- k- order The k-term of Taylor expansion series have thereby the expression

$$\mathbf{W}_k = \frac{1}{2} (\mathbf{W}_{k-1} \nabla \mathbf{u} - \nabla \mathbf{u}^T \mathbf{W}_{k-1}^T)$$

Appendix B

Objective interpolation

B.1 Objective Interpolation

The objectivity of the interpolation is first tested in the planar beam case. We assume the Antman strain measure, the material form is

$$\epsilon = (1 + u_{,1}) \cos \varphi + v_{,1} \sin \varphi - 1 \quad \gamma = -(1 + u_{,1}) \sin \varphi + v_{,1} \cos \varphi \quad \chi = \varphi_{,1}$$

while for the spatial form we have that

$$\epsilon = 1 + u_{,1} - \cos \varphi \quad \gamma = v_{,1} - \sin \varphi \quad \chi = \varphi_{,1}$$

The quantities will be interpolated as

$$\begin{aligned} u_{,1} &= \frac{u_j - u_i}{l} \\ v_{,1} &= f_s \frac{\varphi_i - \varphi_j}{2} + f_e \left(\frac{\varphi_i + \varphi_j}{2} - \frac{v_j - v_i}{l} \right) + \frac{v_j - v_i}{l} \\ \varphi &= v_{,1} \\ \varphi_{,1} &= f_{s,1} \frac{\varphi_i - \varphi_j}{2} + f_{e,1} \left(\frac{\varphi_i + \varphi_j}{2} - \frac{v_j - v_i}{l} \right) \end{aligned}$$

with

$$f_s = 1 - 2\frac{s}{l} \quad f_e = \frac{1}{l^2}(6s^2 - 6sl + l^2)$$

A rigid body motion make the following displacement field

$$u = s(\cos \phi - 1) \quad , \quad v = s \sin \phi$$

The discrete quantities are

$$u_i = 0 \quad u_j = l(\cos \phi - 1) \quad v_i = 0 \quad v_j = l \sin \phi \quad \varphi_i = \varphi_j = \phi$$

Using the interpolation law

$$\begin{aligned} u_{,1} &= \frac{u_j}{l} = \cos \phi - 1 \\ v_{,1} &= \varphi = f_e(\phi - \sin \phi) + \sin \phi \\ \varphi_{,1} &= f_{e,1}(\phi - \sin \phi) \end{aligned}$$

The evaluation of deformation gives for the material form

$$\epsilon = \frac{f_e}{6}\phi^4 \quad \gamma = \frac{\phi^3}{6} \quad \chi = \frac{f_e\phi^3}{6}$$

while for the spatial form

$$\epsilon = \frac{f_e - 1}{6}\phi^4 \quad \gamma = \frac{\phi^3}{6} \quad \chi = \frac{f_e\phi^3}{6}$$

When the quantities will be interpolated as

$$\begin{aligned} u_{,1} &= \frac{u_j - u_i}{l} \\ v_{,1} &= f_s \frac{\varphi_i - \varphi_j}{2} + f_e \left(\frac{\varphi_i + \varphi_j}{2} - \frac{v_j - v_i}{l} \right) + \frac{v_j - v_i}{l} \\ \varphi &= v_{,1} + \bar{\gamma} \\ \varphi_{,1} &= f_{s,1} \frac{\varphi_i - \varphi_j}{2} + f_{e,1} \left(\frac{\varphi_i + \varphi_j}{2} - \frac{v_j - v_i}{l} \right) \end{aligned}$$

with

$$f_s = 1 - 2\frac{s}{l} \quad f_e = \frac{1}{l^2}(6s^2 - 6sl + l^2)$$

A rigid body motion make the following displacement field

$$u = s(\cos \phi - 1) \quad , \quad v = s \sin \phi$$

The discrete quantities are

$$u_i = 0 \quad u_j = l(\cos \phi - 1) \quad v_i = 0 \quad v_j = l \sin \phi \quad \varphi_i = \varphi_j = \phi \quad \varphi = \phi$$

Using the interpolation law

$$\begin{aligned} u_{,1} &= \frac{u_j}{l} = \cos \phi - 1 \\ v_{,1} &= \varphi = f_e(\phi - \sin \phi) + \sin \phi \\ \varphi_{,1} &= f_{e,1}(\phi - \sin \phi) \end{aligned}$$

The evaluation of deformation gives for the material form

$$\epsilon = \frac{f_e}{6}\phi^4 \quad \gamma = \frac{f_e\phi^3}{6} \quad \chi = \frac{f_e\phi^3}{6}$$

while for the spatial form

$$\epsilon = 0 \quad \gamma = \frac{f_e \phi^3}{6} \quad \chi = \frac{f_e \phi^3}{6}$$

Alternative interpolation, we assume that

$$\begin{aligned} u_{,1} &= \frac{u_j - u_i}{l} \\ v_{,1} &= \frac{v_j - v_i}{l} \\ \varphi &= \phi_m \\ \varphi_{,1} &= f_{s,1} \frac{\varphi_i - \varphi_j}{2} + f_{e,1} \left(\frac{\varphi_i + \varphi_j}{2} - \phi_m \right) \end{aligned}$$

The discrete material representation of strain measures becomes

$$\begin{aligned} \epsilon &= \left(1 + \frac{u_j - u_i}{l}\right) \cos \phi_m + \frac{v_j - v_i}{l} \sin \phi_m - 1 \\ \gamma &= -\left(1 + \frac{u_j - u_i}{l}\right) \sin \phi_m + \frac{v_j - v_i}{l} \cos \phi_m \\ \chi &= f_{s,1} \frac{\varphi_i - \varphi_j}{2} + f_{e,1} \left(\frac{\varphi_i + \varphi_j}{2} - \phi_m \right) \end{aligned}$$

Assuming

$$\phi_m = \arctan \frac{v_j - v_i}{l + u_j - u_i}$$

we have that

$$\begin{aligned} \epsilon &= \left(1 + \frac{u_j - u_i}{l}\right) \cos \phi_m + \frac{v_j - v_i}{l} \sin \phi_m - 1 \\ \gamma &= 0 \\ \chi &= f_{s,1} \frac{\varphi_i - \varphi_j}{2} + f_{e,1} \left(\frac{\varphi_i + \varphi_j}{2} - \phi_m \right) \end{aligned}$$

B.1.1 Equivalence with Corotational Formulation

Remembering the linear strain measure

$$\epsilon = \bar{u}_{,1} \quad \gamma = \bar{v}_{,1} - \bar{\varphi} \quad \chi = \bar{\varphi}_{,1}$$

The displacements in corotational frame will be interpolated as

$$\begin{aligned} \bar{u}_{,1} &= \frac{\bar{u}_j - \bar{u}_i}{l} \\ \bar{v}_{,1} &= f_s \frac{\bar{\varphi}_i - \bar{\varphi}_j}{2} + f_e \left(\frac{\bar{\varphi}_i + \bar{\varphi}_j}{2} - \frac{\bar{v}_j - \bar{v}_i}{l} \right) + \frac{\bar{v}_j - \bar{v}_i}{l} \\ \bar{\varphi} &= \bar{v}_{,1} \\ \bar{\varphi}_{,1} &= f_{s,1} \frac{\bar{\varphi}_i - \bar{\varphi}_j}{2} + f_{e,1} \left(\frac{\bar{\varphi}_i + \bar{\varphi}_j}{2} - \frac{\bar{v}_j - \bar{v}_i}{l} \right) \end{aligned}$$

Assuming $\phi_m = \arctan \frac{v_j - v_i}{l + u_j - u_i}$, the strain measure becomes

$$\epsilon = \left(1 + \frac{u_j - u_i}{l}\right) \cos \phi_m + \frac{v_j - v_i}{l} \sin \phi_m - 1$$

$$\gamma = 0$$

$$\chi = f_{s,1} \frac{\varphi_i - \varphi_j}{2} + f_{e,1} \left(\frac{\varphi_i + \varphi_j}{2} - \phi_m\right)$$

Appendix C

The use of material-spatial model in Koiters analysis

C.1 Shallow Frame - Analytical Solution

Exploiting the structure symmetry, we can only study the left side of the whole structure. The geometric and material characteristic are

$$\begin{aligned} L_0 &= 15 & H_0 &= 0.45 \\ EA &= 10^6 & EJ_3 &= 10^4 \end{aligned}$$

The structure is analyzed in local frame. This simplify the expression of the the energy, but the boundary condition become:

$$\begin{aligned} u_1[0] &= 0 & , & & u_1[L] \cos \alpha - u_2[L] \sin \alpha &= 0 \\ u_2[0] &= 0 & , & & N_1[L] \sin \alpha + N_2[L] \cos \alpha &= \lambda \hat{p}_2 \\ M_3[0] &= 0 & , & & \varphi_3[L] &= 0 \end{aligned} \quad (C.1)$$

where $\hat{p}_2 = -1$, $\tan \alpha = \frac{H_0}{L_0}$ and $L = \sqrt{L_0^2 + H_0^2}$. The first step consist in the evaluation of fundamental path. The variational equation to be solved is

$$\Phi_0'' \hat{u} \delta u - \hat{p} \delta u = 0 \quad (C.2)$$

we have that

$$\begin{aligned} \Phi_0'' \hat{u} \delta u &= \int_0^L (\delta N_1 \hat{u}_{1,s} + \hat{N}_1 \delta u_{,s} + \delta N_2 (\hat{u}_{2,s} - \hat{\varphi}_3) \\ &+ \hat{N}_2 (\delta u_{2,s} - \delta \varphi_3) + \delta M_3 \hat{\varphi}_{3,s} + \hat{M}_3 \delta \varphi_{3,s} \\ &- \frac{1}{2} (\frac{\delta N_1 \hat{N}_1}{EA} + \frac{\delta N_2 \hat{N}_2}{EA} + \frac{\delta M_3 \hat{M}_3}{EJ_3})) ds \\ &+ \hat{p}_2 [\delta u_1[L] \sin \alpha + \delta u_2[L] \cos \alpha] \end{aligned} \quad (C.3)$$

The Euler-Lagrange equations, associate to variational principle (C.2) could be separated into two groups: compatibility and equilibrium equations. For compatibility equations we have:

$$\begin{aligned}\hat{N}_1 &= EA \hat{u}_{1,s} \\ \hat{N}_2 &= EA (\hat{u}_{2,s} - \hat{\varphi}_3) \\ \hat{M}_3 &= EJ_3 \hat{\varphi}_{3,s}\end{aligned}\tag{C.4}$$

while for equilibrium equation

$$\begin{aligned}\hat{N}_{1,s} &= 0 \\ \hat{N}_{2,s} &= 0 \\ \hat{M}_{3,s} + \hat{N}_2 &= 0\end{aligned}\tag{C.5}$$

The boundary conditions obviously coincide with (C.1). To solve the groups of equations (C.4) and (C.5) , it's convenient substituting compatibility equation into equilibrium:

$$\begin{aligned}\hat{u}_{1,ss} &= 0 \\ (\hat{u}_{2,s} - \hat{\varphi}_3)_{,s} &= 0 \\ \hat{\varphi}_{3,ss} + \frac{EA}{EJ}(\hat{u}_{2,s} - \hat{\varphi}_3) &= 0\end{aligned}\tag{C.6}$$

The solution of the system of the equation give using the constraints

$$\begin{aligned}\hat{u}_1 &= -k_1 (L^2 + \beta H_0) s \\ \hat{u}_2 &= k_2(-s + \frac{s^3}{L^2}) - k_3(s + \beta \frac{H_0}{L_0^2} s + \frac{L^2}{L_0^2} s - \frac{1}{2} \frac{s^3}{L^2}) \\ \hat{\varphi}_3 &= k_4(s^2 - L^2) = a_0 + a_2 s^2\end{aligned}\tag{C.7}$$

where

$$\begin{aligned}\beta &= 3 \frac{EJ_3}{EA H_0} \quad , \quad k_1 = \frac{1}{2} \frac{1}{(EA (1 + \beta) H_0 L)} \\ k_2 &= \frac{L_0 H_0}{2} k_1 \quad , \quad k_3 = \frac{L_0^3}{H_0} k_1 \quad , \quad k_4 = \frac{3}{2} \frac{L_0}{H_0} k_1\end{aligned}$$

Using the compatibility, with some algebra, the internal forces are

$$\begin{aligned}\hat{N}_1 &= -EA k_1 (L^2 + \beta H_0) \\ \hat{N}_2 &= EA (-k_2 - k_3(1 + \beta \frac{H_0}{L_0^2} + \frac{L^2}{L_0^2}) + k_4 L^2) \\ \hat{M}_3 &= 2EJ_3 k_4 s\end{aligned}$$

As reference the numerical value of \hat{N}_1 and \hat{N}_2 constant in the beam local frame are reported

$$\hat{N}_1 = -14.524 \quad , \quad \hat{N}_2 = -0.06449$$

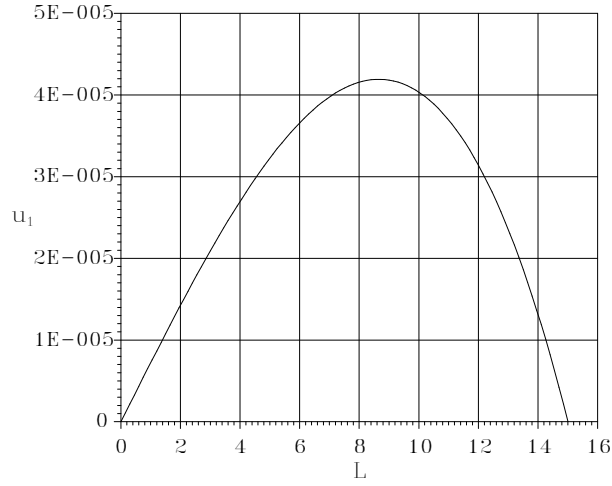


Fig. C.1: Function \hat{u}_1

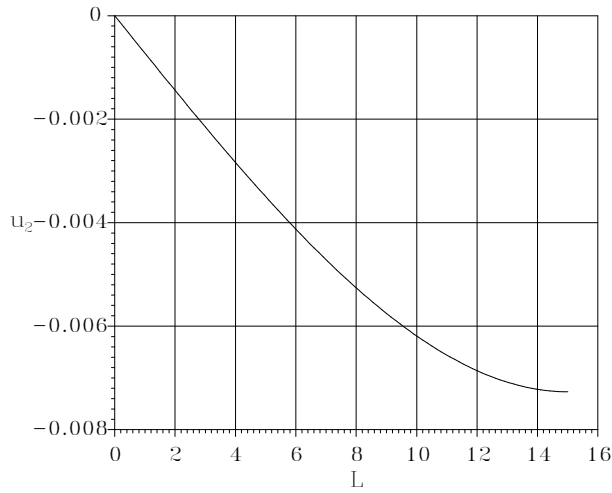


Fig. C.2: Function \hat{u}_2

The second step is the evaluation of the bifurcation problem

$$\Phi_b'' \hat{u} \delta u = 0 \tag{C.8}$$

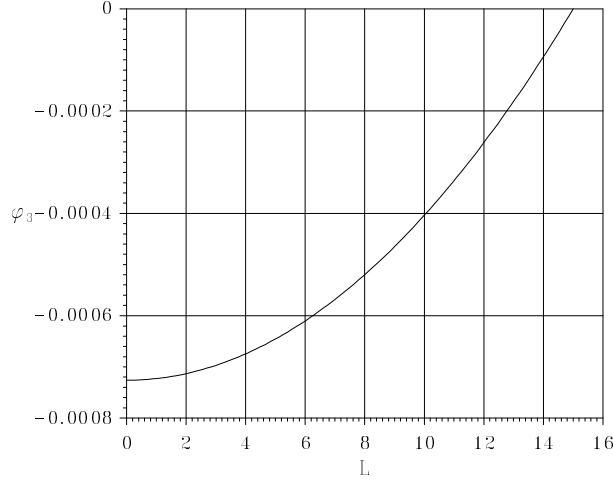


Fig. C.3: Function $\hat{\varphi}_3$

so, we have

$$\begin{aligned}
\Phi_b'' \dot{u} \delta u &= \int_0^L (\delta N_1 (\dot{u}_{1,s} + \lambda \hat{\varphi}_3 \dot{\varphi}_3) + \dot{N}_1 (\delta u_{1,s} + \lambda \hat{\varphi}_3 \delta \varphi_3) \\
&+ \delta N_2 (\dot{u}_{2,s} - \dot{\varphi}_3) + \dot{N}_2 (\delta u_{2,s} - \delta \varphi_3) \\
&+ \delta M_3 \dot{\varphi}_{3,s} + \dot{M}_3 \delta \varphi_{3,s} + \lambda \hat{N}_1 \delta \varphi_3 \dot{\varphi}_3 \\
&- \frac{1}{2} \left(\frac{\delta N_1 \dot{N}_1}{EA} + \frac{\delta N_2 \dot{N}_2}{EA} + \frac{\delta M_3 \dot{M}_3}{EJ_3} \right) ds = 0
\end{aligned}$$

neglecting the terms higher than λ^2 . The Euler-Lagrange equations associate to variational principle (C.8), give the as compatibility equations

$$\begin{aligned}
\dot{N}_1 &= EA(\dot{u}_{1,s} + \lambda \hat{\varphi}_3 \dot{\varphi}_3) \\
\dot{N}_2 &= EA(\dot{u}_{2,s} - \dot{\varphi}_3) \\
\dot{M}_3 &= EJ_3 \dot{\varphi}_{3,s}
\end{aligned} \tag{C.9}$$

and as equilibrium equations

$$\begin{aligned}
\dot{N}_{1,s} &= 0 \\
\dot{N}_{2,s} &= 0 \\
\dot{M}_{3,s} + \dot{N}_2 - \lambda \dot{N}_1 \hat{\varphi}_3 - \lambda_b \hat{N}_1 \dot{\varphi}_3 &= 0
\end{aligned} \tag{C.10}$$

The boundary conditions are homogeneous

$$\begin{aligned}
\dot{u}_1[0] &= 0 \quad , \quad \dot{u}_1[L] \cos \alpha - \dot{u}_2[L] \sin \alpha = 0 \\
\dot{u}_2[0] &= 0 \quad , \quad \dot{N}_1[L] \sin \alpha + \dot{N}_2[L] \cos \alpha = 0 \\
\dot{M}_3[0] &= 0 \quad , \quad \dot{\varphi}_3[L] = 0
\end{aligned} \tag{C.11}$$

As solution strategy, the compatibility equations (C.9) are substituted into equilibrium equations (C.10), obtaining

$$\begin{aligned}
(\dot{u}_{1,s} + \lambda \hat{\varphi}_3 \dot{\varphi}_3)_{,s} &= 0 \\
(\dot{u}_{2,s} - \dot{\varphi}_3)_{,s} &= 0 \\
\dot{\varphi}_{3,ss} + \frac{EA}{EJ_3} ((\dot{u}_{2,s} - \dot{\varphi}_3) - \lambda(\dot{u}_{1,s} + \lambda \hat{\varphi}_3 \dot{\varphi}_3)) - \frac{\lambda \hat{N}_1}{EJ_3} \dot{\varphi}_3 &= 0
\end{aligned} \tag{C.12}$$

The solution of the system (C.12) of the equations gives:

$$\begin{aligned}
\dot{u}_1 &= \int \left(\frac{c_1}{EA} - \lambda \hat{\varphi}_3 \dot{\varphi}_3 \right) ds + c_5 \\
\dot{u}_2 &= \int \left(\frac{c_2}{EA} + \dot{\varphi}_3 \right) ds + c_6
\end{aligned}$$

where c_1, c_2, c_5, c_6 are constant that will be evaluated using the boundary condition (C.11). The functions \dot{u}_1 and \dot{u}_2 depend from $\dot{\varphi}_3$ solution of the differential equations:

$$\dot{\varphi}_{3,ss} + \psi^2 [\lambda] \dot{\varphi}_3 = \dot{f}[\hat{u}]$$

with $\psi^2[\lambda] = -\frac{\lambda \hat{N}_1}{EJ_3}$ and $\dot{f}[\lambda \hat{u}] = \frac{(-c_2 + \lambda \hat{\varphi}_3 c_1)}{EJ_3}$. Solving

$$\dot{\varphi}_3 = \sin(\psi s) c_4 + \cos(\psi s) c_3 + \frac{\dot{f}}{\psi^2} - \frac{2\lambda c_1 a_2}{EJ_3 \psi^4}$$

The compatibility (C.9) allow to evaluated the internal forces. Using the boundary condition and filtering the homogeneous solution, the constant become

$$\begin{aligned}
c_2 &= c_1 \\
c_3 &= -c_1 \tan \alpha \\
c_4 &= -\frac{c_1 \sin(\alpha)}{\cos(\psi_b L) \psi_b^2 EJ_3 \cos(\alpha) (1 + \beta)} \\
&\quad - \frac{c_1 \sin(\alpha) \beta}{\cos(\psi_b L) \psi_b^2 EJ_3 \cos(\alpha) (1 + \beta)} \\
&\quad + \frac{3}{2} \frac{\lambda L_0 c_1}{\cos(\psi_b L) \psi_b^4 LH_0^2 EA EJ_3 (1 + \beta)} \\
c_5 &= 0 \\
c_6 &= 0
\end{aligned}$$

where $\psi_b = \psi[\lambda_b]$ and λ_b the critical value

$$\lambda_b = 21.9653$$

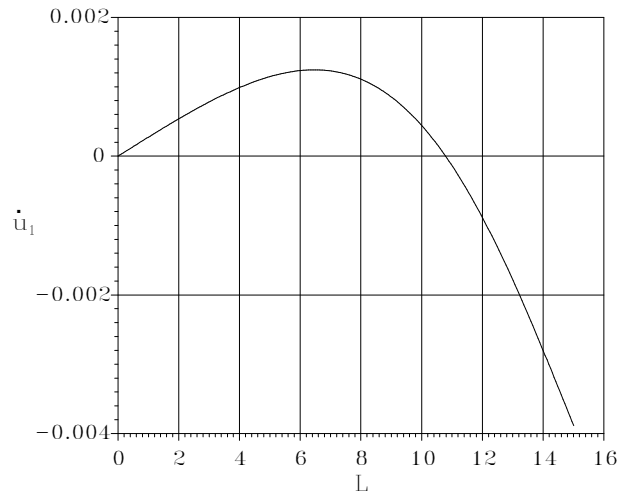


Fig. C.4: Function \dot{u}_1

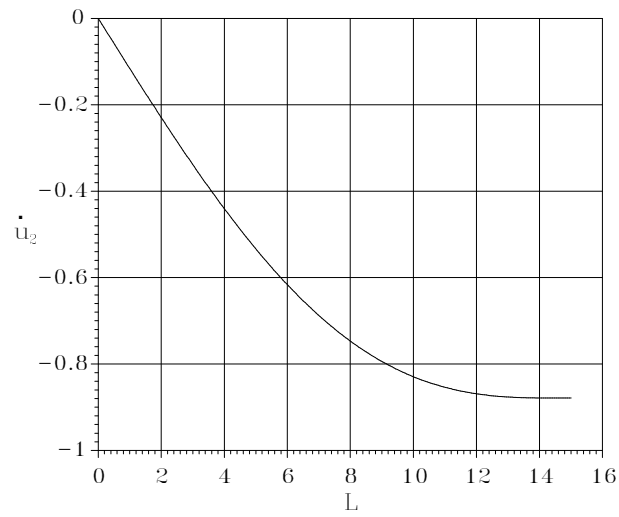


Fig. C.5: Function \dot{u}_2

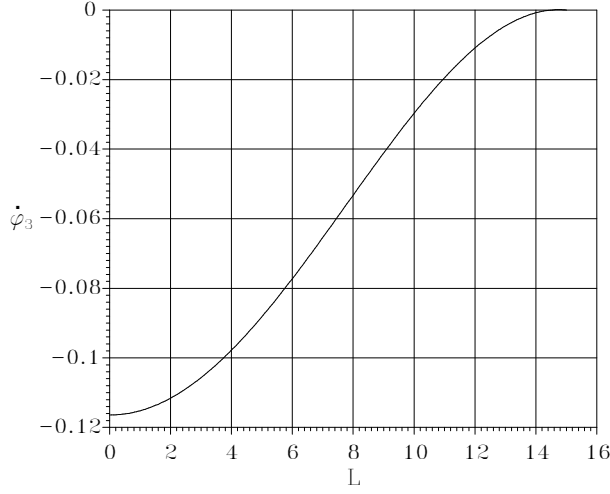


Fig. C.6: Function $\dot{\varphi}_3$

Normalizing the buckling mode so that

$$\dot{u}_1 \sin \alpha + \dot{u}_2 \cos \alpha = -1$$

The evaluation of the energetic quantities gives:

$$\begin{aligned} \Phi_b''' \hat{u} \hat{u}^2 &= \int_0^L (\hat{N}_1 \hat{\varphi}_3^2 + 2\dot{N}_1 \hat{\varphi}_3 \hat{\varphi}_3 + \lambda_b \hat{N}_2 \hat{\varphi}_3^2 \hat{\varphi}_3 \\ &\quad + \lambda_b (\dot{N}_2 \hat{\varphi}_3^2 + 2\dot{N}_2 \hat{\varphi}_3 \hat{\varphi}_3) \hat{\varphi}_3) ds \\ \Phi_b''' \hat{u}^3 &= \int_0^L (3\dot{N}_1 \hat{\varphi}_3^2 + \lambda_b \hat{N}_2 \varphi_3^3 + 3\lambda_b \dot{N}_2 \hat{\varphi}_3^2 \hat{\varphi}_3) ds \\ \Phi_b''' \hat{u}^4 &= \int_0^L (4\dot{N}_2 \varphi_3^3 - \lambda_b \hat{N}_1 \varphi_3^4 - 4\lambda_b \dot{N}_1 \hat{\varphi}_3 \hat{\varphi}_3) ds \end{aligned}$$

the numerical values are

$$\begin{aligned} \Phi_b''' \hat{u} \hat{u}^2 &= -2.7702 \\ \Phi_b''' \hat{u}^3 &= 316.11 \\ \Phi_b''' \hat{u}^4 &= -0.30364 \end{aligned}$$

The last step is the evaluation of the secondary critical modes. The variational problem is:

$$\Phi_b'' \hat{u} \delta u + \Phi_b''' \hat{u}^2 \delta u + c \Phi_b''' \hat{u} \hat{u} \delta u = 0$$

Substituting the variation we have that:

$$\begin{aligned}
\Phi_b'' \ddot{u} \delta u &= \int_0^L (\delta N_1 (\ddot{u}_{1,s} + \lambda_b \hat{\varphi}_3 \ddot{\varphi}_3) + \dot{N}_1 (\delta u_{1,s} + \lambda_b \hat{\varphi}_3 \delta \varphi_3) \\
&\quad + \delta N_2 (\ddot{u}_{2,s} - \ddot{\varphi}_3) + \dot{N}_2 (\delta u_{2,s} - \delta \varphi_3) \\
&\quad + \delta M_3 \ddot{\varphi}_{3,s} + \dot{M}_3 \delta \varphi_{3,s} + \lambda_b \hat{N}_1 \delta \varphi_3 \ddot{\varphi}_3 \\
&\quad - \frac{1}{2} (\frac{\delta N_1 \dot{N}_1}{EA} + \frac{\delta N_2 \dot{N}_2}{EA} + \frac{\delta M_3 \dot{M}_3}{EJ_3})) ds \\
\Phi''' \dot{u}^2 \delta u &= \int_0^L (\delta N_1 \dot{\varphi}_3^2 + 2 \dot{N}_1 \dot{\varphi}_3 \delta \varphi_3 + \lambda_b \hat{N}_2 \dot{\varphi}_3^2 \delta \varphi_3 \\
&\quad + \lambda_b (\dot{N}_2 \dot{\varphi}_3^2 + 2 \dot{N}_2 \dot{\varphi}_3 \delta \varphi_3) \hat{\varphi}_3) ds \\
\Phi''' \dot{u} \hat{u} \delta u &= \int_0^L (\delta N \dot{\varphi}_3 \hat{\varphi}_3 + \dot{N} \dot{\varphi}_3 \delta \varphi_3 + \dot{N} \hat{\varphi}_3 \delta \varphi_3 \\
&\quad + \lambda_b (\hat{N}_2 \dot{\varphi}_3 \delta \varphi_3 + \delta N_2 \dot{\varphi}_3 \hat{\varphi}_3 + \dot{N}_2 \hat{\varphi}_3 \delta \varphi_3) \hat{\varphi}_3 \\
&\quad + \lambda_b \hat{N}_2 \dot{\varphi}_3 \hat{\varphi}_3 \delta \varphi_3) ds
\end{aligned}$$

The constant c are evaluated for the ratio

$$c = -\frac{\Phi_b''' \dot{u}^3}{\Phi_b''' \dot{u}^2 \hat{u}} = 316.11$$

Neglecting as for the critical modes the terms higher than λ . Also in this case, the Euler-Lagrange equations could be subdivided into two groups. We have the compatibility equations:

$$\begin{aligned}
\ddot{N}_1 &= EA(\ddot{u}_{1,s} + \lambda_b \hat{\varphi}_3 \ddot{\varphi}_3 + \dot{\varphi}_3^2 + c \dot{\varphi}_3 \hat{\varphi}_3) \\
\ddot{N}_2 &= EA(\ddot{u}_{2,s} - \ddot{\varphi}_3 + \lambda_b \hat{\varphi}_3 \dot{\varphi}_3^2 + c \lambda_b \dot{\varphi}_3 \hat{\varphi}_3^2) \\
\ddot{M}_3 &= EJ_3 \ddot{\varphi}_{3,s}
\end{aligned} \tag{C.13}$$

and equilibrium equations:

$$\begin{aligned}
\dot{N}_{1,s} &= 0 \\
\dot{N}_{2,s} &= 0 \\
\dot{M}_{3,s} + \dot{N}_2 & \\
&- \lambda_b \hat{N}_1 \dot{\varphi}_3 - \lambda_b \dot{N} \hat{\varphi}_3 - 2 \dot{N}_1 \dot{\varphi}_3 - \lambda_b \hat{N}_2 \dot{\varphi}_3^2 - 2 \lambda_b \dot{N}_2 \hat{\varphi}_3 \dot{\varphi}_3 \\
&- c(\hat{N}_1 \dot{\varphi}_3 + \dot{N} \hat{\varphi}_3 + \lambda_b \hat{N}_1 \dot{\varphi}_3 \hat{\varphi}_3 + \lambda_b \hat{N}_2 \dot{\varphi}_3 \hat{\varphi}_3 + \lambda_b \dot{N}_2 \hat{\varphi}_3^2) = 0
\end{aligned} \tag{C.14}$$

Substituting equilibrium into compatibility

$$\begin{aligned}
(\ddot{u}_{1,s} + \lambda_b \dot{\varphi}_3 \hat{\varphi}_3 + \dot{\varphi}_3^2 + c \dot{\varphi}_3 \hat{\varphi}_3),_s &= 0 \\
(\ddot{u}_{2,s} - \ddot{\varphi}_3 + \lambda_b \dot{\varphi}_3^2 + c \lambda_b \dot{\varphi}_3 \hat{\varphi}_3^2),_s &= 0 \\
EJ_3 \ddot{\varphi}_{3,ss} + EA(\ddot{u}_{2,s} - \ddot{\varphi}_3) & \\
&- (\lambda_b \hat{N}_1 \dot{\varphi}_3 + \lambda_b EA \hat{\varphi}_3 \ddot{u}_{1,s} + \dot{N}_1 \dot{\varphi}_3 + \lambda_b \hat{N}_2 \dot{\varphi}_3^2 + 2 \lambda_b \dot{N}_2 \hat{\varphi}_3 \dot{\varphi}_3) \\
&- c(\hat{N}_1 \dot{\varphi}_3 + \dot{N} \hat{\varphi}_3 + \lambda_b \hat{N}_1 \dot{\varphi}_3 \hat{\varphi}_3 + \lambda_b \hat{N}_2 \dot{\varphi}_3 \hat{\varphi}_3 + \lambda_b \dot{N}_2 \hat{\varphi}_3^2) = 0
\end{aligned} \tag{C.15}$$

The solution of the system (C.15) of the equations gives

$$\begin{aligned}\ddot{u}_1 &= - \int (\lambda_b \ddot{\varphi}_3 \hat{\varphi}_3 + \ddot{\varphi}_3^2 + c \dot{\varphi}_3 \hat{\varphi}_3 - \frac{c_7}{EA}) ds + c_{11} \\ \ddot{u}_2 &= \int (\ddot{\varphi}_3 - \lambda_b \dot{\varphi}_3^2 - c \lambda_b \dot{\varphi}_3 \hat{\varphi}_3^2 + \frac{c_8}{EA}) ds + c_{12}\end{aligned}$$

with $\ddot{\varphi}_3$ solution of the ordinary equation:

$$\ddot{\varphi}_3 + \psi_b^2 \ddot{\varphi}_3 = \ddot{f}[\lambda_b \hat{u}, \dot{u}] \quad (\text{C.16})$$

where

$$\begin{aligned}\ddot{f}[\lambda_b \hat{u}, \dot{u}] &= \frac{1}{EJ_3} (-c_8 + \lambda_b \hat{\varphi}_3 c_7 + 2\dot{N} \dot{\varphi}_3 + \lambda_b \hat{N}_2 \dot{\varphi}_3^2 \\ &\quad + 2\lambda_b \dot{N}_2 \hat{\varphi}_3 \dot{\varphi}_3 + c (\hat{N}_1 \dot{\varphi}_3 + \dot{N} \hat{\varphi}_3 + \lambda_b \hat{N}_1 \dot{\varphi}_3 \hat{\varphi}_3 + \\ &\quad \lambda_b \hat{N}_2 \dot{\varphi}_3 \hat{\varphi}_3 + \lambda_b \dot{N}_2 \hat{\varphi}_3^2)\end{aligned}$$

for the further manipulation we define

$$\ddot{f}[\lambda_b \hat{u}, \dot{u}] = \frac{1}{EJ_3} \sum_{i=1}^{10} \ddot{f}^{(i)}$$

and

$$\dot{\varphi} = d_1 \cos(\psi_b s) + d_2 \sin(\psi_b s) + d_3 + d_4 s^2$$

where

$$\begin{aligned}\ddot{f}^{(1)} &= -c_8 & \ddot{f}^{(2)} &= \lambda_b \hat{\varphi}_3 c_7 & \ddot{f}^{(3)} &= 2\dot{N} \dot{\varphi}_3 & \ddot{f}^{(4)} &= \lambda_b \hat{\varphi}_3 c_7 \\ \ddot{f}^{(5)} &= 2\lambda_b \dot{N}_2 \hat{\varphi}_3 \dot{\varphi}_3 & \ddot{f}^{(6)} &= c \hat{N}_1 \dot{\varphi}_3 & \ddot{f}^{(7)} &= c \dot{N} \hat{\varphi}_3 \\ \ddot{f}^{(8)} &= c \lambda_b \hat{N}_1 \dot{\varphi}_3 \hat{\varphi}_3 & \ddot{f}^{(9)} &= c \lambda_b \hat{N}_2 \dot{\varphi}_3 \hat{\varphi}_3 & \ddot{f}^{(10)} &= c \lambda_b \dot{N}_2 \hat{\varphi}_3^2\end{aligned}$$

and

$$d_1 = c_4 \quad d_2 = c_5 \quad d_3 = \frac{\dot{f}}{\psi^2} \quad d_4 = -\frac{2\lambda c_1 a_2}{EJ_3 \psi^4}$$

The solution of equation (C.16) can be expressed as:

$$\ddot{\varphi}_3 = \ddot{\varphi}_3^{(0)} + \ddot{\varphi}_3^{(p)}$$

being $\ddot{\varphi}_3^{(0)}$ the homogeneous solution and $\ddot{\varphi}_3^{(p)}$ the particular solution. We have that

$$\ddot{\varphi}_3^{(0)} = c_9 \cos(\psi_b s) + c_{10} \sin(\psi_b s)$$

The particular solution is

$$\ddot{\varphi}_3^{(p)} = \frac{1}{EJ_3} \sum_{i=1}^{10} \ddot{\varphi}_3^{(i)}$$

being $\ddot{\varphi}_3^{(i)}$ the particular solution associate to each terms of $f[\lambda_b \hat{u}, \hat{u}]$. In particular follow that

$$\begin{aligned}
\ddot{\varphi}_3^{(1)} &= -\frac{c_8}{\psi_b^2} \\
\ddot{\varphi}_3^{(2)} &= \lambda_b \left(\frac{a_0}{\psi_b^2} - 2 \frac{a_2}{\psi_b^4} + \frac{a_2 s^2}{\psi_b^2} \right) c_7 \\
\ddot{\varphi}_3^{(3)} &= \dot{N}_1 \left(\frac{d_1 \cos(\psi_b s)}{\psi_b^2} + \frac{d_1 s \sin(\psi_b s)}{\psi_b} + 2 \frac{d_3}{\psi_b^2} + 2 \frac{d_4 s^2}{\psi_b^2} \right. \\
&\quad \left. - 4 \frac{d_4}{\psi_b^4} - \frac{\cos(\psi_b s) d_2 s}{\psi_b} \right) \\
\ddot{\varphi}_3^{(4)} &= \lambda_b \hat{N}_2 \left(\left(-\frac{2}{3} \frac{d_1 d_2 \cos(\psi_b s)}{\psi_b^2} + \frac{1}{3} \frac{d_1 d_4 s^3}{\psi_b} \right. \right. \\
&\quad \left. \left. + \frac{1}{2} \frac{d_2 d_4 s^2}{\psi_b^2} + \left(\frac{d_1 d_3}{\psi_b} - \frac{1}{2} \frac{d_1 d_4}{\psi_b^3} \right) s - \frac{1}{2} \frac{d_2 d_4}{\psi_b^4} \right) \sin(\psi_b s) \right. \\
&\quad \left. + \left(\frac{1}{3} \frac{d_2^2}{\psi_b^2} - \frac{1}{3} \frac{d_1^2}{\psi_b^2} \right) (\cos(\psi_b s))^2 + \left(-\frac{1}{3} \frac{d_2 d_4 s^3}{\psi_b} \right. \right. \\
&\quad \left. \left. + \frac{1}{2} \frac{d_1 d_4 s^2}{\psi_b^2} + \left(\frac{1}{2} \frac{d_2 d_4}{\psi_b^3} - \frac{d_2 d_3}{\psi_b} \right) s + \frac{d_1 d_3}{\psi_b^2} \right) \cos(\psi_b s) \right. \\
&\quad \left. + \frac{s^4 d_4^2}{\psi_b^2} + \left(2 \frac{d_4 d_3}{\psi_b^2} - 12 \frac{d_4^2}{\psi_b^4} \right) s^2 + \frac{2}{3} \frac{d_1^2}{\psi_b^2} + \frac{1}{3} \frac{d_2^2}{\psi_b^2} \right. \\
&\quad \left. - 4 \frac{d_4 d_3}{\psi_b^4} + \frac{d_3^2}{\psi_b^2} + 24 \frac{d_4^2}{\psi_b^6} \right)
\end{aligned}$$

$$\begin{aligned}
\ddot{\varphi}_3^{(5)} &= \lambda_b \dot{N}_2 \left(\frac{1}{3} \frac{a_2 d_1 s^3}{\psi_b} + \frac{1}{2} \frac{a_2 d_2 s^2}{\psi_b^2} + \right. \\
&\quad \left. \left(-\frac{1}{2} \frac{a_2 d_1}{\psi_b^3} + \frac{a_0 d_1}{\psi_b} \right) s - \frac{1}{2} \frac{a_2 d_2}{\psi_b^4} \right) \sin(\psi_b s) \\
&\quad + \left(-\frac{1}{3} \frac{a_2 d_2 s^3}{\psi_b} + \frac{1}{2} \frac{a_2 d_1 s^2}{\psi_b^2} + \left(-\frac{a_0 d_2}{\psi_b} + \frac{1}{2} \frac{a_2 d_2}{\psi_b^3} \right) s \right. \\
&\quad \left. + \frac{a_0 d_1}{\psi_b^2} \right) \cos(\psi_b s) + 2 \frac{d_4 s^4 a_2}{\psi_b^2} + \left(2 \frac{a_0 d_4}{\psi_b^2} \right. \\
&\quad \left. - 24 \frac{a_2 d_4}{\psi_b^4} + 2 \frac{a_2 d_3}{\psi_b^2} \right) s^2 + 48 \frac{a_2 d_4}{\psi_b^6} + 2 \frac{d_3 a_0}{\psi_b^2} \\
&\quad \left. - 4 \frac{a_0 d_4}{\psi_b^4} - 4 \frac{a_2 d_3}{\psi_b^4} \right) \\
\ddot{\varphi}_3^{(6)} &= \frac{\hat{N}_1}{2 \dot{N}_1} \ddot{\varphi}_3^{3p} c \\
\ddot{\varphi}_3^{(7)} &= \frac{c \dot{N}_1}{\lambda_b c_7} \ddot{\varphi}_3^{2p} c \\
\ddot{\varphi}_3^{(8)} &= \frac{\hat{N}_1}{2 \dot{N}_2} \ddot{\varphi}_3^{5p} c \\
\ddot{\varphi}_3^{(9)} &= \frac{\hat{N}_1}{2 \dot{N}_2} \ddot{\varphi}_3^{5p} c \\
\ddot{\varphi}_3^{(10)} &= c \lambda_b \dot{N}_2 \left(\frac{a_2^2 s^4}{\psi_b^2} + \left(2 \frac{a_2 a_0}{\psi_b^2} - 12 \frac{a_2^2}{\psi_b^4} \right) s^2 - 4 \frac{a_2 a_0}{\psi_b^4} \right. \\
&\quad \left. + 24 \frac{a_2^2}{\psi_b^6} + \frac{a_0^2}{\psi_b^2} \right) c
\end{aligned}$$

The constants in the evaluated functions are determined imposing the boundary conditions

$$\begin{aligned}
\ddot{u}_1[0] &= 0 \quad , \quad \ddot{u}_1[L] \cos \alpha - \ddot{u}_2[L] \sin \alpha = 0 \\
\ddot{u}_2[0] &= 0 \quad , \quad \ddot{N}_1[L] \sin \alpha + \ddot{N}_2[L] \cos \alpha = 0 \\
\ddot{M}_3[0] &= 0 \quad , \quad \ddot{\varphi}_3[L] = 0
\end{aligned}$$

and filtering the homogeneous solution. The numerical values are

$$\begin{aligned}
c_7 &= 1233.48 & c_8 &= -37.00 & c_9 &= 489.77 \\
c_{10} &= 0 & c_{11} &= 0 & c_{12} &= 0
\end{aligned}$$

Finally we could evaluated the energy quantities associate to the secondary

mode

$$\begin{aligned} \Phi''[\lambda_b \hat{u}] \ddot{u} \ddot{u} = & \int_0^L (2\ddot{N}_1(\ddot{u}_{1,s} + \lambda_b \hat{\varphi}_3 \ddot{\varphi}_3) + 2\ddot{N}_2(\ddot{u}_{2,s} - \ddot{\varphi}_3) \\ & + 2\ddot{M}_3 \ddot{\varphi}_{3,s} + \lambda_b \hat{N}_1 \ddot{\varphi}_3 \ddot{\varphi}_3 \\ & - \frac{1}{2}(\frac{\ddot{N}_1 \ddot{N}_1}{EA} + \frac{\ddot{N}_2 \ddot{N}_2}{EA} + \frac{\ddot{M}_3 \ddot{M}_3}{EJ_3})) ds \end{aligned}$$

numerically

$$\Phi''[\lambda_b \hat{u}] \ddot{u}^2 = -43.65$$

As references value the internal forces become

$$\ddot{N}_1 = 1233.49 \quad \ddot{N}_2 = -37.00$$

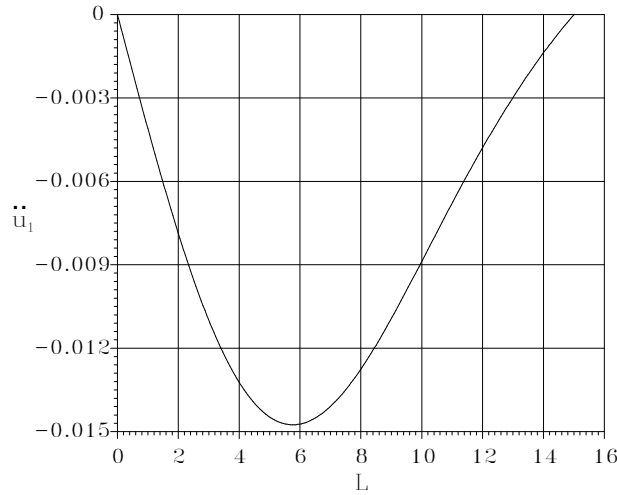


Fig. C.7: Function \ddot{u}_1

C.1.1 Shallow frame solution using - material model

The shallow frame could be solved using material beam model:

$$\bar{\epsilon} = (1 + u_{1,1}) \cos \varphi_3 + u_{2,1} \sin \varphi_3 - 1$$

$$\bar{\gamma} = -u_{2,1} \sin \varphi_3 + (1 + u_{1,1}) \cos \varphi_3$$

$$\bar{\chi} = \varphi_{3,1}$$

The potential energy in mixed form is

$$\Phi''[\lambda \hat{u}] = \int_0^L \{ \bar{N}_1 \bar{\epsilon} + \bar{N}_2 \bar{\gamma} + \bar{M}_3 \bar{\chi} - \frac{1}{2}(\frac{\bar{N}_1^2}{EA} + \frac{\bar{N}_2^2}{EA} + \frac{\bar{M}_3^2}{EJ_3}) \} dX_1$$

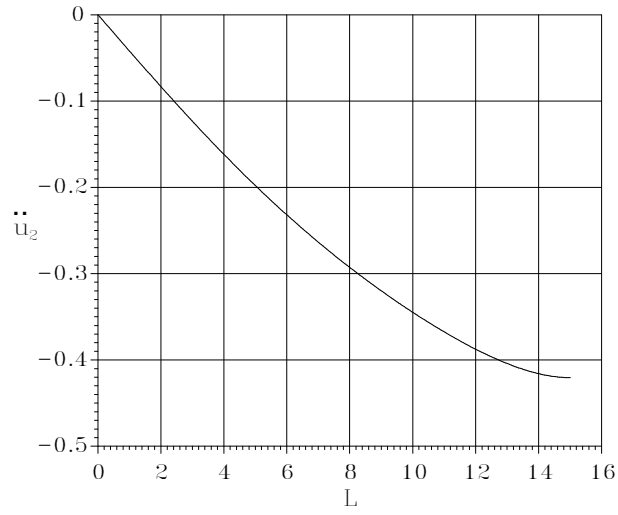


Fig. C.8: Function \ddot{u}_2

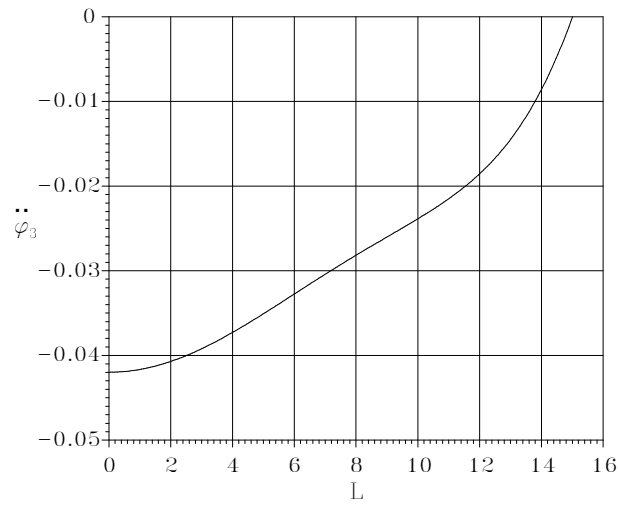


Fig. C.9: Function $\ddot{\varphi}_3$

Using the material model the solution in term of displacement field is the same of that obtained using spatial model. Really, for the fundamental path the problem is the same of (C.3). The solution is the same in term of kinematics and static quantities. The bifurcation problem is defined from linearized second variation energy. By some algebra it is easy to demonstrate that the equilibrium equation are the same of (C.9). The static quantities are obtained from compatibility equation. The compatibility equations are

$$\begin{cases} \dot{\tilde{N}}_1 = EA(\dot{u}_{1,1} + (\dot{u}_{2,1} - \dot{\varphi}_3)\lambda\varphi_3 + \lambda u_{2,1} \dot{\varphi}_3) \\ \dot{\tilde{N}}_2 = EA(\dot{u}_{2,1} - \dot{\varphi}_3 - \dot{u}_{1,1} \lambda\varphi_3 - \dot{\varphi}_3 \lambda u_{1,1}) \\ \dot{\tilde{M}}_3 = EJ_3 \dot{\varphi}_{3,1} \end{cases} \quad (\text{C.17})$$

These last are obviously the linearization of the consistent compatibility equations

$$\begin{cases} \dot{\tilde{N}}_1 = EA(\dot{u}_{1,1} \cos(\lambda\varphi_3) - \dot{\varphi}_3 \sin(\lambda\varphi_3)(1 + \lambda u_{1,1}) \\ \quad + \dot{u}_{2,1} \sin(\lambda\varphi_3) + u_{2,1} \cos(\lambda\varphi_3)\lambda\dot{\varphi}_3) \\ \dot{\tilde{N}}_2 = EA(-\dot{u}_{1,1} \sin(\lambda\varphi_3) - \dot{\varphi}_3 \cos(\lambda\varphi_3)(1 + \lambda u_{1,1}) \\ \quad + \dot{u}_{2,1} \cos(\lambda\varphi_3) - \lambda u_{2,1} \sin(\lambda\varphi_3)\dot{\varphi}_3) \\ \dot{\tilde{M}}_3 = EJ_3 \dot{\varphi}_{3,1} \end{cases} \quad (\text{C.18})$$

Using the displacement fields obtained with the spatial model is possible to obtain the static quantities associate to the critical mode. Using exact

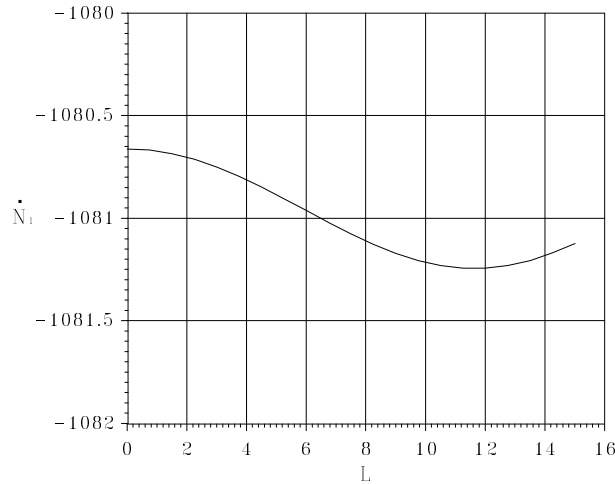


Fig. C.10: Function $\dot{\tilde{N}}_1$

compatibility equation we have while using linearized compatibility The

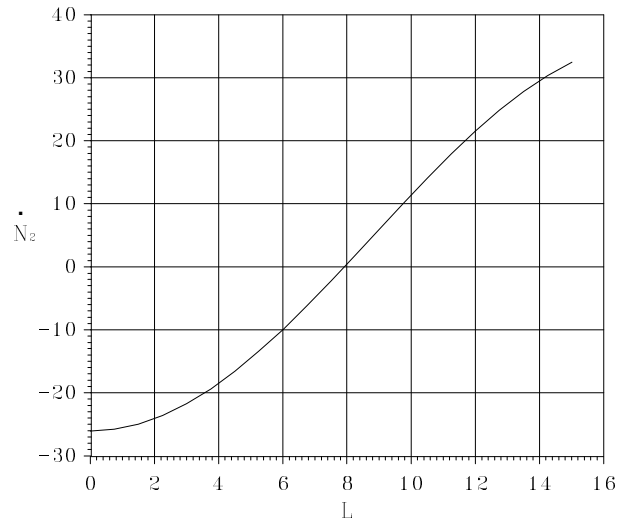


Fig. C.11: Function \dot{N}_2

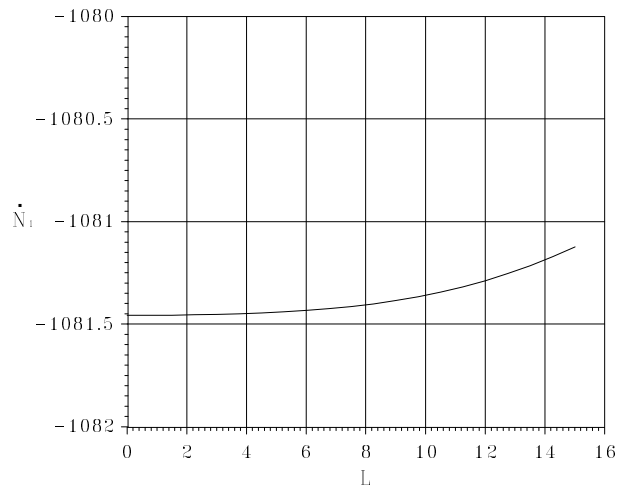


Fig. C.12: Function \dot{N}_1

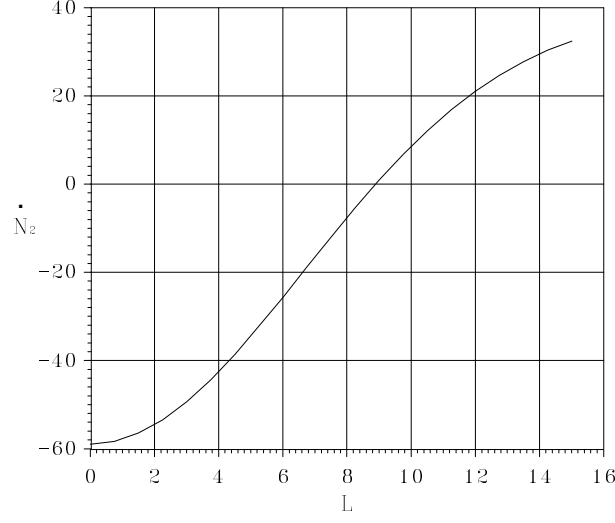


Fig. C.13: Function \dot{N}_2

evaluation of the energy quantities $\Phi''''[\lambda_b \hat{u}]$ will be analyzed.

$$\begin{aligned} \Phi''''[\lambda_b \hat{u}] = & -12 \dot{\varphi}_3^2 \dot{N}_1 \dot{u}_{1,1} + 4 \dot{\varphi}_3^3 \dot{N}_2 - 12 \dot{\varphi}_3^2 \dot{N}_2 \dot{u}_{1,2} \\ & + \left(4 \frac{\dot{\varphi}_3^3 \dot{N}_2}{EA} + \dot{\varphi}_3^4 - 4 \dot{\varphi}_3^3 \dot{u}_{1,2} \right) \lambda_b \hat{N}_1 \\ & + \left(4 \dot{\varphi}_3^3 \dot{u}_{1,1} - 4 \frac{\dot{\varphi}_3^3 \dot{N}_1}{EA} \right) \lambda_b \hat{T}_1 \\ & + \left(-12 \dot{\varphi}_3^2 \dot{N}_1 \dot{u}_{1,2} + 12 \dot{\varphi}_3^2 \dot{N}_2 \dot{u}_{1,1} \right) \lambda_b \hat{\varphi}_3 \end{aligned}$$

The use of the compatibility equation (C.18) or (C.17) give very different result. In particular for exact and approximate compatibility equation we have

$$\Phi''''[\lambda_b \hat{u}] = -1.900 \quad \Phi''''[\lambda_b \hat{u}] = -4.108$$

The fourth variation substituting linearized compatibility in the energy quantities evaluated for the material and spatial model are respectively

$$\begin{aligned} \Phi''''[\lambda_b \hat{u}] = & EA(12 \dot{\varphi}_3^2 \dot{u}_{2,1}^2 - 12 \dot{\varphi}_3^3 \dot{u}_{2,1} + 12 \dot{\varphi}_3^2 \dot{u}_{1,1}^2 \\ & + (6 \dot{\varphi}_3^4 - 12 \dot{\varphi}_3^3 \dot{u}_{2,1}) \lambda_b \hat{u}_{1,1} + 12 \dot{\varphi}_3^3 \dot{u}_{1,1} \lambda_b \hat{u}_{2,1} \\ & + (-16 \dot{\varphi}_3^3 \dot{u}_{2,1} + 12 \dot{\varphi}_3^2 \dot{u}_{1,1}^2 + 12 \dot{\varphi}_3^2 \dot{u}_{2,1}^2) \lambda_b \hat{\varphi}_3^2 \\ & + 4 \dot{\varphi}_3^4 \lambda_b \hat{u}_{2,1}^2 + 4 \dot{\varphi}_3^4 \lambda_b \hat{u}_{1,1}^2 + 16 \dot{\varphi}_3^3 \lambda_b \hat{u}_{1,1} \dot{u}_{1,1} \lambda_b \hat{\varphi}_3 \\ & + (-8 \dot{\varphi}_3^4 + 16 \dot{\varphi}_3^3 \dot{u}_{2,1}) \lambda_b^2 \hat{\varphi}_3 \hat{u}_{2,1} \end{aligned}$$

$$\Phi''''[\lambda_b \hat{u}] = EA(4 \dot{\varphi}_3^3 \dot{u}_{2,1} - 4 \dot{\varphi}_3^4 - 4 \dot{\varphi}_3^3 \varphi_3 \dot{u}_{1,1} - 4 \dot{\varphi}_3^4 \varphi_3^2 - u_{1,1} \dot{\varphi}_3^4)$$

So the different value is associate to a different extrapolation quantities describing the problem. The same treatment could be done for the secondary mode.